Charles University in Prague

1st Faculty of Medicine

Institute of Inherited Metabolic Disorders

Center for Applied Genomics

Molecular Basis of Hereditary Hyperuricaemic Nephropathies

Ph.D. Thesis

Petr Vylet'al

Prague 2008

Dedicated to my grandmother Antonie.

(† 17. 8. 1999, RIP)

Věnováno mojí babičce Antonii.

(† 17. 8. 1999, Odpočívej v pokoji)

ACKNOWLEDGEMENTS

My acknowledgements go to:

Stanislav Kmoch - my boss and supervisor. He was always friendly, supportive and willing to discuss. Many times, he assisted with the advice as well as the action.

Milan Elleder - Institute head, always putting much effort to create convenient environment for Ph.D. students and for the research in general.

My workgroup colleagues:

Martina Živná (nee Kublová) - principal collaborator; always friendly, cheerful and inventive.

Kateřina Hodaňová, Marie Kalbáčová, Marie Zikánová, Hana Blažková, Veronika Barešová and Blanka Stibůrková - provided their friendship, knowledge and results of their work.

Other workgroups colleagues:

Miroslav Janošík, Bohumila Janošíková, Petra Zavaďáková and Jitka Sokolová (Homocysteine Metabolism Disorders research group supervised by Viktor Kožich - they all taught me many).

Linda Berná, Jitka Hlavatá, Helena Hůlková, Helena Poupětová and Jakub Sikora (Lysosomal Metabolism Disorders research group supervised by Jana Ledvinová)

Technicians:

Eva Richterová - DNA and RNA isolation expert technician.

Jana Sovová - immunostaining expert technician.

Office:

Eva Oliveriusová and Eva Horáková - provided indispensable help in administrative jungle.

Collaborators from other institutions:

Květa Pelinková - quality control manager from Institute of Clinical Biochemistry and Laboratory Diagnostics (biochemical analyses of urines).

Zdislava Vaníčková - senior researcher from the same institute (ELISA support).

Family:

I am grateful to my spouse Zuzana, devoted and solicitous person, always willing to listen and advice and also to critically read this thesis, and our son Tadeáš (born on January 2005), giving me a lot of joy and showing me new aspects of life.

My parents were always by my side during my undergraduate as well as Ph.D. studies, sharing my troubles and successes. Without their attitude, I could have never followed my way of life.

Friends:

My mates from Mai Gei Wong Wing Chun International kung fu school in Prague leaded by Sifu Ivan Rzounek, genuine friends always providing great company and mental relaxation.

Funding:

During my Ph.D. studies, I was financially supported by 1st Faculty of Medicine of Charles University in Prague, by grants VZ-111100003 and MSM0021620806 from the Ministry of Education, Youth and Sports of the Czech Republic, 5NE/7046 from the Grant Agency of Ministry of Health of the Czech Republic and by grants 203200, 257672, 257750 and 258105 from the Grant Agency of Charles University in Prague.

Table of Contents

1 INTRODUCTION

Patients with abnormalities in uric acid metabolism form a significant portion of cases evaluated in metabolic centres such as the Institute of Metabolic Disorders in Prague [1]. Mechanisms of uric acid handling in the kidneys are mostly unknown. They include glomerular filtration, reabsorption, secretion and postsecretory reabsorption.

Involved uric acid metabolism contributes to complex traits such as the metabolic syndrome X. The possible way to understand those complex traits is to examine molecular basis of extreme hereditary forms of hyperuricaemia. They include particularly disorders leading to hyperuricaemia due to urate overproduction (phosphoribosylpyrophosphate synthetase superactivity, Lesch-Nyhan syndrome, Kelley-Seegmiller syndrome) and due to urate underexcretion in the kidneys.

This work was focused on the latter disorders represented by familial juvenile hyperuricaemic nephropathy and nephronophthisis-medullary cystic kidney disease complex.

The introduction describes the history of identification of those disorders and presents in chronological order knowledge gathered on clinical presentation and genetic dissection of hereditary nephropathies associated with hyperuricaemia and gout up to 2001 when I started to work on this subject.

1.1 Familial juvenile hyperuricaemic nephropathy (FJHN, OMIM 162000)

In 1960, Duncan and Dixon described a family with hyperuricaemia, gout and renal insufficiency [2]. The patient was 19 years old man suffering from acute gouty arthritis, hyperuricaemia, hypertension and severe renal failure. Both his kidneys were abnormally small. All his seven first-degree relatives had hyperuricaemia and five of them had renal failure. Since then, more than 50 kindreds of various ethnic origin - Whites [3-14], Japanese [15-17], Chinese [18], Polynesian [19], Chilean [20] - had been described in the literature by 2001.

The disorder is inherited in consecutive generations. Both males and females are equally affected. The condition is transmitted from father to son and about half of the offspring is affected. This suggested autosomal dominant (AD) inheritance with high penetrance.

Clinical presentation

Hyperuricaemia, resulting from reduced urate excretion, is usually diagnosed in childhood, adolescence or early adult life but cases presenting later have also been observed. Disease progresses to gouty arthritis and renal insufficiency in second decade of life. The renal

insufficiency progresses further to renal failure between 20^{th} and 40^{th} year of life and affected individuals end up on dialysis and require renal transplantation in third to fourth decade of life.

Isolated attack of gout in one or more family members is an important factor drawing attention to kindreds being until then diagnosed as familial nephritis or familial renal disease [7, 21]. However, gout is not constant feature of the condition [7, 21], which is therefore meant to have been missed and underdiagnosed in the past. For the same reason, gout in clinical description of "familial nephropathy with gout" or "familial juvenile gouty nephropathy", having been used in the past, is preferentially replaced by "hyperuricaemia" or "hyperuricaemic nephropathy" as more appropriate terms. The majority of patients are normotensive, although hypertension may be found in later stages of renal disease and conversely accelerates the progression of chronic renal failure.

Biochemistry

There are two biochemical hallmarks of FJHN: i) hyperuricaemia disproportionate to age, sex or degree of renal involvement, ii) markedly decreased fractional excretion of urate (FE_{ur} = (urate clearance/creatinine clearance)*100). The mean FE_{ur} in FJHN 5.1% is equally low in young men, women and children [22]. However, as low as 1% FE_{ur} were reported, whereas normal values range from 7% to 12%. Even more obvious discrepancy can be seen in children, in which normal values ranges from 12% to 30% [23]. Important thing with respect to the pathogenesis of the disease is that the low FE_{ur} precedes all other symptoms in apparently normal, though affected individuals [22, 24]. Proteinuria is minimal or absent in FJHN patients as are abnormalities of urinary sediment. Microscopic haematuria may be present. In differential diagnosis, there are taken into account mainly hypoxanthine-guanine phosphoribosyl transferase (HGPRT) deficiency and phosphoribosyl pyrophosphate synthetase (PRPS) superactivity in erythrocytes.

Pathology

Renal manifestation of FJHN has features of non-specific interstitial nephropathy. The kidneys show interstitial fibrosis associated with infiltration of lymphocytes and histiocytes, focal atrophy of distal tubules, thickening and sometimes reduplication of basal membranes in distal tubules and collecting ducts and partial glomerular sclerosis [22, 25-27]. Crystals of urate were detected only in fraction of examined biopsies, which however could be caused by unsuitable sample fixation [27] or by their reabsorption [26].

Management and treatment of clinical and biochemical symptoms

Approaches to management of FJHN were and still remain a subject of heated discussions. Using of xanthine oxidase inhibitor allopurinol to reduce hyperuricaemia and to slow down the progression of renal disease remains controversial. Its beneficial effect was emphasised in several studies [22, 24, 27] but disputed in other [7, 28, 29].

The control of high blood pressure, if present, is generally meant to be a prerequisite for successful treatment.

More efficient approach to treatment may be the combination of allopurinol to reduce renal urate load and benzbromarone or probenecid to block tubular anion exchanger and thus restoring FE_{ur} towards normal, provided that the decreased uric acid excretion is caused by gain-of-function mutation in proximal tubule (PT) anion exchanger [11, 30]. Others suggested that blockade of renin-angiotensin system in patients with early stage nephropathy may delay the progression of renal insufficiency [31, 32].

Pathogenesis

The pathogenesis of FJHN was not clear. Decreased FE_{ur} can be proven in FJHN patients before any renal malfunctions occur, suggesting a primary defect in urate handling [22, 24]. A gain-of-function mutation of the luminal urate/anion exchanger would be consistent with decreased FE_{ur}, dominant inheritance and PT epithelial cells apoptosis, hypothetically caused by increased transcellular flux of urate [11]. Possible candidate could have been human urate transporter hUAT, localised to chromosome 17p [33], or another not fully characterised anion exchanger [34]. Alternatively, hyperuricaemia induced in rat model by uricase inhibition was shown to cause hypertension and renal fibrosis by a crystal-independent mechanism [35], further suggesting primary role of urate in the renal damage. On the contrary, others suggested uric acid underexcretion and hyperuricaemia to be a consequence of primary impairment of renal hemodynamics [7, 36]. This was observed not only in patients from five kindreds, but also in obligate carriers in preclinical status [37]. This hypothesis was further supported by ultrasound imaging and colour Doppler studies in FJHN patients showing renal vasoconstriction [38]. Another proposal was that the abnormal urate handling in this condition is a result of primary renal disease consisting in abnormal nephronogenesis due to a defect in G protein-coupled receptor [12].

1.2 Complex Nephronophthisis-Medullary Cystic Kidney Disease (NPH-MCKD, OMIM 174000, 603860, 256100, 602088, 604387)

MCKD

Medullary cystic kidney disease was first described by Thorn et al. in 1944 as "salt-loosing nephritis" [39], although some authors state that it were Smith and Graham in 1945 who reported first case [40]. They used the term "congenital medullary cystic disease of the kidney" in relation to 8-years-old girl suffering from severe anaemia, hyposthenuria and uraemia. Since then, there had been reported further cases and families presenting with renal failure, medullary cysts, anaemia and salt loss [41-46]. It is a rare disorder. By 2001, MCKD had been described in more than 50 families mainly from Europe and North America [47].

NPH

In 1951, Fanconi et al. recognised very similar familial renal disease affecting children 4-14 years old characterised by renal insufficiency, anaemia, polyuria, hyposthenuria and tubulointerstitial involvement [48]. Medullary cysts were also present, although not mentioned in the article [47]. The condition was designated nephronophthisis (NPH) by the authors. It was recognised early that NPH and MCKD share several clinical (polyuria, polydipsia, anaemia), pathological (cysts primarily located at the cortico-medullary border) and histological (tubular atrophy, interstitial fibrosis, cell infiltration) features.

NPH-MCKD

In the 1960s, inability to clearly distinguish both entities and confused diagnoses lead to proposal of the term NPH-MCKD complex and several studies tried to prove the identity of the two disorders [44, 49-51]. Further decades, however, have also shown differences, namely mode of inheritance (autosomal recessive in NPH versus autosomal dominant in MCKD), age of onset of clinical symptoms and progression to end-stage renal disease (ESRD; usually childhood or adolescence in NPH and adulthood in MCKD) and extrarenal organ involvement (tapeto-retinal degeneration in NPH and hyperuricaemia with or without gout in MCKD).

Distinction of these two entities had become more obvious through the identification of underlying genetic loci by linkage analyses. NPH, at present referred to as NPHP, had been linked to three loci by 2001, namely 2q13 (NPHP1) [52, 53], 9q22 (NPHP2) [54] and 3q21 (NPHP3) [55], while MCKD had been mapped to different loci (see later). Mutations in *NPHP1* gene encoding for nephrocystin were found causative in case of NPHP1 [56, 57]. Additional loci and underlying genes in NPHP were identified later (see Results and Discussion).

Clinical presentation and biochemistry of MCKD

Reduced urine concentrating ability with salt wasting, preceding decreased glomerular filtration rate (GFR), can be the only finding early in the course. Proteinuria is absent or

minimal, urinary sediment is non-specific. When urine-concentrating ability decreases substantially, polyuria usually accompanied by polydipsia appears in early or later adulthood (average 28 years). It is usually in this stage the affected individuals are diagnosed. Following anaemia, metabolic acidosis and uraemia are related to progressive renal insufficiency. Hypertension is usual and often precocious, despite the presence of polyuria. The renal insufficiency usually slowly progresses to ESRD in the third to fifth decade of life and affected individuals end up on dialysis and require renal transplantation [58].

It is of note that there were described families, in which onset of clinical symptoms was in childhood or adolescence [43, 59] as well as occurrence of juvenile and adult form within one family [50]. These findings decrease the value of age of onset for differential diagnosis in the eyes of some authors [47].

Pathology of MCKD

Histological findings such as diffuse tubulointerstitial nephritis, thickened tubular basement membranes, focal tubular atrophy, interstitial fibrosis and inflammatory cells infiltration are typical. Tubular dilation is present and formation of cysts at the cortico-medullary border and/or in the medulla may be seen (in contrast to FJHN). The kidneys, overall, are small and echogenic.

Management and treatment of clinical and biochemical symptoms in MCKD

There were no specific therapeutic approaches to MCKD. Before the development of ESRD, the control of water and electrolyte imbalance and later, when ESRD breaks out, dialysis followed by kidney transplantation are applied.

Pathogenesis of MCKD

The pathogenesis of MCKD had been unclear. Without the knowledge of causative genes, it had been impossible to speculate about observed clinical and pathological features. It was observed that the condition never occurred again after kidneys transplantation. This suggested kidney restricted involvement.

MCKD and FJHN

Besides renal involvement, hyperuricaemia with or without gout had been observed in portion of MCKD families. In 1978 for example, Thomson et al. described a family clinically resembling FJHN but medullary cysts were also present [60]. Hyperuricaemia and gouty arthritis occurred at late adolescence and preceded renal failure. Similar condition, complicated by epilepsy, was reported by Burke et al. in 1982 [61]. Since then, more MCKD families with

hyperuricaemia and/without gout had been reported [12, 59, 62] but also MCKD families in which portion of affected members showed hyperuricaemia but did not have cysts, resembling thus FJHN phenotype [62, 63]. Unfortunately, only little data were available on FE_{ur} in MCKD patients [64] and none from affected patients in pre-symptomatic period.

As can be seen, there were recognised remarkable similarities in phenotype between FJHN and MCKD associated with hyperuricaemia with or without gout. Together with advances in molecular genetics of the two disorders, their relationship and molecular bases had become clearer.

1.3 Molecular genetics of MCKD/FJHN

MCKD

The first genetic linkage to chromosome 1q21 found Christodoulou et al. in two large Cypriot MCKD families in 1998 [62]. MCKD in those families was associated with hyperuricaemia, gout and late onset of ESRD (means 62.2 and 51.5 years).

One year later, Scolari et al. found linkage to another locus on chromosome 16p12 in large Italian family with MCKD associated with hyperuricaemia and gouty arthritis [63]. In all families was previously excluded linkage to NPHP1 locus on chromosome 2q13. These observations lead to differentiation of MCKD to two variants: (AD)MCKD1 with the linkage to chromosome 1q21 and (AD)MCKD2 with the linkage to chromosome 16q12.

Further linkage studies in MCKD families revealed two important points: i) further genetic heterogeneity of the disease and ii) no concordance of phenotype with identified locus. Kroiss et al. excluded genetic linkage to both MCKD1 and MCKD2 loci in five MCKD families with the absence of hyperuricaemia and gout [65]. Both loci were excluded from linkage also in one of six Finnish families reported by Auranen et al. [17]. This single family presented hyperuricaemia, while remaining five families, mapped to chromosome 1q21, did not. Interestingly, Parvari et al. proved linkage to MCKD1 locus in large family of Jewish origin, clinically characterised by hypertension and progressive renal insufficiency. No polyuria, anaemia, gout, haematuria or proteinuria was observed. Renal histology showed extensive tubulointerstitial fibrosis and global glomerulosclerosis [66]. This study further broadened the spectrum of clinical presentations linked to 1q21 locus. Finally, Hateboer et al. reported linkage to MCKD2 locus in large Welsh MCKD family, which however did not present hyperuricaemia or gout [67]. This indicated that these clinical features are not invariably related to MCKD2 mutations.

FJHN

In 2000, Kamatani et al. performed genome-wide linkage analysis in a large Japanese family with FJHN to find locus segregating with the disease [68]. The family transmitting gouty arthritis, renal failure and hypertension in autosomal dominant mode was originally described by Yokota et al. in 1991 [28]. Kamatani et al. at first found linkage to chromosome 16p and using additional 12 polymorphic markers they delimited candidate interval of 9 cM in the 16p12 region. In the same year, Stibůrková et al. reported linkage to 16p11.2 in two of three Czech FJHN families presenting with hyperuricaemia, decreased FE_{ur}, gouty arthritis and renal insufficiency [10]. This study also provided other important results: i) genetic heterogeneity of FJHN and ii) variable penetrance of the disease. In further study, Dahan et al. confirmed linkage to 16p12 locus in large Belgian family [12] and among others promoted hypothesis that FJHN and MCKD2 are in fact allelic disorders. However, alternate hypothesis of two disease genes in close proximity could not be excluded as well. Solution of this situation was possible only through the identification of responsible gene(s) in 16p12 locus.

2 AIMS OF THE STUDY

The main goal of this thesis has been to contribute to understanding of FJHN and other inherited diseases presenting with familial occurrence of hyperuricaemia, gouty arthritis and progressive kidney failure at an early age. We have been especially interested in molecular bases and mechanisms underlying these disorders. The project was based on the following strategy:

1. Continuous collection and characterization of FJHN/MCKD patients and families.
2. Identification of disease causing genes in affected families by positional cloning approaches.
3. Characterisation of the identified proteins and their mutated forms by standard molecular biology methods and evaluation of mechanisms involved in the disease pathogenesis.
4. Isolation and characterisation of interacting partners of newly identified proteins as a parallel approach to the positional cloning in definition of potential candidate disease causing genes and disease related pathways.

3 RESULTS AND DISCUSSION

During last years, considerable achievements have been reached in molecular characterisation of inherited kidney diseases. Characterisation of nephronophthisis and its distinction from MCKD has been evidenced by identification of further NPHP loci and

underlying genes. So far, six NPHP genes have been identified [56, 69-74] and there is evidence of further genetic heterogeneity [75]. At the same time, common pathogenesis of NPHP and polycystic kidney disease (PKD) involving cilium/centrosome pathology has been revealed [70, 76, 77].

A couple of years ago, MCKD and FJHN were partially genetically characterised and their close relationship came out [10, 12, 63]. The following section describes and discusses results obtained in our four partially overlapping projects addressing strategic concepts outlined in previous chapter. Results are presented with respect to four published manuscripts, one manuscript prepared for the publication and one unpublished work. Each part is structured in introduction, specific methods, results and their discussion. Unless otherwise stated, water mentioned in specific methods sections was ultrapure water prepared from common distilled water in Milli-Q® RG Ultrapure Water Purification System (Millipore).

3.1 Collection and characterisation of additional FJHN/MCKD patients and families (2001-2003) -

European Journal of Human Genetics **11**(2): p. 145-154, 2003

3.1.1 Introduction

In the situation described in chapter 1.3, we had the opportunity to obtain biological samples from additional FJHN/MCKD families from abroad to perform further molecular genetic analyses. We collected samples from members of 15 families coming mainly from the United Kingdom and also from Spain and Belgium. Thus we were driven into the international race of finding the first gene responsible for FJHN/MCKD, in which participated in addition to countries mentioned also the USA, Japan, Germany and Italy. In question, there was mainly the ability of presymptomatic detection of the disease, related helpfulness of allopurinol for the therapy in increasing number of families and allelism of FJHN and MCKD2.

3.1.2 Specific methods

Bioinformatics

Information on gene organisation and DNA sequences of exons, introns and gene promotors were obtained from The Entrez Nucleotide database (http://www.ncbi.nlm.nih.gov/sites/entrez?db=nuccore) and The UCSC Genome Browser database using BLASTN tool (http://blast.ncbi.nlm.nih.gov/Blast.cgi) for pairwise alignment of nucleotide sequences. Results of sequencing were confronted with the UniGene database

(http://www.ncbi.nlm.nih.gov/sites/entrez?db=unigene) and the Entrez SNP database (http://www.ncbi.nlm.nih.gov/sites/entrez?db=snp).

Primer design

Polymerase chain reaction (PCR) and sequencing primers were designed on retrieved sequences by Oligo 6.44 software (Molecular Biology Insights) in automatic mode with high stringency and filtration of frequent 6-mers of human and primate origin. Where automatic approach failed, primers were designed by hand following the recommendation of higher internal stability (ΔG) at the 5´ end or in the middle of the primer and relatively lower internal stability at the 3´ end of the primer.

Other used methods are described in General methods section, chapters 5.4 - 5.7.

3.1.3 Results and discussion

Following the work of Stibůrková et al. [10], we performed linkage analysis to previously identified locus on chromosome 16p12 in 15 families consistent with FJHN diagnosis [78]. We were able to prove linkage in six families. In two families, linkage was excluded based on logarithm of odds (LOD) score ≤ -2 criterion. In the rest of families, negative LOD scores but not reaching the -2 threshold or inconsistency of segregating haplotypes with linkage was detected. Haplotype analysis was used in this work as an alternative approach for determination of linkage rate in the group of studied families. This was shown to be 0.4 (6/15) compared to value of parameter $\alpha = 0.374$ maximizing the LOD score in linkage analysis. We were therefore able to estimate that between 37% and 40% of FJHN cases from our cohort could be explained by linkage to 16p11.2. Haplotype analysis also showed that there was no common haplotype or allele segregating with the disease that would be shared across families. This suggested either independent mutational events or one ancestral but ancient mutation.

Compilation of our haplotyping data with similar data from other studies in both FJHN and MCKD2 kindreds [10, 12, 63, 67, 68] suggested possible existence of two non-overlapping candidate regions in close proximity on chromosome 16p. Similar conclusion (without our data) was at the same time presented by Scolari et al [47]. It brought further confusion to understanding the genetic bases of FJHN and its relationship to MCKD2. Providing genetic distinctness of FJHN and MCKD2, there were possible up to three disease genes. Providing FJHN and MCKD2 allelism, two loci still came into consideration.

To evaluate genetic content and make possible the assessment of candidate genes, we constructed integrated genetic, physical and transcript map of 16p chromosome region comprising both critical intervals. Compilation of four genomic contigs and three gap-closing bacterial artificial chromosome (BAC) clones provided contiguous sequence of 7.5 mega-base pairs (Mbp) harbouring, according to NCBI annotation that time, 45 genes and 129 gene-like sequences. Taking the multilocus hypothesis into account, we selected seven candidate genes involved in G-protein signalling, regulated protein degradation, thyroid hormone homeostasis and hypertension for sequence analysis. Kidney specific *UMOD* (encoding Tamm-Horsfall protein, or uromodulin) and *ACSM3* (encoding acyl-CoA synthetase medium-chain family member 3) genes, proposed as promising candidates by Scolari et al. in 1999 [63] were not analysed by us as the sequence analysis performed by Pirulli et al. in 2001 in single MCKD2 family showed no mutations [79]. In all of the seven candidate genes analysed by us, no classic deleterious mutations were found within promoter region, exon/intron junctions and coding sequences.

Identification and characterisation of UMOD as a disease-causing gene

At the time of acceptance of our manuscript (end of the year 2002), Hart et al. came out with work in which they clearly described mutations in the *UMOD* gene (OMIM 191845), encoding for uromodulin, in two FJHN families as well as in one MCKD2 family, proving thus allelism of both disorders [80]. Thus the USA actually won the international race mentioned in chapter 3.1.1.

Based on their findings, authors suggested using the term "uromodulin-associated kidney disease" (UAKD) for both FJHN and MCKD2 for the sake of clarity. Some researchers, including us, currently prefer this term [80-82], while others prefer the term "uromodulin storage diseases" [83, 84] (see later).

It is of note, that the obvious contradiction with data of Pirulli et al. [79] (see above) was resolved after they revised their data and identified the *UMOD* mutation as well [85].

Another gene in single FJHN family with atypical clinical presentation

Interestingly, another research group studied one of our families in parallel. Onset of the diabetes type 2 in this family, originally described by Calabrese et al. in 1990 [86], led the group to the identification of the mutation in *HNF-1β* gene located on chromosome 17q21.3. This finding was also published at the time our publication was coming out [87]. Clinical features in affected members included renal cysts, renal development abnormalities and diabetes. *HNF-1β* gene has been previously associated with "renal cysts and diabetes syndrome" (OMIM 137920),

the disorder comprising i) nondiabetic renal disease resulting from abnormal renal development and ii) disorder consistent with a diagnosis of maturity-onset diabetes of the young (MODY) [88, 89].

Uromodulin

A mucoprotein was isolated by salt precipitation from human urine in 1950 by Tamm and Horsfall as a potent inhibitor of virus-mediated haemagglutination [90]. Same authors characterised the protein chemically two years later [91]. Gottschalk and Odin showed that about 30% of molecular weight (MW) of the protein, called from now on Tamm-Horsfall protein (THP), is formed by glycans with a high sialic acid content [92, 93]. A study of THP complexes with influenza virions by electron microscopy (EM) showed that the protein aggregates to fibrils with a diameter of 4-24 nm, further creating filamentous network [94]. Similar observations were made much later, in 1987 by Wiggins who studied THP aggregation under various conditions [95], and by Jovine et al. in 2002 [96]. The protein was further characterised by series of studies in 1970s [97-101]. They showed that uromodulin runs in SDS-PAGE as a single band with MW of 80-90 kDa, is the most abundant protein in normal urine being excreted at the rate of about 50 mg/day and is present in urine of other mammals.

Interestingly, Muchmore and Decker reported in 1985 isolation of uromodulin, a glycoprotein with immunosuppressive properties *in vitro*, from urine of pregnant women. This protein has been studied independently [102-106], until Pennica et al. proved the identity of uromodulin and THP based on complementary DNA (cDNA) analysis [107]. In the following text, the name uromodulin (UMOD) will be used for this protein.

Since its discovery in 1950, uromodulin was extensively studied and hundreds of articles addressing its biochemistry, physicochemical properties, purification, determination, detection, biology, clinical relevance, and genetics have been reported. Its role has been assessed in defence against urinary tract infection (UTI) [108-110], cast nephropathy [111-115], urolithiasis [116-120], tubulointerstitial nephritis [121-125] and recently also in UAKD (see above). Uromodulin urinary excretion in various pathological conditions including nephropathy has also been evaluated [126-131]. Despite this extensive research, physiological role of uromodulin remains unclear. Although its various potential roles were studied *in vitro*, due to its occurrence restricted to urinary tract and parts of nephron *in vivo* (see later), only some of them come to question.

Uromodulin precursor is composed of 640 amino acids (AA), based on cDNA analysis [107]. 48 of them are cysteine residues, all probably involved in disulfide bonds [97, 132]. Motifs identified in uromodulin structure include signal peptide (residues 1-24), three calcium-

binding epidermal growth factor (cbEGF) domains (residues 31-64, 65-107 and 108-149), zona pellucida (ZP) domain (residues 334-585), the glycosyl phosphatidylinositol (GPI) attachment site (residue 614) and eight potential N-glycosylation sites (http://smart.embl.de/smart/show_motifs.pl?ID=P07911). There is a debate about the region between third cbEGF domain and ZP domain (residues 150-333). Although similarity searches showed no resemblance to any of known protein domains, some researches state that there is possibly a fourth EGF domain spanning residues 281-336 [83, 133, 134], or residues 297-335 [135]. Meanwhile, Yang et al. reported in the debated region a new domain, spanning residues 199-287, named D8C (Figure 3.1), that is in common to a new family of proteins including liver-specific ZP domain-containing protein (LZP), glycoprotein 2 (GP2), UMOD and several other uncharacterised proteins [136].

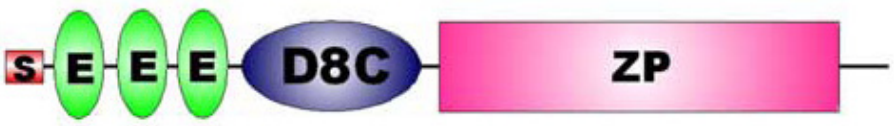

Figure 3.1 Domain structure of uromodulin. S - signal peptide, D8C - D8C domain, E - EGF domain, ZP - zona pellucida domain. Acquired from [136].

UMOD gene is located in cytogenetic band p12.3 on chromosome 16 according to Ensembl (http://www.ensembl.org/Homo_sapiens/geneview?db=core;gene=ENSG00000169344), UCSC (http://genome.ucsc.edu/cgi-bin/hgTracks?db=hg18&acembly=full&hgt.out1=1.5x&est=dense&position=chr16:20271538-20251874) and Entrez gene (http://www.ncbi.nlm.nih.gov/entrez/query.fcgi?db=gene&cmd=Retrieve&dopt=full_report&list_uids=7369) databases while in band 16p13.11 according to HGNC (http://www.gene.ucl.ac.uk/nomenclature/data/get_data.php?hgnc_id=12559) and Geneatlas (http://www.dsi.univ-paris5.fr/genatlas/fiche.php?n=825) databases. It spans 19.66 kilo-base pairs (kbp) of genomic sequence on minus strand (http://www.ncbi.nlm.nih.gov/entrez/viewer.fcgi?val=NC_000016.8&from=20251874&to=20271538&strand=2&dopt=gb). Two major transcripts encoding the full-length protein were observed. They differ in 5' untranslated region (UTR) (Figure 3.2).

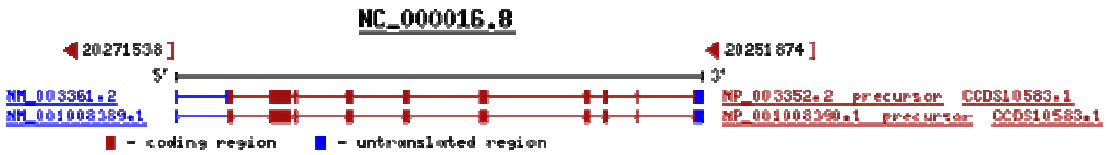

Figure 3.2 *UMOD* gene organisation. Two organisations representing two major transcripts are given. On top, there is the accession number of *UMOD* genomic sequence. Numbered arrows indicate the position of the gene on the sequence of chromosome 16 and its orientation. On the left side, GenBank accession numbers of two major mRNAs are given. On the right side, accession numbers of corresponding protein sequences and consensus coding sequences are given. Acquired from Entrez Gene database (http://www.ncbi.nlm.nih.gov/entrez/query.fcgi?db=gene&cmd=Retrieve&dopt=full_report&list_uids=7369).

UMOD is expressed solely in the kidney [107] (http://symatlas.gnf.org/SymAtlas), namely in epithelial cells of the thick ascending limb of the loop of Henle (TALH) and early distal convoluted tubule (DCT), as showed by immunofluorescence and immunohistochemical studies [137-139]. During biosynthesis, uromodulin enters the endoplasmic reticulum (ER) and signal peptide is cleaved. In the ER, GPI anchor replacing C-terminal sequence is added probably to serine 614, disulfide bridges are formed and glycans are synthesised on seven of eight potential N-glycosylation sites [140, 141]. N-glycans are further trimmed in Golgi apparatus. Both glycans and GPI anchor act as a sorting signal for transport of the protein to the apical membrane of epithelial cells, where anchorage by means of GPI takes place [142, 143]. Uromodulin urinary excretion results from proteolytic cleavage at the site 66 residues upstream of GPI attachment site [144]. Overall, uromodulin found in urine is by 166 AA shorter than the precursor.

The knowledge of the occurrence of uromodulin in TAL and subsequently in downstream parts of nephron and the whole urinary tract together with *in vitro* experiments raised the discussion about its role *in vivo*. The ability to bind uropathogenic strains of *E. coli* and abundance in urine predetermines uromodulin to be an effective agent in preventing adhesion of bacteria to glycoproteins and glycolipids at luminal plasma membrane. Its tendency to form large polymers in urine seems to favour this role by forming polyvalent ligand with high affinity [110, 145]. Involvement of uromodulin in urinary stone formation has been extensively studied and several studies showed its inhibitory effect on both calcium oxalate [146-148] and hydroxyapatite [149] crystals aggregation and growth. Among other polyanionic macromolecules present in urine, it may potentially act as substantial inhibitor of calcium crystallization in tubular fluid. Finally, specific localisation of uromodulin on luminal plasma membrane of TAL cells led to suggestion that it could take part in ion transport and maintaining

of counter current gradient in interstitium by formation of the water barrier in this segment of nephron.

3.2 UMOD mutations in our cohort and their characterisation - Kidney International **70**(6): p. 1155-1169, 2006

3.2.1 Introduction

After identification of *UMOD* as the first gene underlying FJHN and MCKD2, we focused on its analysis with respect to our cohort, comprising that time 19 families. They came from our previous studies [10, 78] or were obtained from abroad but also several Czech families were newly recognised, while we quit working on Spanish families in the meantime [78].

First, we were aimed at identification of *UMOD* mutations in out cohort and determination of true linkage rate and, second, at examination of the impact of these mutations on urinary UMOD excretion and on its processing in the kidney. Third, to be able to define and evaluate potential mechanisms involved in the disease pathogenesis, we intended to analyse affected tissues and to express and characterise identified mutations on cellular level in cell culture models.

3.2.2 Specific methods

3.2.2.1 Urine uromodulin and biochemical analyses

Urine biochemical analysis

Urine total protein, creatinine, uric acid, magnesium, calcium, and phosphate were determined in random spot urine samples stored at -80°C by the Protein (urine) (BioSystems), CREA (Roche), UA Plus (Roche), Mg (Roche), Ca (Roche), and PHOS (Roche) kits, respectively, on a Hitachi Modular analyser (Roche). Sodium, potassium, and chloride were determined by ion-selective electrodes. Osmolality was determined by freezing point method using FISKE 2400 osmometer (Advanced Instruments-Fiske Associates).

All these analyses were performed by Květa Pelinková, M.Sc. at the Institute of Clinical Biochemistry and Laboratory Diagnostics of General University Hospital and First Faculty of Medicine of Charles University in Prague.

Uromodulin enzyme-linked immunosorbent assay (ELISA)

Buffers and solutions:

TEA buffer: 0.5% (v/v) Triton X-100, 0.02 M EDTA, pH 7.5 adjusted by 1 M NaOH (OP-274 pH/Ion Analyser, Radelkis) [150].

PBS: see chapter 5.3.

Blocking buffer (PBS/2%BSA): 2% (w/v) BSA dissolved in PBS.

Washing buffer (PBS-T): see chapter 5.3.

Detection solution: 0.09% (w/v) *o*-phenylenediamine (OPD) and 0.03% (v/v) H_2O_2 dissolved/diluted in PBS.

Stop solution: 2 M H_2SO_4.

For quantitative analysis of urinary uromodulin, we established sandwich ELISA with mouse monoclonal anti-THP antibody (Cedarlane) as capture antibody, rabbit polyclonal anti-THP antibody (Biogenesis) as detecting antibody and HRP-linked goat anti-rabbit IgG (Pierce) as secondary antibody.

Wells of F96 Maxisorp immuno-plate (Nunc) were coated by monoclonal anti-THP antibody by incubation with 100 μL of antibody dilution (1:9000 in PBS) overnight at 4°C. Following day, wells were washed three times by PBS-T with short horizontal shaking in between washes (ELx50™ Microplate Strip Washer, BioTek). Wells were then blocked by 100 μL of Blocking buffer one hour at room temperature (RT). Following washing three times by PBS-T with shaking, urine samples diluted 1:250 in TEA buffer, calibration curve solutions and blanks were incubated in wells one hour at RT (100 μL per well). Calibration curve TEA solutions were prepared by serial dilution of uromodulin isolated from healthy male urine. Concentrations of 0 ng/mL, 1 ng/mL, 10 ng/mL, 50 ng/mL, 100 ng/mL, 140 ng/mL and 160ng/mL were used. Following washing three times by PBS-T with shaking, polyclonal anti-THP antibody diluted 1:5000 in PBS was added to wells (100 μL per well) and incubated one hour at RT. After washing three times by PBS-T with shaking, secondary HRP-conjugated antibody, diluted 1:10000 in PBS was added to wells (100 μL per well) and incubated one hour at RT. After final washing three times by PBS-T with shaking, 100 μL of detection solution was added to each well and the plate was put in the dark. After colour development, HRP reaction was stopped by 50 μL of the Stop solution. Plate was then analysed in automatic Spectra ELISA reader (SLT) at 492 nm with 620 nm filter and absorbance data were processed by KimW software (Schoeller Pharma).

Urinary sediment preparation

For qualitative analysis of uromodulin in urinary sediment, 35 µL of total urine was centrifuged at 5000g/10 minutes, supernatant was discarded, the pellet was resuspended in 1X SDS-PAGE sample buffer and analysed by SDS-PAGE followed by Sypro Ruby (Molecular Probes) staining or WB analysis.

Urine concentration

If concentrated for SDS-PAGE and/or WB analysis, 250 µL of total urine was loaded on Microcon YM-30 filter (Millipore) and 1.5 mL tube assembly and centrifuged at 12000g until volume on the filter reached less then about 50 µL. Ultrafiltrate was discarded and retentate was recovered to a new tube at 10000g. Aliquot equivalent to 10 µg of total protein (based on total urinary protein determination) was mixed with SDS-PAGE sample buffer, denatured at 100°C/5 minutes (Dri-Block DB-3 thermostat, Techne) and analysed by SDS-PAGE followed by Sypro Ruby (Molecular Probes) staining or WB analysis.

3.2.2.2 Recombinant uromodulin analysis

Cultured cells lysis

Cells were harvested to PBS into 1.5 mL tubes, pelleted by centrifugation at 800g/5 minutes and washed twice in PBS. The pellet was then resuspended in PBS with 1% (v/v) protease inhibitor cocktail (PIC) (Sigma) and sonicated twice for 30 seconds at output of 50% in the cuphorn filled with mixture of ice and water and connected to Ultrasonic Homogeniser (4710 series, Cole-Parmer Instrument Co). The suspension was then centrifuged at 14000g/5 minutes at 4°C to remove cell debris. The supernatant was collected to a new tube and analysed, or stored at -20°C.

Uromodulin deglycosylation

For analysis of glycosylation patterns of wildtype and mutant uromodulins expressed in cell cultures, we used GlycoPro™ Enzymatic Deglycosylation Kit (ProZyme) according to manufacturer's instructions. Briefly, cell lysate was mixed with 5X Reaction buffer (kit component) and Denaturation buffer (kit component) in 0.2 mL tubes (Eppendorf). Reaction mix was then denatured at 100°C/5 minutes in the thermal cycler (PTC-225 DNA Engine Tetrad, MJ Research), let cool down to RT and Detergent solution (kit component) was added. Glycosidases N-glycanase® PNGase F, Sialidase A™ or O-Glycanase® (kit components) or their combinations were added to reaction mix and incubated at 37°C/3 hours in biological thermostat

(BT 120 M, Ekom). Reactions were then mixed with 6X SDS-PAGE sample buffer, denatured at 100°C/5 minutes in the thermal cycler and analysed by SDS-PAGE and WB.

Antibodies fluorescein labelling

For fluorescent automated cell sorting (FACS) analysis, we conjugated polyclonal anti-THP antibody (Biogenesis) with fluorescein by Fluorescein Protein Labelling Kit (Roche) according to manufacturer's instructions. Briefly, 20 mg/mL FLUOS reagent [5(6)-carboxyfluorescein-N-hydroxysuccinimide ester] solution was prepared by dissolution of lyophilised reagent in dimethyl sulfoxide (DMSO). 1 mg of polyclonal antibody was dissolved in 1 mL of PBS (kit component) and 7.9 μL of FLUOS solution was added. Reaction mix was incubated at RT protected from light during gentle stirring in rotamixer (Multi RS-60, Biosan). Meanwhile, Sephadex G-25 column (kit component) was blocked by Blocking reagent (kit component) and rinsed by PBS several times. Reaction mix was then applied onto the column to remove non-reacted FLUOS. Labelled antibody was eluted from the column by PBS and fractions of about 0.5 mL were collected. The amount of antibody in individual fractions and labelling yield were calculated based on extinctions at 280 nm (protein) and 495 nm (fluorescein) measured by means of photometer (UV/VIS Spectrometer UV4-100, Unicam Ltd.) and applying the equation provided by the manufacturer.

Other used methods are described in General methods section, chapters 5.1 - 5.3.

3.2.3 Results and discussion

In this work, we completed molecular genetic examination of altogether 19 families [151]. In summary, we performed linkage analysis in all families to all known FJHN/MCKD loci, and analysed the *UMOD* genomic sequence. We found the genetic linkage to the *UMOD* candidate locus on chromosome 16p12 in nine families and excluded this linkage in three families based on LOD ≤ -2 criterion. In the rest of families, no haplotypes consistent with the linkage to any of currently known FJHN/MCKD loci were detected.

UMOD gene sequence analysis revealed missense mutations in six of nine families linked to 16p12 locus. In remaining three families, in addition to coding sequence, 5.7 kbp of *UMOD* promoter region was analysed. Here, several family-specific nucleotide changes were identified in two of these families, but their potential pathogenic effect was not further investigated.

Of six missense mutations identified, three were reported previously and three were novel. To examine their functional consequences, we transiently transfected tissue culture cells by wildtype and all six mutant cDNA constructs. By time-course FACS experiments, we investigated the dynamics of the amount of uromodulin expressed on plasma membrane. All mutant proteins had decreased ability to reach the plasma membrane but to a different extent. Accordingly, it was possible to distinguish two separate groups of mutants, one with pattern similar to wildtype protein but still lower exposition on plasma membrane (group I) and second (group II) with even lower ability to reach the plasma membrane as compared to both wildtype and group I proteins.

We then performed biochemical characterization of all transiently expressed mutant proteins by deglycosylation and WB. Wildtype protein was detected on WBs of cultured cells lysates in two separate zones obviously composed of several not properly resolved bands, probably representing different degrees of glycans processing. This pattern was observed also in other studies [140, 152-154]. It was also shown that lower MW zone represents ER precursor lacking branched sialic acid chains added as late as in Golgi apparatus [152, 154], while higher MW zone represents properly glycosylated, GPI modified and membrane anchored uromodulin. The precursor probably accumulates in transient cultures due to protein overexpression as we observed only negligible amounts of it in lysate of wildtype uromodulin stable cell line. All group I mutants showed similar level of fully processed protein as the wildtype on WB. On the other hand, group II mutants showed low amounts of fully processed protein. Regarding precursor form, one group I mutant and all group II mutants manifested zone of somewhat lower molecular weight compared to wildtype and other group I mutants.

Complete deglycosylation of all expressed proteins followed by WB produced double band of about 30% lower MW compared to untreated proteins in case of wildtype and group I mutants. Observed polypeptides most probably represented uromodulin precursor (higher MW) and the precursor after C-terminus cleavage and GPI anchor attachment (lower MW). Incomplete processing might be again ascribed to protein overexpression [155, 156]. On the contrary, no GPI processing could be observed in group II mutants and it was also less evident in one group I mutant. These results were in good agreement with the experiment in which were HeLa cells expressing uromodulin treated by the inhibitor of GPI synthesis [153].

Sialic acid specific deglycosylation of mutant proteins resulted in three different patterns. Two group I mutants produced, likewise the wildtype protein, single zone corresponding to the ER precursor, while other mutants produced additional zone of two different lower MWs. This suggested that polypeptides not properly glycosylated in the ER reached the Golgi apparatus where sialic acid modification takes place.

Immunofluorescence analysis of all transiently expressed proteins showed plasma membrane localisation and almost no detectable intracellular retention of wildtype protein while all mutant proteins exhibited granular retention in the ER. It was, however, less apparent in group I mutants. Group I mutants also showed considerable plasma membrane display contrary to group II mutants that showed almost no localization to plasma membrane.

To elaborate the idea of altered uromodulin biology to be common to all UAKD cases irrespective of underlying genetic defect, we performed in this study extensive qualitative and quantitative analysis of urinary uromodulin excretion in 12 and 15 families, respectively. Both WB and ELISA revealed significantly decreased urinary uromodulin excretion in all but one examined family. In addition, we performed immunohistochemical analysis of uromodulin and epithelial membrane antigen mucin (MUC1) in kidney sections representing four different genetic defects leading to UAKD. We found abnormal uromodulin staining patterns including massive intracellular accumulation in case of *UMOD* mutation and presence in hyaline casts accompanied by low intracellular positivity, irregular staining pattern or strongly reduced expression in patients with not yet identified genetic defect. Interestingly, uromodulin staining patterns were mostly correlated with those of MUC1.

Ultrastructural EM examination of kidney specimen from patient with one of group I mutant showed, besides numerous morphological abnormalities, large amounts of fibrillar material stored in the ER of TALH epithelial cells. By means of immunofluorescence colocalisation studies of kidney sections from the same patient, we were able to show that stored material was uromodulin.

UMOD mutations analysis and functional studies in other families

Currently there have been reported about 60 FJHN kindreds of various ethnic origin, but it is clear that including unpublished data there are much more kindreds being studied, as for example in the United Kingdom alone about 70 investigated kindreds were reported [23] and our cohort comprises more than 30 kindreds.

Following the initial report of Hart et al. [80], a lot of studies identified *UMOD* mutations in formerly as well as newly described FJHN/MCKD families. Interestingly, Rampoldi et al. in 2003 [133] included to *UMOD* mutation analysis in their FJHN and MCKD2 families also a family, originally reported by Gusmano et al. in 2002, with autosomal dominant glomorulocystic kidney disease (ADGCKD) [157]. Re-evaluation of clinical status in this family revealed hyperuricaemia and isosthenuria in affected members. GCKD associated with maturity-onset diabetes was excluded by *HNF-1β* sequencing and glucose tolerance test. Although linkage to 16p12 locus was not significant, causal mutation in *UMOD* gene was identified in this

family and thus a new Mendelian disorder was established (OMIM 609886). Lens et al. reported additional GCKD family with UMOD mutation in 2005 [135].

Up to date, 42 different mutations in the *UMOD* gene were reported in the literature [13, 80, 82, 133-135, 151, 158-164]. Importantly, the rate of linkage to 16p12 region in those studies was found to be 50% at most, reflecting thus underlying genetic heterogeneity. In the rest of families, no significant linkage was detected. Moreover, *UMOD* mutations were not found in all 16p12 linked families, suggesting either false positivity of linkage analysis, yet unidentified mutations or existence of another disease gene in this region.

Most of *UMOD* mutations (39) are missense. Remaining three mutations are in-frame deletions leading to the loss of 5 to 33 AA. They are summarised in Table 3.1. *UMOD* mutations show clustering in two neighbouring exons (in the literature referred to as exons 4 and 5, respectively, based on Hart's et al. gene organization analysis, which is currently invalid) and more than 50% of missense mutations affect one of 48 conserved cysteine residues.

Table 3.1 Summary of reported uromodulin mutations.

Mutation		**Exon**	**Reference**
cDNA	**Protein**		
c.95G>A	p.C32Y	3	[151]
c.156T>G	p.C52W	3	[161]
c.176A>C	p.D59A	3	[159]
c.299T>G	p.C77G	3	[164]
c.230G>A	p.C77Y	3	[158]
c.278_289del/insCCGGCTCCT	p.V93_G97del/insAASC	3	[160]
c.307G>T	p.G103C	3	[80]
c.334T>C	p.C112R	3	[159]
c.376T>C	p.C126R	3	[158]
c.383A>G	p.N128S	3	[158]
c.403T>A	p.C135S	3	[161]
c.443G>A	p.C148Y	3	[80]
c.444T>G	p.C148W	3	[133]
c.449G>C	p.C150S	3	[133]
c.509G>A	p.C170Y	3	[159]
c.529_555del	p.H177_R185del	3	[80]
c.553C>G	p.R185G	3	[165]
c.553C>A	p.R185S	3	[159]
c.563_661del	p.E188_L221del	3	[159]
c.584G>T	p.C195F	3	[161]
c.605G>C	p.W202S	3	[161]
c.610C>G	p.R204G	3	[159]

c.649T>C	p.C217R	3	[80]
c.649T>G	p.C217G	3	[159]
c.665G>C	p.R222P	3	[159]
c.668G>A	p.C223Y	3	[163]
c.674C>T	p.T225M	3	[159]
c.674C>A	p.T225K	3	[160]
c.686T>C	p.M229R	3	[151]
c.707C>T	p.P236L	3	[161]
c.707C>G	p.P236R	3	[162]
c.744C>G	p.C248W	3	[160]
c.764G>A	p.C255Y	3	[158]
c.817G>T	p.V273F	3	[151]
c.844T>C	p.C282R	3	[160]
c.898T>G	p.C300G	4	[158]
c.899G>A	p.C300Y	4	[82]
c.920A>C	p.K307T	4	[13]
c.943T>C	p.C315R	4	[133]
c.947A>C	p.Q316P	4	[135]
c.950G>A	p.C317Y	4	[133]
c.1039T>G	p.C347G	5	[134]

Positions of mutations in cDNA sequence are indicated "c." (base counting starts at adenosine in the initiation ATG codon). Positions in the protein sequence are indicated "p.". Exon counting is based on GeneBank sequence NM_003361.2.

First functional studies on *UMOD* mutations reported Dahan et al. and Rampoldi et al. in 2003. By means of kidney sections immunohistochemistry and WB of urines, Dahan et al. showed that *UMOD* mutations lead to gross accumulation of uromodulin in TALH epithelial cells, together with a drop in the urinary excretion of the protein [159]. Interestingly, biochemical analysis including SDS-PAGE of urines under both reducing and non-reducing conditions and after deglycosylation together with mass spectrometry analysis of urines showed that only the wildtype uromodulin is excreted by patients. These observations suggested that *UMOD* mutations affect the function and expression of uromodulin accompanied by abnormal accumulation of the mutated protein in tubular epithelial cells.

Rampoldi et al., who in a more detail studied effect of cysteine mutations on uromodulin trafficking in transiently transfected tissue culture cells [133], supported results of Dahan et al. Using time-laps transfection experiments, colocalisation studies and FACS analysis, they showed that compared to a wildtype protein, mutant isoforms were delayed in transport to the plasma membrane with a prolonged retention time in the ER, probably reflecting an abnormal folding of the protein due to the inability to form intrachain disulfide bridges. This behaviour

was truly simulated by culturing cells expressing wildtype protein in reducing conditions, proving thus the importance of cysteine residues for proper folding and maturation of uromodulin. Immunohistochemistry of kidney sections and WB analysis of uromodulin urinary excretion provided results consistent with Dahan et al. Heaps of fibrillar material most probably coinciding with uromodulin deposits were visualised in the ER of TALH cells by EM.

Decrease in urinary excretion of uromodulin, which seems to be a consequence of its altered processing, was further examined by Bleyer et al. [165]. They tested a set of patients from several families harbouring various *UMOD* mutations, unaffected family members and unrelated controls. They found significant decrease of urinary uromodulin excretion independent on age, gender or level of renal involvement in the group of individuals with mutation compared to groups with no mutation.

Data on urinary uromodulin excretion from all three studies revealed that the extent of reduction is greater than could be expected for heterozygous mutation status. This finding gave support for negative dominant effect of *UMOD* mutations, in which the mutated protein interferes with the wildtype protein and blocks its proper processing. Although simulation of heterozygous state by cotransfecting tissue culture cells by both mutant and wildtype constructs was not fully consistent with this model, it should not be rejected, as the situation in this kind of experiment is obviously very different from the situation in the kidney [133].

Group of doctor Rampoldi further reported functional consequences of the only missense mutation identified so far to involve ZP domain of uromodulin [134]. They again used FACS and immunofluorescence analysis of transfected tissue culture cells to investigate mutant protein dynamics. As in their previous study, they found that this cysteine mutation caused a delay in transport to plasma membrane due to its retention in the ER.

Behaviour of uromodulin mutants revealed by tissue culture and immunohistochemistry studies suggested consideration of UAKD as the ER storage disease. The hypothesis that apoptosis caused by ER storage of mutant uromodulin may be involved in UAKD pathogenesis was tested by Choi et al. [152]. Studying two cell lines stably transfected by both wildtype and two mutant uromodulin cDNAs, they showed accumulation of mutant proteins in the ER and their decreased excretion to culture media by means of immunofluorescence, selective deglycosylation, ELISA and WB. Annexin V and propidium iodide assay with FACS analysis proved significant increase in early apoptotic signal in both mutant cell lines, indicating a possible role of apoptosis in progressive renal damage in UAKD. Evaluating the influence of several chemical chaperones, they were able to show that colchicine and sodium 4-phenylbutyrate significantly improved delivery of mutant proteins from ER to plasma membrane as well as cell viability.

Right after our study, further reports addressing functional consequences of *UMOD* mutations appeared and their conclusions were generally concordant with our results. Doctor Rampoldi's group provided extensive study of intracellular trafficking and sub cellular localization of wildtype and 12 mutant uromodulin proteins [162]. Three of these mutants were characterised in a more detail by numerous experimental techniques. Besides methods used in other studies, they employed live imaging with fluorescence recovery after photo bleaching (FRAP) and immunogold-EM analysis to study real-time dynamics of uromodulin intracellular traffic and to quantitatively assess the intracellular distribution of transiently expressed proteins. Contrary to our results, they showed that at least in three mutants investigated in a detail, GPI modification was not altered as revealed by comprehensive phosphatidylinositol-phospholipase C (Pi-PLC) assay.

Jennings et al. aimed to characterise the effects of *UMOD* mutations on membrane targeting and direction of secretion [166]. They employed stably transfected and polarised renal epithelial cell cultures to study two uromodulin mutants in a detail. By means of immunohistochemistry and quantitative immunoassay, they showed the two mutants to be properly targeted to apical membrane, although their secretion to apical compartment was less efficient compared to wildtype protein, most probably due to decreased synthesis rate. By caspase 3 and proteasome inhibition studies, they showed that both mutants did not significantly activate apoptosis and proteasome-dependent degradation did not contribute significantly to their amelioration from the cytoplasm.

UMOD knockout mice models

Up to date, two *UMOD*$^{-/-}$ mice models were generated by independent groups [167, 168]. In both of them, targeted disruption of certain parts of the *UMOD* gene led to a complete shut down of its expression. Examination of both models proved that knockout (KO) mice suffered significantly more frequently from urinary tract infections. This observation confirmed one of the long proposed physiological roles of uromodulin in host defence against type 1-fimbriated *E. coli* [110]. Indeed, it was shown that uromodulin could act as a general host defence factor against UTI [169].

Second extensively discussed topic, the role of uromodulin in calcium oxalate stones formation was also evaluated using this model. Mo et al. showed that considerable portion of KO mice on special diet spontaneously formed calcium oxalate stones in the collecting duct of the medulla, while stone formation has never been observed in wildtype littermates on the same diet [170]. This observation supported hypothesis of inhibitory effect of uromodulin on kidney stones formation.

Several issues related to UAKD pathophysiology were also investigated. Examination of renal histological samples derived from these mice showed no developmental or morphological changes typically seen in UAKD patients [167, 168], even in several years course [171, 172]. This observation is not surprising, as *UMOD*$^{-/-}$ mice do not represent truly the situation in UAKD patients' kidneys in which intracellular accumulation of mutated protein is meant to be the primary cause of morphological changes. The same difference most probably accounts also for the absence of kidney stones and increased UTI events in UAKD patients that excrete certain, yet sufficient amount of wildtype protein to their urine.

Examination of steady state electrolyte handling showed no abnormalities in KO mice [172]. However, creatinine clearance was significantly reduced. Impaired urine concentration ability, a feature found with high prevalence in UAKD patients, was observed under water deprivation conditions. Moreover, biochemical and histochemical quantitative approaches used to asses changes in the biosynthesis of proteins related to NaCl transport along the nephron revealed upregulation of major distal transporters and downregulation of juxtaglomerular apparatus (JGA) components, consistently with the adaptation to altered NaCl reabsorption in the TALH. The same authors further observed significant difference in ratio of urinary sodium concentrations and urinary urate concentrations between KO and wildtype mice [84]. KO mice excreted less uric acid for a given amount of sodium, a result consistent with previously observed dysregulation of NaCl transport-related proteins. Interestingly, mRNA levels of PT urate transporters were found to be normal, suggesting that the upregulation of their expression is not responsible for increased urate reabsorption.

UMOD related pathogenesis of UAKD

As briefly discussed in chapter 1.1, major biochemical (decreased urine concentration ability, hyperuricaemia, decreased FE_{ur}) and histological (tubulointerstitial fibrosis, cystogenesis) features of UAKD has always been difficult to establish. Opinions on pathogenic mechanisms before invention of relationship between FJHN/MCKD/GCKD and uromodulin were also summarised.

Idea of gain-of-function mutation in urate/anion transporter became less promising after identification of second urate transporter of PT, URAT1 [173]. *URAT1* gene was localised to chromosome 11q. However, neither 17p (hUAT locus) nor 11q loci have been associated with UAKD so far.

Hypothesis of impaired renal hemodynamics as primary cause of hyperuricaemia was disputed by London group [23, 174] and defended by its authors [175]. However, this argument

has faded away after identification of causative *UMOD* mutations also in kindreds studied by authors of this hypothesis [158].

At the same time, discussion about efficacy of allopurinol treatment and related role of hyperuricaemia in the disease progression raised again. Fairbanks et al. reported results of long-term allopurinol treatment study supporting its beneficial role in ameliorating the progression of renal disease [174]. They stressed, however, that efficacy of the treatment decreases with the progression of renal impairment and is dependent on patient compliance as well. This underscored the importance of pre-symptomatic diagnosis, especially in children, as successful management may prevent or delay dialysis and ultimate renal transplantation. On the contrary, studies of two other groups could not confirm beneficial role of allopurinol [175-178]. Nevertheless, in view of London group, this was due to lack of compliance to the treatment in case of Bleyer et al. and late therapy commencement in case of Puig et al. [23, 179].

Regarding the primacy of hyperuricaemia in pathogenesis of UAKD, in the view of Bleyer et al. this discussion also lost significance as hyperuricaemia is secondary to UMOD dysfunction, the primary cause of the disease [177].

Nevertheless, identification of mutations in *UMOD* gene as a cause of UAKD in 25% to 50% of patients in different series [23] has not shed much more light on UAKD pathogenesis. There cannot be found a direct link between impaired uromodulin biology and decreased FE_{ur} and other major clinical findings. However, as we propose the impaired uromodulin biology to be responsible for most of the cases, it makes sense to discuss indirect mechanisms leading from UMOD dysfunction to major symptoms.

Cellular pathology

Right after invention of causative *UMOD* mutations in a proportion of FJHN/MCKD/GCKD families, experiments addressing cellular effects of these mutations started. Immunohistochemical analyses of kidney tissue sections from UAKD patients showed large uromodulin deposits in cytoplasm. They were associated with the ER and visualised as stacks of fibrillar material by the electron microscopy [133, 151]. Several cell tissue culture models of different mutations showed decreased presentation of uromodulin on the plasma membrane compared to wildtype due to decreased processing rate and accumulation in the ER. This effect was initially observed with mutations affecting conserved cysteine residues [133], but later on has been proved in all mutations studied so far. Nevertheless, there is a great variability among mutations suggesting different severity of molecular lesion and possibly different pathogenic mechanisms [151, 162]. However, genotype-phenotype correlations for individual UMOD mutations are lacking at present due to small number of families and

inadequate clinical data. Such a correlation could have been made only on cellular level in a single case where results from cell culture model corresponded well with immunohistochemical and ultrastructural findings in kidney tissue from the patient [151].

In our study of six UMOD mutations, based on biochemical and immunofluorescent analyses of transient cell cultures, we were able to outline two different pathogenic mechanisms, both consistent with negative dominant model [151]. In mutants susceptible to GPI modification, which are able to exit the ER, enter the secretory pathway and reach the plasma membrane, underlying pathogenic mechanisms might be impaired intracellular trafficking, decreased ability to be internalised and exposed on the plasma membrane or inability to form protein filaments on the plasma membrane. *In vivo*, impaired trafficking might be caused by co-occurrence of mutant and wildtype protein in transport vesicles [180]. The same co-occurrence on the plasma membrane may hamper uromodulin polymerisation and filaments formation [96], compromising thus the biological function of the protein. In mutants not susceptible to GPI modification, proteins with uncleaved GPI signal peptide probably cannot escape and accumulate in the ER [156] causing the expansion of the organelle and consequent triggering of ER stress signalling pathways [181, 182].

Generally, ER stress is a condition resulting from compromised ER functions for any reason. The most common cause of ER stress, accumulation of misfolded or malfolded proteins in the lumen of the organelle, induces stress response traditionally referred to as unfolded protein response (UPR). The ER has resident machinery of chaperones that assist proteins to acquire proper conformation. If the protein fails to acquire its natural conformation for any reason, it is degraded by the process called ER-associated degradation (ERAD). The process involves translocation of the protein through the ER membrane to cytoplasm, polyubiquitination and degradation in the proteasome. However, if the capacity of ER chaperones and ERAD is exceeded, accumulation of the protein in the ER occurs and UPR is triggered. UPR activation leads to downregulation of overall proteosynthesis to decrease the protein load on the ER and upregulation of ER chaperones and ERAD components to deal with accumulated protein. If these compensatory mechanisms do not solve the situation, apoptotic mechanisms are activated as the last line of defence. Currently, there are known three different UPR signalling pathways and several UPR-related apoptotic pathways. Their role in UAKD pathogenesis is, however poorly understood. Choi et al. showed significant increase in early as well as late apoptotic signals in two cell culture models of two UMOD mutations and reported reversibility of apoptotic changes by chemical chaperones [152]. On the other hand, Jennings et al. did not proved activation of caspase 3-dependent apoptotic pathway in two different cell culture models and two different mutations [166]. They also excluded involvement of ERAD in amelioration of

mutant uromodulin from the ER by proteasome inhibition studies. More studies in this area are therefore needed to evaluate the role of ER stress response and apoptosis in pathogenesis of UAKD.

A group of diseases in which abnormal ER accumulation of proteins occurs as a consequence of any ER related malfunction are called ER storage diseases (ESRD). There are known seven groups of those disorders caused by mutated cargo molecules (four subgroups), a defect in ER folding or transport machinery, a defect in UPR signalling or by inhibition of UPR-regulated adaptive responses [183]. According to this division, UAKD might be considered as a member of one of the first group's subgroup characterised by non-functional mutant cargo molecule that is not susceptible to ERAD. This proposal, however, needs to be evaluated in further studies.

Pathophysiology

Hyperuricaemia in UAKD is caused by increased tubular reabsorption of urate, as judged from normal urinary urate excretion in patients on purine free diet [23]. It is found in 65-75% of cases [83]. There was found an inverse correlation between urine osmolarity and uricaemia [83], inverse correlation between FE_{ur} and creatinine clearance [178] and we found positive correlation between urinary urate and uromodulin concentrations in UAKD patients [151]. These results suggest implication of blood volume, renal function and uromodulin in abnormal urate handling. The influence of uromodulin is considered indirect as urate reabsorption, secretion and postsecretory reabsorption are believed to be finished on the level of PT while uromodulin expression was repeatedly shown to be confined to TALH and early DCT [145]. However, minor *UMOD* expression was recently found also in PT cells [184] and therefore possibility of direct involvement of urate transport by mutant uromodulin should not be dismissed entirely. Most discussed hypothesis of hyperuricaemia in UAKD is based on long proposed function of uromodulin in salt uptake and formation of water barrier in TALH [185, 186]. Disruption of this barrier should lead to increased water uptake in this segment, which would compromise sodium reabsorption by the Na-K-2Cl cotransporter and maintenance of interstitial countercurrent gradient. This would cause not only the compensatory increase in sodium reabsorption in PT but also the impaired urine concentration ability and volume contraction and consequently the increased reabsorption of urate [83, 133, 187, 188]. This hypothesis was supported by results from *UMOD* KO mice that showed decreased urine concentration ability under water deprivation [172] and decreased excretion of urate relatively to the excretion of sodium [84]. Although it is currently not known a sodium-linked urate transporter in PT, such a transporter or transporter upregulated together with PT sodium

transport might to be invented. Alternatively, urate may non-specifically permeate along with water through disrupted water barrier in the TALH. Another possibility is a defect in urate secretion or enhanced postsecretory reabsorption of urate linked to the absence of uromodulin in distal tubules or collecting duct. Effect of uromodulin on distal urate handling through direct binding of urate was nevertheless excluded by uromodulin-urate binding assays [189]. Regarding decreased urine concentration ability, we hypothesise that impaired water reabsorption may be due to enhanced urine flow consequently to the absence of uromodulin in urine and compromised cast formation in distal and collecting tubules. This notion is supported by abnormalities in urine flow and dysregulation of major distal tubule transporters observed in KO mice [172].

Tubulointerstitial nephritis in UAKD is probably not due to a mere lack of uromodulin in the kidney. KO mice lacking uromodulin entirely did not show any kidney tissue abnormalities even after several years follow up [171, 172]. Most common opinion on development of histological findings in UAKD is that they are the result of events following abnormal processing and accumulation of uromodulin in the ER of respective cells. For example, massive cytoplasmic storage of uromodulin could ultimately lead to apoptosis that would lead to fibroblast infiltration and induction of interstitial inflammatory response by the cell debris. Moreover, inflammation caused by release of uromodulin aggregates to the interstitium could also play role. Several studies described abnormal interstitial deposits of uromodulin in various conditions where tubulointerstitial fibrosis occurs, including MCKD [124, 190, 191]. Uromodulin was shown to stimulate cytokine production in monocytes and granulocytes [192-194]. Moreover, tubulointerstitial nephritis with presence of anti-uromodulin antibodies was experimentally induced in rabbits and rats administrated by uromodulin [195, 196]. Alternatively, abnormal processing of uromodulin in TALH cells could lead to loss of polarity and mistargeting of the protein to interstitium. However, available data on immunohistochemical staining of uromodulin in kidney sections from UAKD patients did not prove its interstitial localisation [81, 82, 133, 151, 159]. Yet another possibility is that inflammatory signals initiates in uromodulin storing cells. It was shown that one of the UPR pathways can lead to nuclear factor κB (NF-κB) activation, a well-known mediator of inflammatory and immune responses [197-199].

Formation of cysts is only occasionally observed in UAKD patients [23, 59, 83]. They were observed in two variants, as glomerular cysts in GCKD patients and as medullary cysts in MCKD2 patients with *UMOD* mutations. Different cystic presentation of *UMOD* mutations suggests involvement of modifier genes or two-hit mechanism. Essentially, there is currently impossible to find the link between uromodulin dysfunction and cysts formation. Medullary

cysts originate from tubules enlargements and remain connected to the original nephron. It was speculated that tubule swelling might occur because of water income due to impaired uromodulin water barrier in the TALH [83]. On the other hand, formation of glomerular cysts found invariably in GCKD patients with *UMOD* mutations most probably follows different mechanism [47, 135]. It could be the result of tubular obstruction, urine reflux and increased pressure in Bowman's space [83, 133]. In favour of this hypothesis could speak abnormal presence of uromodulin in glomerular cysts of patients with GCKD of unknown molecular basis [124]. However, this has not been observed in GCKD due to *UMOD* mutations so far [83].

In conclusion, pathogenesis of UAKD is mostly unclear and it will require further formal studies of urate tubular handling as well as specific studies addressing cellular effects of *UMOD* mutations.

3.3 UMOD in other diseases with renal involvement - Journal of Inherited Metabolic Disorders, **31**(4): p. 508-517, 2008

3.3.1 Introduction

In previous chapters, I described current knowledge of UMOD processing in UAKD. We were further interested if changes in UMOD expression, cellular localisation and urinary excretion are specific to FJHN/MCKD/UAKD and what is the range of these changes in various genetic diseases with severe renal involvement. Examination of these issues was enabled by our affiliation to Institute of Inherited Metabolic Disorders, where are several such diseases under investigation. In the first round, we focused on Fabry disease (OMIM 301500), caused by α-galactosidase A (GLA) (EC 3.2.1.22) deficiency, in which renal involvement is very well documented and which has a long investigation history at our institute.

3.3.2 Specific methods

Total urine deglycosylation

For analysis of uromodulin glycosylation patterns in urines, we used GlycoPro^{TM} Enzymatic Deglycosylation Kit (ProZyme) according to manufacturer's instructions. Briefly, spot urine sample was thawed, thoroughly vortexed and 15 μL were mixed with 5X Reaction buffer (kit component) and Denaturation buffer (kit component) in 0.2 mL tubes (Eppendorf). Reaction mix was denatured at 100°C/5 minutes in the thermal cycler (PTC-225 DNA Engine Tetrad, MJ Research), let cool down to RT and Detergent solution (kit component) was added.

Glycosidase N-glycanase® PNGase F was added to reaction mix and incubated at 37°C/3 hours in biological thermostat (BT 120 M, Ekom). Reactions were then mixed with 6X SDS-PAGE sample buffer, denatured at 100°C/5 minutes in the thermal cycler and analysed by SDS-PAGE and WB.

Urine concentration

If concentrated for SDS-PAGE analysis, 500 µL of total urine was loaded on Microcon YM-50 filter (Millipore) and 1.5 mL tube assembly and centrifuged at 10000g until volume on the filter reached about 20-30 µL. Ultrafiltrate was discarded, retentate was recovered to a new tube, mixed with SDS-PAGE sample buffer, denatured at 100°C/5 minutes (Dri-Block DB-3 thermostat, Techne) and separated by SDS-PAGE followed by Coomassie blue R 250 staining, as described in chapter 5.2.

Other methods applicable to this section are described in General methods, chapters 5.1 - 5.3.

3.3.3 Results and discussion

For urinary UMOD excretion analysis, we selected 15 male patients to cover the age range, severity of symptoms and treatment regimens. We also randomly selected 9 female carriers for comparison and for completeness' sake.

First, we analysed pretreatment urine samples by WB and found significant quantitative and qualitative changes in urinary UMOD excretion in about half of the hemizygous male patients as well as in 7 out of 9 heterozygous carriers. These changes consisted in strongly decreased or reduced UMOD excretion and presence of abnormal anti-UMOD immunoreactive protein of lower molecular mass or combination of both.

Deglycosylation of the urine from one patient with abnormal anti-UMOD immunoreactive protein suggested that it was not UMOD glycoform but rather different form of the protein.

We recovered normal as well as abnormal UMOD proteins from the concentrated urine of the same patient by SDS-PAGE and subjected them to mass spectrometry analysis. Abnormal polypeptide was shown to be UMOD lacking its C-terminal part, with cleavage site located somewhere between AA residues K432 and R449 (see chapter 3.1.3)

Our male patients were enrolled in different types of clinical trials - one using substrate reduction therapy (SRT) with ceramide glucosyltransferase (EC 2.4.1.80) inhibitor and two using enzyme replacement therapy (ERT) by different recombinant GLA preparations. To assess

the impact of different treatment regimens on UMOD excretion and processing, we analysed urine samples collected during individual courses along with pretreatment samples by WB. Abnormal processing clearly normalised in all patients on both ERTs, while the effect of SRT was not as striking.

To shed light on observed abnormalities in UMOD excretion and processing, we examined UMOD immunohistochemical and Gb3 storage patterns in different parts of the nephron in kidney sections from three untreated patients (different from those 15 male and 9 female patients mentioned above). We observed abnormal UMOD localisation in TALH and collecting duct, with UMOD expression in TALH epithelial cells to be inversely proportional to the degree of storage.

Based on our results, we were not able to define the site and mechanisms leading to observed abnormalities in urinary UMOD processing. Basically, it may occur either intracellularly (for example due to storage-related proteasome and/or specific protease activation) or extracellularly, on the cell membrane as a result of abnormal ectodomain shedding. This process could be activated by glomerulopathy-related changes in tubular fluid composition altering the tertiary structure of UMOD and making it susceptible to aberrant cleavage. Another possibility might be that alternative processing takes place in desquamated storing epithelial cells.

Reduced urinary UMOD excretion observed in some patients may be considered as a consequence of inverse proportion of the storage and UMOD expression, while normal, fully processed UMOD is most probably produced by cells not affected by the storage.

In this work, we showed for the first time a biochemically defined alteration of tubular cell biology reflecting the process of storage in defined parts of the nephron. Our results warrant evaluation of tubular functions in Fabry disease patients and suggest UMOD as a potential biochemical marker of the therapy response.

3.4 Identification of a new UAKD locus - Kidney International **68**(4): p. 1472-1482, 2005

3.4.1 Introduction

Beside our work on UMOD-related issues (search for and collection of new families, mutation analysis, characterisation of mutations, the role of UMOD in other kidney-involved diseases), we attempted to identify new FJHN/MCKD loci in those families not linked to any of previously known loci on chromosomes 16p12 and 1q21. For this study, we selected large and

promising Belgian family (BE1) from our previous study [78], in which we tested only the linkage to locus 16p12, to perform genome-wide linkage analysis. [81]

3.4.2 Specific methods

Specific methods applicable to this section are described in chapter 3.2.2.1. Other used methods are described in General methods section, chapter 5.

3.4.3 Results and discussion

First, we focused on detailed clinical and biochemical characterisation of family members to minimise the risk of the disease status misclassification and consequent failure of the linkage analysis. The clinical phenotype was found to be atypical. In addition to usual signs of the disease like small kidney size, anaemia, hyperuricaemia, elevated plasma creatinine and hypouricuria appearing in early age [174], precocious anaemia, absence of gout and relatively late onset of renal insufficiency were also observed.

First, we analysed qualitatively and quantitatively available spot urine samples from family members to obtain their up-to-date biochemical status.

Qualitative SDS-PAGE and Western blot analyses showed reduction or absence of UMOD in urines as well as urinary sediments from affected members.

Quantitatively, we determined several biochemical parameters including UMOD concentration to assess kidney functions. When comparing healthy family members and controls, no statistically significant changes in any parameter were found. On the other hand, we found significantly changed almost all biochemical parameters in affected individuals when compared to controls. We employed all of these significantly changed parameters as disease status characteristics in discriminant analysis to calculate posterior probabilities that individuals belonged to either affected or unaffected group. This kind of analysis provided a high degree of certainty in classification and confirmation of affection status.

Comparison of biochemical parameters between affected and unaffected family member groups showed significantly reduced excretion of urate, calcium and UMOD in the former. No obvious explanation of decreased calcium excretion could be provided. One hypothesis might be that UMOD contributes to the regulation of calcium metabolism through its calcium binding domains. Unlike decreased urate excretion, which is one of the hallmarks of FJHN/MCKD2, reduced UMOD excretion in these patients with no *UMOD* mutation was surprising. Similar UMOD excretion pattern was so far observed only in patients with *UMOD* mutations [165].

Hence we further performed immunohistochemical analysis of kidney section from one affected family member to elucidate the cause of decreased urinary excretion in this family. It showed significantly and uniformly reduced UMOD staining in TALH epithelial cells and minimal tubulointerstitial involvement. In control kidney tissue, we observed cytoplasmic distribution of UMOD with maximal staining on the apical membranes of TALH epithelial cells. In contrast to both of these observations, kidney tissue from FJHN patient with *UMOD* mutation showed strong cytoplasmic (ER) accumulation of UMOD. Yet another staining pattern, characterised by irregular UMOD staining accompanied by interstitial fibrosis and tubular atrophy was detected in kidney section from FJHN patient coming from a family without proven linkage to any locus. These results suggested three different mechanisms of UMOD depletion and pathogenesis in FJHN/MCKD2 but featuring UMOD as a common denominator.

Genome-wide linkage analysis in studied family employing 93 microsatellite markers revealed only one candidate region on chromosome 1 with relatively low LOD score (1.69). Fine mapping using 38 additional markers in this region provided LOD score of 3.27 and haplotype analysis identified a single haplotype segregating with the disease. Recombination events detected in affected individuals delimited critical region of 37.2 Mbp on chromosome 1q41 containing about 300 genes. Consequently, we examined the linkage to this locus in eight FJHN families from our previous study [78] and in one additional MCKD family described earlier [17] and showing no linkage to already established FJHN/MCKD loci on chromosomes 16p12 and 1q21. However, we were unable to confirm linkage to this newly identified locus in any of those families. On the other hand, atypical clinical presentation of FJHN in this Belgian family together with our immunohistochemical analysis is suggestive of different genetic origin and gives support to the validity of our linkage analysis.

Due to relatively high gene content in newly identified critical region, we applied several bioinformatic tools to effectively select for candidate genes. We focused first on genes specifically expressed in kidney and second on genes of which defect could be responsible for decreased UMOD expression observed in kidney tissue. As none kidney specific genes could be found in the critical region, we tried to identify genes possibly related to UMOD expression - transcription factors, hormones or proteins involved in posttranslational modification or cellular trafficking.

Eventually, we selected nine candidate genes for sequence analysis. In none of these genes, however, classical deleterious mutation was found within the promoter regions, exon/intron junctions or coding sequences. That time, we proposed that further progress in finding and cloning of responsible disease gene was unfortunately hampered by the size of the critical region and number of genes to be considered and that the identification of other families

linked to this region would be needed to further confirm and hopefully narrow the critical region.

3.5 Evaluating *REN* as a candidate gene in 1q41 region - manuscript in preparation, 2008

3.5.1 Introduction

In previous chapter, I described results of our attempt to identify new UAKD loci. In single Belgian family (BE1), we were able to perform advanced clinical characterisation and classification and to identify significant locus segregating with the disease on chromosome 1q41 by medium-density genome-wide scan. In this region, we analysed sequences of 9 candidate genes and found no deleterious mutation.

Besides those genes, we also analysed the sequence of renin precursor (preprorenin) encoding gene (*REN*). In affected member of BE1 family, we found heterozygous mutation in exon 1 of *REN* gene, which was not present in healthy family member as well as in 200 healthy controls. However, we postponed the publication of this finding to further characterise and to functionally study wildtype and mutant preprorenin and the impact of the mutation on cell biology and its potential role in the disease pathogenesis.

Renin

Renin and prorenin are secretory proteins active in the renin-angiotensin system (RAS) [200] and the (pro)renin receptor signal transduction pathway which is distinct from RAS receptor signalling [201]. Both pathways play an important role in kidney physiology and pathology.

Renin precursor or preprorenin is composed of 406 AA. It harbours several motifs - two potential N-glycosylation sites, signal peptide (residues 1-23), A1 propeptide (residues 31-59) and aspartyl protease domain (residues 85-405) (http://smart.embl.de/smart/show_motifs.pl?ID=P00797).

REN gene is located in cytogenetic band q32 on chromosome 1 according to Entrez gene (http://www.ncbi.nlm.nih.gov/sites/entrez?Db=gene&Cmd=ShowDetailView&TermToSearch=5972&ordinalpos=1&itool=EntrezSystem2.PEntrez.Gene.Gene_ResultsPanel.Gene_RVDocSum) as well as Ensembl, UCSC, HGNC and Geneatlas databases. It spans 11.5 kbp of the genomic sequence on minus strand (http://www.ncbi.nlm.nih.gov/entrez/viewer.fcgi?val=NC_000001.9&from=202390571&to=202402088&strand=2&dopt=gb).

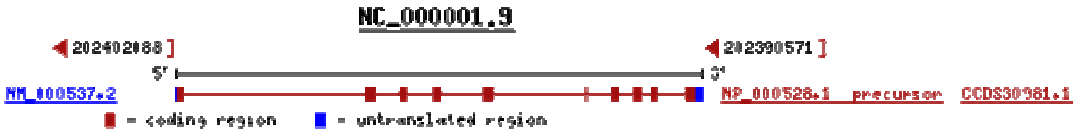

Figure 3.3 *REN* gene organisation. On top, there is the accession number of *REN* genomic sequence. Numbered arrows indicate the position of the gene on the sequence of chromosome 1 and its orientation. On the left side, GenBank accession number of mRNA is given. On the right side, accession numbers of corresponding protein sequence and consensus coding sequence are given. Acquired from Entrez Gene database (http://www.ncbi.nlm.nih.gov/sites/entrez?Db=gene&Cmd=ShowDetailView&TermToSearch=5972&ordinalpos=1&itool=EntrezSystem2.PEntrez.Gene.Gene_ResultsPanel.Gene_RVDocSum)

REN is expressed most profoundly in the ovary, the uterus and the kidney (http://symatlas.gnf.org/SymAtlas). In the kidney, the expression is restricted to juxtaglomerular (granular) cells of the JGA. The hydrophobic core structure of the signal peptide binds to signal recognition particle (SRP), which ensures insertion of the signal peptide into translation-translocation channel in the membrane of the ER [202]. Following proteosynthesis, glycosylation, signal sequence removal and proteolytic processing, both the prorenin and renin are sorted to secretory granules from which they are released in highly regulated manner into the circulation [203].

3.5.2 Specific methods

Recombinant renin analysis

Cultured cells lysis

Cells were harvested to PBS into 1.5 mL tubes, pelleted by centrifugation at 800g/5 minutes and washed twice in PBS. The pellet was then resuspended in PBS with 1% (v/v) PIC (Sigma) and sonicated 5x10 seconds at output of 50% in the cuphorn filled with mixture of ice and water and connected to Ultrasonic Homogeniser (4710 series, Cole-Parmer Instrument Co). The suspension was then centrifuged at 14000g/5 minutes at 4°C to remove cell debris. The supernatant was collected to a new tube and analysed, or stored at -20°C.

Preparation of cell culture medium for secreted renin analysis

For secreted renin analysis, the foetal calf serum free medium was collected and centrifuged first at 800g/5 min at 4°C and then at 15000g/5 min at 4°C to remove residual cells and cellular debris, respectively. To the resulting supernatant, PIC (Sigma) was added to 1% (v/v). 500µl of the medium was then concentrated to a small volume and brought to PBS by two

successive rounds of concentration-refill on Microcon YM-10 filter and 1.5 mL tube assembly (Millipore) at 10000g. Retentate was then recovered to a new tube at 10000g and analysed by SDS-PAGE and WB as is or after the deglycosylation.

Renin deglycosylation

For analysis of glycosylation patterns of wildtype and mutant renins expressed in cell cultures, we used GlycoPro™ Enzymatic Deglycosylation Kit (ProZyme) according to manufacturer's instructions. Briefly, cell lysate or concentrated cell culture medium (previous paragraph) was mixed with 5X Reaction buffer (kit component) and Denaturation buffer (kit component) in 0.2 mL tubes (Eppendorf). Reaction mix was denatured at 100°C/5 minutes in the thermal cycler (PTC-225 DNA Engine Tetrad, MJ Research), let cool down to RT and Detergent solution (kit component) was added. Glycosidase N-glycanase® PNGase F was then added to reaction mix and incubated at 37°C/3 hours in biological thermostat (BT 120 M, Ekom). Reactions were then mixed with 6X SDS-PAGE sample buffer, denatured at 100°C/5 minutes in the thermal cycler and analysed by SDS-PAGE and WB.

Antibodies fluorescein labelling

For FACS analysis, polyclonal Anti Preprorenin (21-64)(Human) Serum and Anti Preprorenin (288-317)(Human) Serum antibodies (Yanaihara Institute) were conjugated to fluorescein by Fluorescein Protein Labelling Kit (Roche) according to manufacturer's instructions. Briefly, 20 mg/mL FLUOS reagent [5(6)-carboxyfluorescein-N-hydroxysuccinimide ester] solution was prepared by dissolution of lyophilised reagent in DMSO. 1 mg of each polyclonal antibody was dissolved in 1 mL of PBS (kit component) and 7.9 μL of FLUOS solution were added. Reaction mix was incubated at RT protected from light during gentle stirring in the rotamixer (Multi RS-60, Biosan). Meanwhile, Sephadex G-25 column (kit component) was blocked by Blocking reagent (kit component) and rinsed by PBS several times. Reaction mix was then applied onto the column to remove non-reacted FLUOS. Labelled antibody was eluted from the column by PBS and fractions of about 0.5 mL were collected. The amount of antibody in individual fractions and labelling yield were calculated based on extinctions at 280 nm (protein) and 495 nm (fluorescein) measured by means of photometer (UV/VIS Spectrometer UV4-100, Unicam Ltd.) and applying the equation provided by the manufacturer.

Other used methods are described in General methods section, chapters 5.2 - 5.3.

3.5.3 Results and discussion

To confirm and to define chromosome 1 candidate region more precisely, we performed again linkage analysis in BE1 family, that time using Affymetrix 10K SNP microarrays. It provided LOD score of 3.24 on chromosome 1. Haplotype analysis delimited candidate region of 24.7 Mbp containing that time 224 genes.

This region overlapped partially with the candidate region of Gordon hyperkalemia-hypertension syndrome (OMIM 145260), presenting some clinical features found also in BE1 family.

The mutation in exon 1, mentioned in the chapter 3.5.1, causes the deletion of one leucine from pentaleucine hydrophobic core of renin precursor (preprorenin) signal peptide. In this work, we provided several lines of evidence indicating that this deletion leads to aberrant renin biosynthesis, secretion and localisation in the kidney, which may account for the phenotypic abnormalities observed in affected individuals.

Two independent *in silico* analyses showed that the deletion leads to the decrease in hydrophobicity of signal peptide while preserving predicted cleavage site and binding to SRP.

In vitro translation (IVT) analysis followed by SDS-PAGE suggested that the leucine deletion in signal peptide reduces the translocation efficiency into the rough ER (microsomes). Assay in similar system focused only on signal peptide revealed altered processing of deletion harbouring signal peptide compared to the wildtype.

We constructed transient cell culture models to establish effects of the deletion on (pro)renin translocation efficiency, post-translational processing and secretion rate and renin enzymatic activity *in vivo*. Compared to the wildtype, we found no change in the enzymatic activity either in cell lysates or in cell culture media but we found significant decrease of total prorenin and renin amount in both cell lysates and cell culture media. We further observed decreased rate and time delay in biosynthesis of deletion harbouring protein compared to the wildtype. However, we have never observed any qualitative differences in post-translational processing between both recombinant proteins as assessed by WB.

To broaden the range of available assays, we constructed also stable wildtype and deletion cell lines. Similarly to transient cultures, we found even more pronounced decrease in total amount of renin and prorenin in cell lysates as well as culture media in case of deletion. However, qualitative WB analysis with the potential, contrary to quantitative assay, to detect all protein forms showed marked accumulation of renin and prorenin in deletion harbouring clones. Again, no qualitative differences in post-translational processing between wildtype and deletion

proteins, as assessed by WB, were observed. Continuous monitoring of renin activity secretion by live cells, employing modified commercial fluorescent assay, showed its significant decrease in case of deletion.

The impact of deletion on cell viability was also assessed using stable cell lines. During the first three days of cultivation, cultures with deletion showed significant delay in reaching the lag phase accompanied by the doubling-time increase from 46 hours to 78 hours when compared to wildtype and reference, antibiotic-selected culture with no renin expression. Following this three-day period, all cell lines became similar in their growth curves and doubling-times. Moreover, RT-PCR analysis showed in deletion cells the presence of the spliced *XBP1(S)* mRNA variant, which is a key effector of the mammalian UPR [204]. Examination of levels of early and late apoptotic signals (Annexin V and propidium iodide) showed no significant differences among cultures.

We further investigated subcellular localisation of renin and prorenin in stable cell lines by immunofluorescence and confocal microscopy. In wildtype cultures, we observed renin specific granular material in the cytoplasm. Neither significant changes in granules' shape, size or localisation nor signs of prorenin nor renin retention in ER, Golgi apparatus, cytoskeleton or plasma membrane were observed in deletion cell lines.

EM examination of fixed stable cell lines pellets revealed membrane delimited granules compatible with characteristics of renin secretory granules in cytoplasm of both wildtype and deletion cells, but not in non-transfected cells. In both types of cell lines there were also observed membraned bodies of probably macroautophagic origin and considerable distension of predominantly rough endoplasmic reticulum cisternae. Those features seemed to be more frequent and pronounced in deletion cell lines.

Finally, renin was examined also in patients from BE1 family to confront results of *in vitro* and *in vivo* analyses with the real situation. Plasma renin activity and aldosterone concentrations measured in three patients were in normal ranges. We further broadened immunohistochemical examinations of UMOD and MUC1 expression presented in the previous study [81]. Here we further examined the expression of other RAS components (renin receptor, angiotensinogen (AGT), angiotensin II), KCNK2 (TREK-1) (as another candidate protein, of which gene is located within the chromosome 1 region and as the marker of proximal tubule brush border) and WNK4 kinase (as a protein involved in the pathogenesis of the Gordon hyperkalemia-hypertension syndrome [205]) in kidney sections from three patients. Compared to control tissues, we found considerably reduced expression of both, renin and prorenin. The observed pattern was disease-stage dependent. On the other hand, we observed abnormal localization/induction of both renin and prorenin inside the vessel wall of several arterioles and

small arteries in all three patients. Expression of renin receptor, detected on the basolateral pole of DCT and TALH in a set of controls, was unchanged in patients. Reduced expression of renin and other local kidney RAS components in both JGA and tubular epithelium was accompanied by AGT and angiotensin II tubular staining either comparable to controls or decreased, reflecting the disease stage. TREK-1 (apical pole of PT) and WNK4 (apical pole of TALH and CD) showed tendency to weakened immunostaining similarly to UMOD and MUC-1 [81].

Generally, patients' kidneys showed progressive destruction of both glomeruli and renal tubules with some differences in severity between individual nephrons.

Manuscript in preparation is presented in the appendix chapter 9.2

Renin in disease

Mutations in the RAS system components cause autosomal recessive renal tubular dysgenesis (RTD) [206-208]. The (pro)renin receptor knockout in mouse was lethal [209] and human (pro)renin receptor transgenic rats developed gradual proteinuria and glomerulosclerosis [210]. Moreover, selective ablation of juxtaglomerular cells in mouse resulting into renin insufficiency led to severe reduction of the kidney size, glomeruli hyperplasia and atrophy, tubular dilatation and alteration of renal functions [211].

Amino acids changes within the hydrophobic core of signal peptides have potential to affect co-translational translocation and post-translational processing of corresponding proteins [212] and there were described several autosomal dominant phenotypes associated with such changes [213-215] and altogether about 30 human genetic diseases [216-219]. Functional characterisation of signal sequence mutations showed that their pathogenic potential depends on the site and the type of the mutation.

We found that our mutation decreases signal sequence hydrophobicity required for efficient ER translocation, changes property of the off-cleaved signal sequence and limits biosynthesis of secretory competent and catalytically active prorenin and renin proteins. The mutation further causes intracellular retention of prorenin and renin, and cells expressing mutant protein have shown reduced growth rate, signs of activated ER stress, unfolded protein response (UPR) and pronounced autophagy, a features having potentially serious consequences especially for tissues dedicated to extracellular protein synthesis [220]. Constant ER stress and activated UPR signalling have generally serious impact on ER function and structure, trigger apoptosis, inflammation and eventually lead to reduced viability or even cell death [221] and disease development [222]. This pathogenetic mechanism is well plausible for this mutation as is in ER-stress and apoptosis inducing signal sequence mutations found in autosomal dominant

neurohypophyseal diabetes insipidus [223], carbonic anhydrase IV causing retinitis pigmentosa [224, 225] or parathyroid hormone in autosomal dominant form of hypoparathyroidism [218].

Based on our results of *in silico*, *in vitro*, quantitative and qualitative and immunohistochemical experiments and observations, it is conceivable to predict, that our mutation reduces ability of regulated renin secretion *in vivo*. This probably affects renal development [206], sensitivity of the tubuloglomerular feedback mechanism and autoregulation of renal blood flow [226], which through altered renal hemodynamics and resulting hypoxia may lead to loss of glomeruli, tubulointerstitial injury and end-stage renal disease [227]. Mechanism of RAS blockage corresponds to anaemia, hyperkalemia and reduced GFR presented in the patients [228] and renal ischaemia well explains reduced expression of UMOD [229] and other tubular proteins.

These proposed mechanisms with their consequences are consistent with multiple changes in kidney morphology, altered tubular function and clinical and biochemical abnormalities observed in patients from BE1 family.

In conclusion, we identified mutation in signal sequence of preprorenin that, based on several lines of evidence, causes aberrant ER translation/translocation and intracellular accumulation of prorenin and renin. We suggest that these events lead gradually to cytotoxic stress of juxtaglomerular cells and result in autosomal dominant kidney phenotype. Detailed clinical, biochemical and molecular investigations of the patients together with further characterization of the wildtype and mutant preprorenin expressing cell lines are therefore of great interest.

3.6 UMOD protein-protein interaction studies

In early years of my Ph.D. studies, when the role of UMOD in FJHN/MCKD was not known but the genetic heterogeneity of the disease was evident, we hypothesised the existence of a protein complex, of which components' defects would lead to similar clinical presentations. After establishment of UMOD as one of the major player in the pathogenesis of the disease, we considered it as the component of such hypothetical protein complex and, as an alternative to positional cloning approach, we have attempted to apply protein-protein interaction approaches to hopefully identify other causal proteins and consequently genes underlying the disease.

That time, we took into consideration first of all a yeast two-hybrid system, probably the most common and available approach to identify unknown interaction partners of the protein of interest. In parallel, we tried to utilize high glycan content of UMOD protein to prepare solid, UMOD-bound matrix for probing complex mixtures of proteins in pull-down assay.

3.6.1 Yeast two-hybrid system (YTHS)

3.6.1.1 Introduction

This approach relies on expression of the protein of interest or its part in fusion with DNA-binding domain (so called bait) of a transcription factor in a yeast cell. Potential interacting protein, on the other hand, is expressed in the same cell in fusion with transcription-activating domain (so called prey) of the same transcription factor. If bait and prey physically interact in the yeast cell nucleus, both domains of transcription factor are brought to close proximity on promoters of certain genes and their transcription takes place. These so called reporter genes are usually biosynthetic genes engineered under the control of fusion transcription factor and can be easily scored biochemically by nutritionally selective cultivation.

3.6.1.2 Specific methods

Yeast media and solutions

YPAD (Yeast extract-Peptone-Dextrose + Adenine): 1% (w/v) yeast extract, 2% (w/v) peptone, 2% (w/v) D-glucose, 50 mg/L adenine sulphate. All components except glucose were dissolved in water and the resulting solution was autoclaved (MLS-2420 autoclave, Sanyo). Filter sterilised (0.22 μm filter Milex GP, Millipore) 20% (w/v) D-glucose stock solution was added after autoclaving. For plates, agar to 2% (w/v) was added before autoclaving.

SD (Synthetic Dextrose): 0.17% (w/v) yeast nitrogen base without AA and ammonium sulphate, 0.5% (w/v) ammonium sulphate, 2% (w/v) D-glucose. All components except glucose were dissolved in water, pH was adjusted to 6-7 with 1 M NaOH (OP-274 pH/Ion Analyser, Radelkis) and the resulting solution was autoclaved. Filter sterilised (0.22 μm filter Milex GP, Millipore) 20% (w/v) D-glucose stock solution was added after autoclaving. For plates, agar to 1.5% (w/v) was added before autoclaving.

100X tryptophan (trp) solution: 2 mg/mL tryptophan, dissolved in autoclave-sterilised water.

100X histidine (his) solution: 2 mg/mL histidine, dissolved in autoclave-sterilised water.

100X leucine (leu) solution: 10 mg/mL leucine, dissolved in autoclave-sterilised water.

100X methionine (met) solution: 2 mg/mL methionine, dissolved in autoclave-sterilised water.

100X adenine sulphate (ade) solution: 5 mg/mL adenine sulphate, dissolved in autoclave-sterilised water.

100X uracil (ura) solution: 2 mg/mL uracil, dissolved in autoclave-sterilised water.

These 100x nutrient solutions combined with minimal SD medium were used to prepare yeast dropout media and plates for nutritional selection of transformed yeasts. In the text, they are referred to as -"nutrient" dropout medium/plate. For example, -trp dropout medium/plate corresponds to SD + ade, his, met, ura, leu.

Glycerol storage solution: 30% (v/v) glycerol, filter sterilised (0.22 μm filter Milex GP, Millipore). For long-term storage of *S. cerevisiae* clones, overnight liquid culture was mixed 1:1 with the glycerol storage solution, frozen in the mixture of dry ice and denatured ethanol and stored at -70°C.

Yeast vector and strain

Plasmid pGBD-B for construction of bait fusion proteins was a generous gift from David Markie, Ph.D. from Department of Pathology at Dunedin School of Medicine, New Zealand. This plasmid was derived from plasmid pGBD-C1 [230] by the replacement of multiple cloning site with a single *Bam*HI site flanked by the *attB1* and *attB2* sequences that direct homologous recombination with the tagged insert in yeasts. It is a multi-copy shuttle vector containing *TRP1* gene for selection in yeasts and ampicillin resistance gene (Amp^r) for selection in *E. coli* (Figure 3.3).

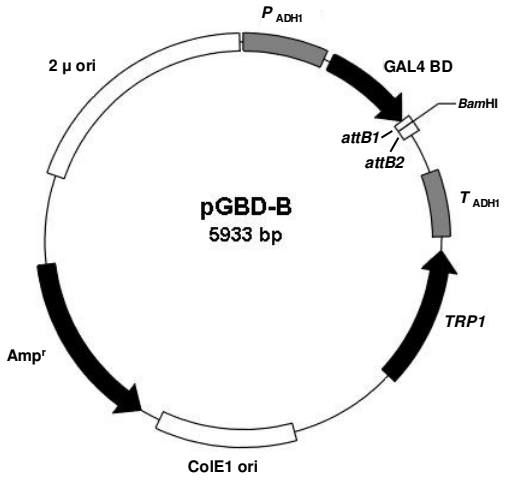

Figure 3.3 Map of pGBD-B vector. P_{ADH1} - ADH1 promoter, GAL4 BD - GAL4 binding domain, T_{ADH1} - ADH1 terminator, *TRP1* - tryptophan biosynthesis gene, ColE1 ori - bacterial ColE1 replication origin, Amp^r - ampicillin resistance gene (*bla*), 2μ ori - yeast 2-micron replication origin

S. cerevisiae host strain PJ69-4A was used for expression of baits [230]. Its genotype is *MATa trp1-901 leu2-3,112 ura3-52 his3-200 gal4Δ gal80Δ LYS2::GAL1-HIS3GAL2-ADE2 met2::GAL7-lacZ* meaning that this strain is deficient in *TRP1*, *LEU2*, *URA3*, *HIS3*, *ADE2* and

MET genes and consequently is able to grow only in presence of adequate concentrations of tryptophan, leucine, uracil, histidine, adenine and methionine in the media. At the same time, *HIS3*, *ADE2* and *lacZ* (β-D-galactosidase) genes are placed under the control of different *GAL4*-responsive promoters and serve as reporter genes in GAL4-based YTHS.

Primer design for bait construction

Oligonucleotides for PCR amplification of bait fragments were designed to contain two distinct parts. The 3' regions were *UMOD* specific and were designed using Oligo 6.44 software (Molecular Biology Insights) as common PCR primers. The 5' regions were tags including sequences identical to *attB1* and *attB2* regions flanking *Bam*HI cloning site in pGBD-B vector and enabling homologous recombination cloning in yeasts. To ensure oriented cloning of the bait fragment in proper reading frame, A1 tag (including *attB1* sequence) was added to upper (sense) primer while A2 tag (including *attB2* sequence) was added to lower (antisense) primer. Oligonucleotides designed for UMOD bait construction are summarised in Table 3.2.

Table 3.2 *UMOD* specific primers used to amplify bait fragment from cDNA.

Bait fragment	**Upper primer*** **Lower primer****	**PCR length*** (bp)**
UMOD ($UMOD^{25-640}$)	A1-GACACCTCAGAAGCAAGATG A2-CCGCTGTCAGTCACTGAA	1924
EGF domains ($UMOD^{25-151}$)	A1-GACACCTCAGAAGCAAGATG A2-GGAGCACTCACAGTGC	447
ZP domain ($UMOD^{331-585}$)	A1-CACAGGCTGGAATGTGG A2-GGTCCCAGAGCAGGTAGG	831

* A1: 5' GAA TTC ACA AGT TTG TAC AAA AAA GCA GGC TGG 3'

** A2: 5' GTC GAC CAC TTT GTA CAA GAA AGC TGG GTG (TTA) 3'

*** Including tags

In A2 tag sequence, the stop codon (in parentheses) was included except for the largest fragment ($UMOD^{25-640}$), in which it was naturally included. Ranges of AAs included are in superscript.

PCR for bait fragments

Solutions:

10 mM deoxynucleoside triphosphates (dNTPs) mix: 10 mM dATP, 10 mM dCTP, 10 mM dGTP, 10 mM dTTP. 100 mM stock solutions of all dNTPs (USB) were mixed together and with water to 1:9 dilutions.

Bait fragments were amplified by "touch-down" approach to increase the chance of the positive result at a first attempt. UMOD cDNA fragments were amplified by *Taq* DNA polymerase (Promega, #M1861-discontinued) together with Deep $Vent_R$™ DNA Polymerase (New England Biolabs) from pCR3.1-UMOD construct (kindly provided by my colleagues

Marie Kalbáčová, Ph.D. and Kateřina Hodaňová, Ph.D.). For one PCR reaction, following mix was set:

Component	Amount (µL)
Thermophilic DNA Polymerase 10X Reaction Buffer, Magnesium Free*	5
10 mM dNTPs mix	1
10 µM upper primer	2.5
10 µM lower primer	2.5
25 mM $MgCl_2$ solution*	4
5U/µL Taq DNA polymerase	0.25
Deep $Vent_R$™ DNA Polymerase (1:20)**	1
50 ng/µL pCR3.1-UMOD plasmid DNA	1
Water	to 50

* #M1901 (discontinued) and #A3511, respectively, supplied together with Taq DNA polymerase

** Diluted in Vent Diluent (New England Biolabs)

Tubes were placed to thermal cycler and the following thermal program was executed:

Segment	Number of cycles	Temperature (°C)	Time (s)
1	1	95	180
2	5	95	10
		60-1 per cycle	30
		72	90
3	25	95	10
		55	30
		72	90
4	1	72	600
5	1	15	for ever

After program termination, 10 µL of PCR reaction were analysed by agarose gel electrophoresis.

Linearisation of pGBD-B vector

Vector pGBD-B was propagated in and isolated from an overnight culture of *E. coli* strain DH5α (chapter *Isolation of plasmid DNA from E. coli*). Isolated plasmid DNA was linearised by restriction endonuclease *Bam*HI in the following reaction:

Component	Amount
10X Buffer BamHI*	2 µL
BamHI (10 U/ µL)*	0.5 µL
pGBD-B plasmid DNA	1 µg
Water	to 20 µL

* Purchased from Fermentas

Reaction mix was incubated at 37°C/1 hour in the incubator (Biological Thermostat BT 120 M, Ekom). Linearised vector was resolved by preparative agarose gel electrophoresis and isolated from the gel as described above (chapters 5.4 and 5.5).

Lithium acetate yeast transformation and bait cloning

Buffers and solutions:

10X Lithium acetate (LiAc) solution: 1 M Lithium acetate, pH 7.5 was adjusted by dilute acetic acid (OP-274 pH/Ion Analyser, Radelkis).

10X TE (Tris-EDTA) buffer: 0.1 M Tris base, 0.01 M EDTA, pH 7.5 was adjusted by concentrated HCl. Solution was filter sterilised (0.22 μm filter Milex GP, Millipore) and stored at RT.

LiAc/PEG/TE transformation buffer: 0.1 M LiAc, 40% (w/v) polyethylene glycol 3,350 (PEG), 0.01 M Tris-Cl, 0.001 M EDTA, pH 7.5. The buffer was prepared by mixing 10X LiAc solution and 10X TE buffer. After addition of PEG, solution was autoclaved and stored at RT.

For up to ten small-scale transformations, 0.7 mL of YPAD broth in 50 mL tube (TPP) was inoculated with fresh colony of PJ69-4A yeast strain and the culture was grown overnight with shaking at 30°C (Cellstar incubator, Queue Systems). In the morning, 10 mL of YPAD broth was added and the culture was grown for next 4-5 hours. Cells were then harvested at 700g/5 minutes (centrifuge MR22i, Jouan or 4K15, SIGMA Laborzentrifugen), resuspended in 1 mL of 1X LiAc solution and transferred to 1.5 mL tube. Cells were harvested again in centrifuge and washed twice in 1 mL of 1X LiAc solution. Pellet was resuspended in 360 μL of LiAc/PEG/TE transformation buffer and 10 μL of 10 mg/mL heat-denatured salmon sperm DNA (Sigma, #D-9156) and 1 μL of *Bam*HI linearised pGBD-B vector solution (about 9 ng of DNA) were added. For each transformation, 32 μL of this suspension was placed into 0.2 mL PCR tube (Eppendorf) and mixed with 4 μL of the bait fragment PCR reaction or 4 μL of sterile water as a transformation negative control. Tubes were incubated in the thermal cycler (PTC-225 DNA Engine Tetrad, MJ Research) at 30°C/30 minutes, 42°C/1 minute and 30°C/1 minute. After transformation, 100 μL of sterile water were added to each tube, mixed well, spread over a selective -trp dropout plate and let grow for three days at 30°C.

Identification of yeast clones containing baits and a test for reporter genes autoactivation

For identification of colonies containing inserts, we used the same PCR reactions as for amplification of bait fragments from UMOD cDNA (chapter *PCR for bait fragments*). As a template, we used yeast lysates prepared as follows. After three days of growth on -trp plates, eight colonies of each bait were picked by sterile toothpick and resuspended each in 50 μL of sterile water dispensed in 96-well plate. In another 96 well plate, 20 μL of freshly prepared 20 mM NaOH solution were dispensed accordingly. 3 μL of each yeast suspension were transferred into corresponding wells of NaOH plate. After incubation at RT/5 minutes, 80 μL of sterile

water were added to each well of NaOH plate. For each PCR reaction, 10 µL of this lysate was used as a template. 10 µL of each PCR reaction were analysed by agarose electrophoresis (chapter 5.4).

To test for reporter genes autoactivation in bait clones, 3 µL of each yeast suspension in water were arrayed in duplicate onto -trp-his and -trp dropout plates and let grow for two days at 30°C.

Isolation of DNA from yeasts

Buffers and solutions:

Prespheroplasting buffer: 0.05 M EDTA, 1% (v/v) BME, pH 8. Solution was prepared from 0.5 M EDTA stock solution, pH 8 (chapter 5.4).

Lyticase buffer: 0.8 M KCl, 0.01 M EDTA, 0.1% (v/v) BME.

Lyticase solution: 5 mg/mL Lyticase (Sigma, # L4025). Lyophilised enzyme preparation was dissolved in water and stored at -20°C.

Lysis solution: 10% (w/v) SDS.

Proteinase K solution: 20 mg/mL Proteinase K (Sigma). Lyophilised enzyme preparation was dissolved in water and stored at -20°C.

Phenol/chloroform: phenol equilibrated with TE buffer (Sigma, #P4557) and chloroform were mixed in 1:1 ratio and stored at -20°C.

Sodium acetate (NaAc) solution: 3 M NaAc, pH 5.5 was adjusted by concentrated acetic acid (OP-274 pH/Ion Analyser, Radelkis).

For isolation of plasmid DNA from PJ69-4A yeast cells containing bait constructs, 10 mL of -trp dropout medium in 50 mL tube were inoculated by a large fresh colony grown on -trp plates and incubated at 30°C overnight with shaking (Cellstar incubator, Queue Systems). The following day, cells were harvested in the centrifuge at 1900g/10 min (MR22i, Jouan or 4K15, SIGMA Laborzentrifugen) and the pellet was resuspended in 0.5 mL of Prespheroplasting buffer. Cell suspension was transferred to 1.5 mL tube (Deltalab) and incubated at RT/20 minutes. Cells were then harvested at 1900g/3 minutes and resuspended in 400 µL of Lyticase buffer. 40 µL of Lyticase solution was added and suspension was incubated at 28°C/1 hour (Dri-Block DB-3, Techne) with turning the tube upside down every fifteen minutes. After the incubation, 40 µL of Lysis solution and 1 µL of Proteinase K solution were added and mixed gently. Following the incubation at 56°C/30 minutes, equal volume (480 µL) of phenol/chloroform mixture was added and vortexed thoroughly (Vortex-Genie 2, Scientific Industries). Phases were separated at 14000g/5 minutes and maximum of the upper aqueous

phase was transferred to a new tube. Equal volume of chloroform was added, vortexed thoroughly and centrifuged at 14000g/5 minutes. Maximum of the upper aqueous phase was transferred to a new tube and 1/10 volume of NaAc solution and 1 mL of 96% ethanol were added. DNA was precipitated at -20°C/1 hour and collected at 14000g/5 minutes. The pellet was washed in 1 mL of 70% (v/v) ethanol solution with vortexing, collected again at 14000g/5 minutes and dried at RT. Dry pellet was dissolved in 30 µL of water.

Sequence analysis of bait constructs

Inserts of bait constructs propagated in E. coli (chapters 5.8.1 and 5.8.2) were sequenced on slab gel platform as described in chapter 5.7.1. The following primers were used in cycle sequencing reactions with $UMOD^{25-640}$ bait constructs:

5' Cy5-CGGAGCAGTTGTGAGCT 3'
5' Cy5-CGTCCGTCCAGGTGAAGG 3'
5' Cy5-GTCGACCACTTTGTACAAGAAAGCTGGGTG 3'

First two primers are *UMOD* cDNA specific primers with antisense orientation and are labelled by Cy5 fluorescent dye. Third primer sequence is identical to A2 tag (without the stop codon) of lower primers used to amplify bait fragments (chapter *Primer design for bait construction*), again labelled by Cy5. For sequencing of EGF ($UMOD^{25-151}$) and ZP ($UMOD^{331-585}$) bait inserts (chapter *Primer design for bait construction*), only the primer Cy5-A2 was used.

Preparation of yeast protein extracts for WB

Buffers and solutions:

Tris-Cl stock solution: 1 M Tris-Cl, pH 6.8 was adjusted by 1 M NaOH (OP-274 pH/Ion Analyser, Radelkis).

Cracking buffer: 8 M urea, 5% (w/v) SDS, 0.04 M Tris-Cl, 0.1 mM EDTA, 1% (v/v) BME, 0.04% (w/v) BPB. 1 M Tris-Cl stock solution, pH 6.8 was used for the preparation of the buffer.

For extraction of proteins from PJ69-4A yeast cells containing bait constructs, 5 mL of -trp dropout medium in 50 mL tube (TPP) were inoculated by a large fresh colony grown on -trp dropout plates and 5 mL of YPAD medium inoculated by untransformed PJ69-4A strain as a negative control. Cultures were incubated at 30°C overnight with shaking (Cellstar incubator, Queue Systems). Overnight cultures were vortexed for 0.5 to 1 minute to disperse cell clumps (Vortex-Genie 2, Scientific Industries) and OD_{600} was determined (BioPhotometer, Eppendorf). Cultures were diluted to OD_{600} 0.15 by fresh medium to 10 mL and incubated until the OD_{600}

reached 0.6 (about 4 to 5 hours). After chilling cultures on ice, cells were harvested at 1000g/5 minutes at 4°C in 15 mL centrifuge tubes (Gama Group). Supernatant was discarded, pellets were resuspended in 5 mL of ice cold water and centrifuged again at 1000g/5 minutes at 4°C. Pellets were then frozen to -70°C and after 10 minutes thawed in turn in Cracking buffer prewarmed to 60°C with PIC (Sigma) added to concentration of 1% (v/v) right before use. 100 µL of Cracking buffer was used for every 7.5 total OD_{600} units (OD_{600} x culture volume). Cell suspensions were transferred to 1.5 mL tubes (Deltalab) containing 80 µL of glass beads (425-600 µm, Sigma, #G-87723) for every 7.5 total OD_{600} units. Samples were incubated at 70°C/10 minutes (Dri-Block DB-3, Techne) and then vortexed vigorously for one minute. Cell debris, unbroken cells and glass beads were pelleted at 14000g/5 minutes and supernatants were transferred to new 1.5 mL tubes. Tubes with pellets were further incubated at 100°C/3-5 minutes in thermal block and then vortexed vigorously for one minute. Debris, unbroken cells and beads were pelleted again at 14000g/5 minutes and resulting supernatants were combined with first supernatants. If no supernatants were obtained in this second round, 50 µL of Cracking buffer were added to pellets and previous four steps were repeated. Extracts were denatured at 100°C/5 minutes and stored frozen at -70°C.

WB analysis of bait expression

Yeast protein extracts were analysed by SDS-PAGE (chapter 5.2) followed by WB (chapter 5.3) as described. Frozen samples were thawed and directly loaded onto SDS-PAGE gel. WBs were probed by monoclonal anti-GAL4 DNA-BD antibody (BD Biosciences Clontech, #5399-1) diluted 1:10000 followed by HRP-conjugated goat anti-mouse secondary antibody (Pierce) diluted 1:10000. In a separate run, WBs were probed by polyclonal anti-THP antibody followed by HRP-conjugated goat anti-rabbit secondary antibody as described.

Construction of UMOD bait by restriction/ligation

As an alternative approach to $UMOD^{25-640}$ bait construction, we cut out the central part of a pGBD-B-UMOD construct prepared by homologous recombination cloning, but containing multiple point mutations, and replaced it with the same part from pCR3.1-$UMOD^{25-640}$ construct (see chapter *PCR for bait fragments*). This approach was designed to avoid PCR in bait construction.

Both constructs were amplified in and isolated from *E. coli* liquid cultures. Ampicillin supplemented LB medium was inoculated by TOP10 glycerol stock culture of pCR3.1-UMOD construct and DH5α glycerol stock culture of pGBD-B-UMOD. Plasmid DNA was isolated as described (chapter 5.8.2). Following reaction was set to double digest each construct:

Component	Amount
Plasmid DNA	10 µg
10X NEBuffer 4*	10 µL
*Sac*II*	3 U
*Ppu*MI*	3 U
Water	to 20 µL

*Purchased from New England Biolabs; analysis of restriction sites was performed in Oligo software (Molecular Biology Insights); *Sac*II and *Ppu*MI cut at positions c.545 and c.1933, respectively (based on GenBank UMOD mRNA sequence NM_003361.2)

Reactions were incubated at 37°C in the incubator (Biological Thermostat BT 120 M, Ekom) for 3 hours. Then, UMOD cDNA part from pCR3.1-UMOD digest and vector part from pGBD-B-UMOD digest were purified by preparative gel electrophoresis (chapters 5.4 and 5.5). Both fragments were ligated overnight at 16°C in the thermal cycler (PTC-225 DNA Engine Tetrad, MJ Research) by T4 DNA ligase. Reaction mix was set as follows:

Component	Amount
10X Buffer for T4 DNA Ligase*	4 µL
10 mM ATP solution*	4 µL
T4 DNA Ligase (1 U/µL)*	1 µL
UMOD fragment	120 ng
pGBD-B fragment	20 ng
Water	to 40 µL

*Purchased from Fermentas

Molar ratio of insert DNA termini to vector DNA was 3:1. Reaction volume was made up to 100 µL and DNA was extracted and precipitated by phenol/chloroform and ethanol as described (chapter *Isolation of DNA from yeasts*). Purified DNA was used to transform DH5α cells by electroporation (chapter 5.8.1) to propagate the construct. Several resulting colonies were used to inoculate LB-ampicillin medium (chapter 5.8.2). Overnight cultures were PCR screened for the presence of the construct (according to chapter *PCR for bait fragments*; 1 µL of each overnight culture was directly used as a template in PCR reactions). 10 µL of each PCR reaction were analysed by agarose electrophoresis (chapter 5.4). The same cultures were further used for the isolation of plasmid DNA (chapter 5.8.2) and *UMOD* insert was sequenced (chapter *Sequence analysis of bait constructs*). Isolated construct was then introduced to PJ69-4A yeast strain by LiAc/PEG transformation (chapter *Lithium acetate transformation and bait cloning*) and resulting yeast clones were tested for reporter genes autoactivation (chapter *Identification of yeast clones containing baits and a test for reporter genes*) and BD fusion expression (chapters *Preparation of yeast lysates for WB* and *WB analysis of bait expression*).

3.6.1.3 Results and discussion

For our experiments, we chose original-like system based on GAL4 transcription factor domains [231] and enabling simple nutritional selection, homologous recombination cloning [232, 233] and mating-based prey library screening [234, 235].

After invention of uromodulin causative role in FJHN/MCKD2 we prepared several uromodulin-based bait clones, comprising the whole coding sequence (CDS) except for N-terminal signal sequence, or particular domains, namely ZP domain and EGF domain cluster (Figure 3.4).

A

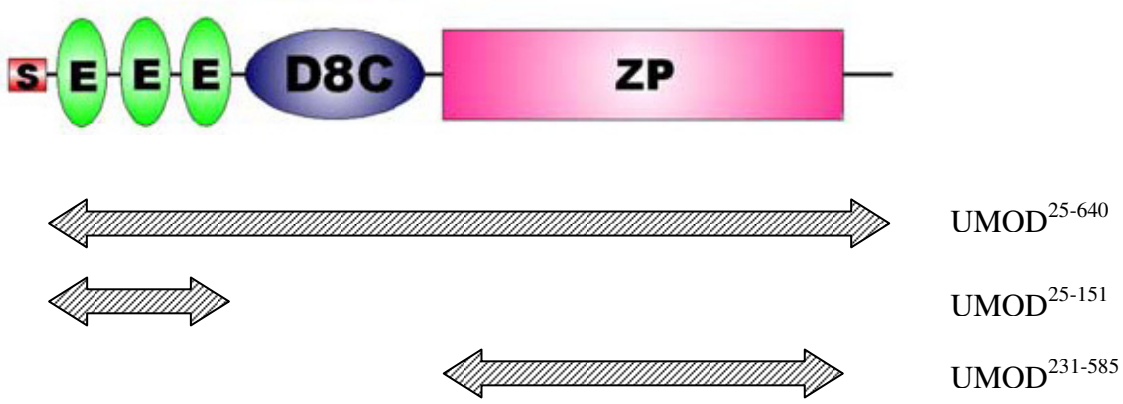

B

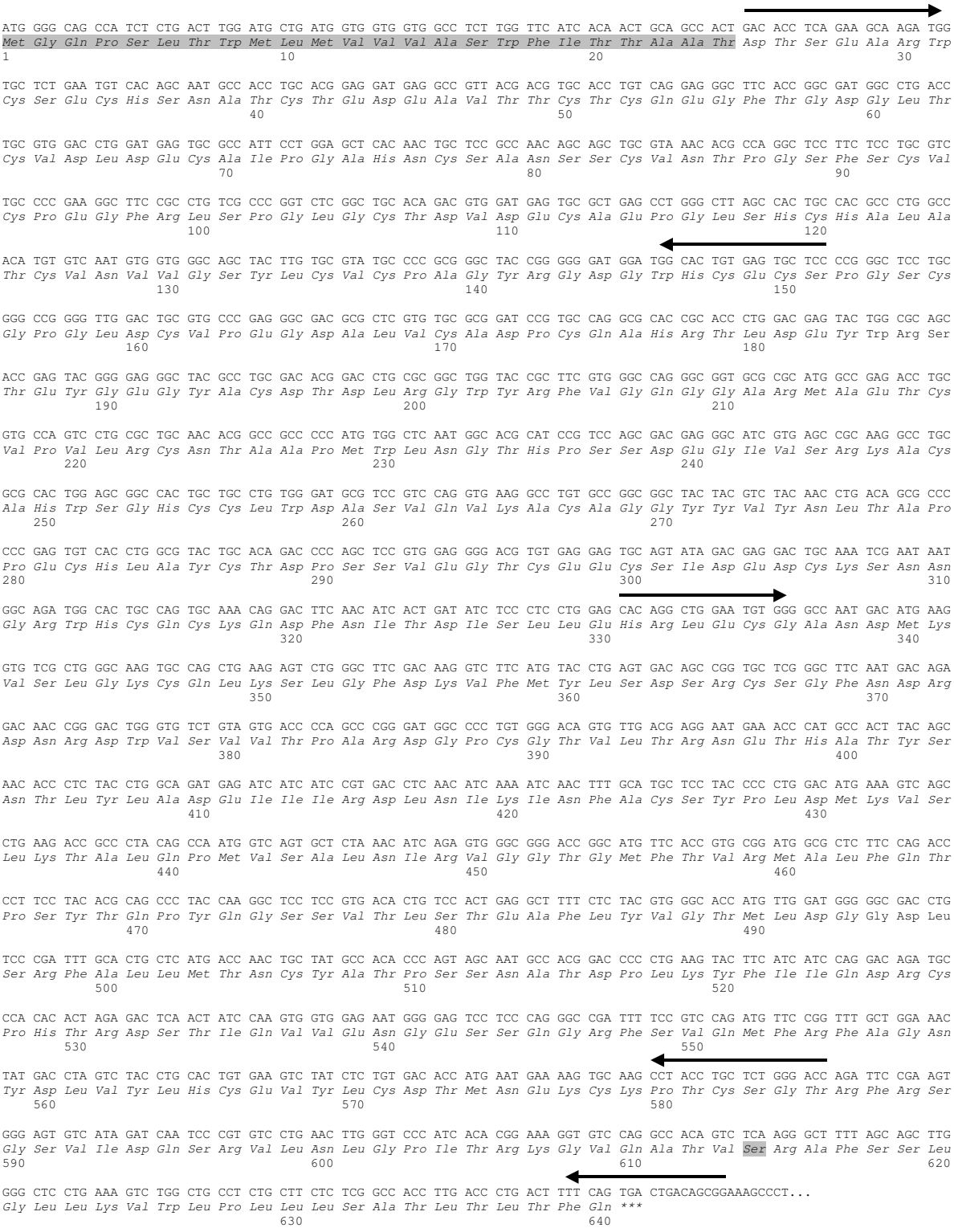

Figure 3.4 Schematic representation of uromodulin bait fragments used in YTHS. A) Double arrows delimit bait fragments on domain structure representation of uromodulin protein. Bait fragment labelling on the right conforms to chapter *Primer design for bait construction*. B) Uromodulin CDS (upper line, based on GenBank sequence NM_003361.2) with numbered three-letter code translation (middle and lower line). Grey-highlighted AAs indicate N-terminal signal sequence and GPI attachment site 614Ser, respectively. Arrows denote position and orientation of PCR amplification primers (according to chapter *Primer design for bait construction*)

N-terminal signal peptide was omitted from UMOD$^{25\text{-}640}$ and UMOD$^{25\text{-}151}$ bait fragments, as YTHS requires fusion proteins to be transferred to the yeast nucleus. Bait fragments were PCR amplified from UMOD cDNA cloned to pCR3.1 eukaryotic expression vector (Figure 3.5) and transformed together with *Bam*HI linearised vector pGBD-B to yeast strain PJ69-4A. Bait construct formation takes place in the yeast cell by homologous recombination between A1 and A2 tags included in bait PCR primers and identical sequences flanking the *Bam*HI site in pGBD-B vector. Resulting clones were tested by PCR for the presence of the construct (Figure 3.6). For this purpose, the same PCR primers as for bait fragment amplification were used as we were unable to perform these screening PCRs with primers based on A1 and A2 sequences.

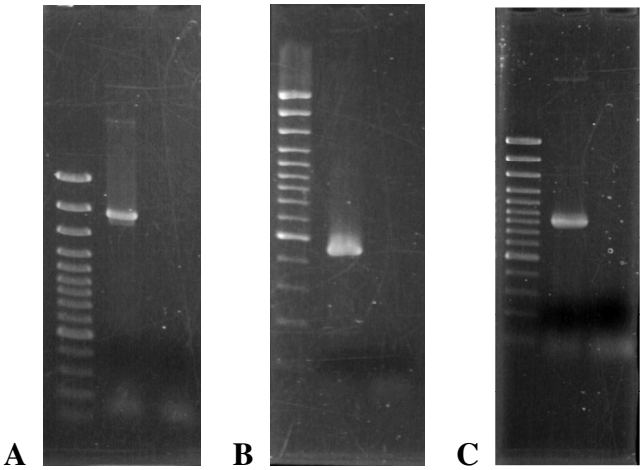

Figure 3.5 Bait fragments PCR products. A) UMOD$^{25\text{-}640}$, B) UMOD$^{25\text{-}151}$, C) UMOD$^{331\text{-}585}$. The order of samples on agarose gels was as follows (from left to right): GeneRuler™ 100bp DNA Ladder Plus marker (Fermentas), bait PCR aliquot, blank (no template) PCR aliquot.

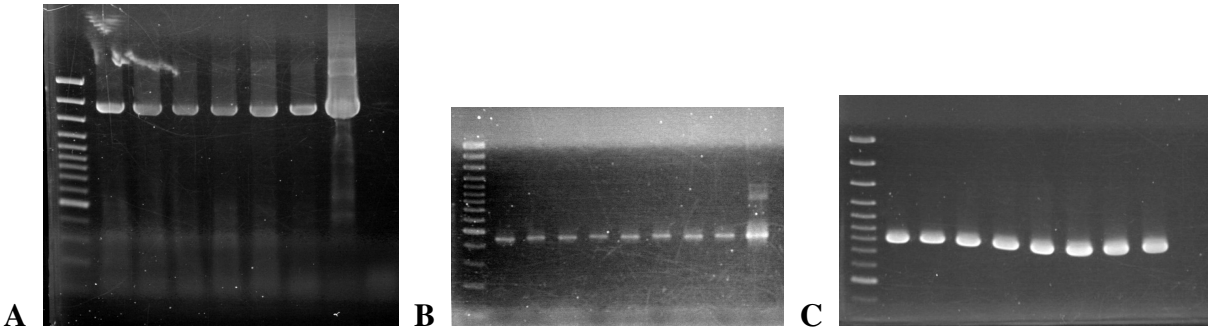

Figure 3.6 PCR screening of yeast bait clones. A) UMOD$^{25\text{-}640}$; order of samples on agarose gel (from left to right): GeneRuler™ 100bp DNA Ladder Plus marker (Fermentas), PCR aliquots of six individual clones, positive control (pCR3.1-UMOD) PCR aliquot, blank (no template) PCR aliquot. B) UMOD$^{25\text{-}151}$; order of samples on agarose gel (from left to right): GeneRuler™ 100bp DNA Ladder Plus marker, PCR aliquots of eight individual clones, positive control (pCR3.1-UMOD) PCR aliquot, blank (no template) PCR aliquot. C) UMOD$^{331\text{-}585}$; order of samples on agarose gel (from left to right): GeneRuler™ 100bp DNA Ladder Plus marker, PCR aliquots of eight individual clones, blank (no template) PCR aliquot.

Positive clones were further tested for activation of reporter genes transcription in the absence of the interactor (autoactivation) by nutritionally selective cultivation on -trp-his dropout plates. Significant autoactivation was observed only in case of some UMOD$^{25\text{-}640}$ bait clones. Only clones showing no autoactivation were selected for further analyses.

Several clones of each bait were tested for expression of bait fusion protein by WB with both anti-GAL4 BD monoclonal antibody and anti-THP polyclonal antibody (Figure 3.7). Two clones with ZP domain bait showed specific signal on WB of correct MW (45 kDa) with anti-GAL4 BD monoclonal antibody. However, this bait fusion protein was not detected by WB with anti-THP polyclonal antibody. One clone with EGF bait showed specific signal on WB with anti-GAL4 BD monoclonal antibody, of which MW (about 19 kDa), however, corresponded to GAL4 BD only (theoretical MW of bait fusion protein was about 30 kDa). In bait clones with the whole UMOD CDS, no specific signal could be detected on WB with either antibody.

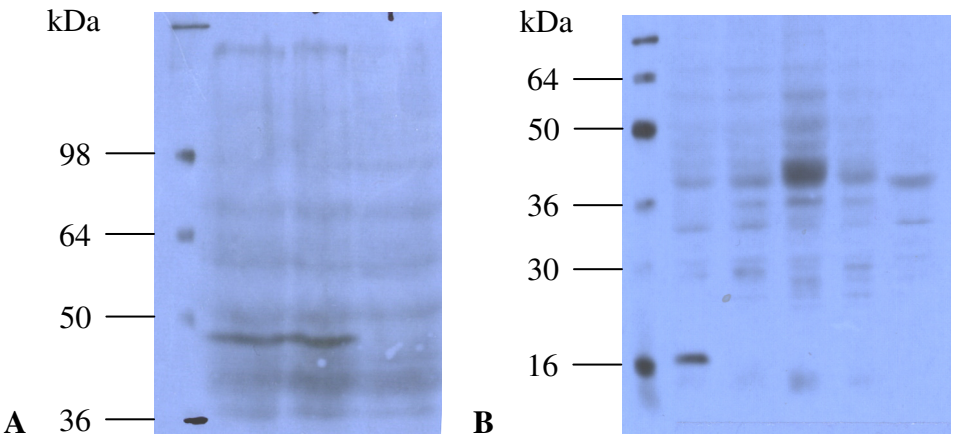

Figure 3.7 GAL4 BD WBs of yeast bait clones lysates. A) UMOD$^{331\text{-}585}$ (ZP) bait; order of samples (from left to right): SeeBlue® Pre-Stained Marker (Invitrogen), lysates of two bait clones, negative control (lysate of nontransformed strain PJ69-4A), B) UMOD$^{25\text{-}151}$ (EGF) bait; order of samples (from left to right): SeeBlue® Pre-Stained Marker, lysates of four bait clones, negative control (lysate of nontransformed strain PJ69-4A).

Selected constructs of each bait were also analysed by sequencing on slab gel platform to verify the correctness of insert sequences. It required DNA isolation from yeasts, its transformation to *E. coli* by electroporation for amplification, isolation from *E. coli* cultures and finally sequencing. We found that all analysed constructs repeatedly showed multiple single nucleotide changes.

To exclude the possibility that these errors arose during PCR amplification of bait fragments, we prepared another UMOD$^{25\text{-}640}$ construct by classical restriction/ligation approach. As a template, we used one of UMOD$^{25\text{-}640}$ bait constructs from which most of the UMOD CDS was cut out by two different restriction endonucleases. The removed part was then replaced by

the same fragment from pCR3.1-UMOD construct. Resulting construct was then transformed to *E. coli* (Figure 3.8) to be amplified and sequenced before the transformation to yeasts. Sequence of the insert was correct. Construct was then transformed to PJ69-4A yeast strain as usually and selected clones were PCR screened (Figure 3.9) and tested as described above. No apparent autoactivation was observed. The sequence of the construct isolated from single yeast clone was proved to be correct. However, expression of bait fusion protein could not be detected by WB with either antibody mentioned above.

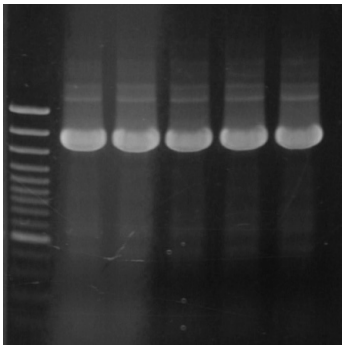

Figure 3.8 PCR screening of *E. coli* bait construct clones. Order of samples on agarose gel (from left to right): GeneRuler™ 100bp DNA Ladder Plus marker (Fermentas), four individual *E. coli* clones PCR aliquots and positive control (pCR3.1-UMOD) PCR aliquot.

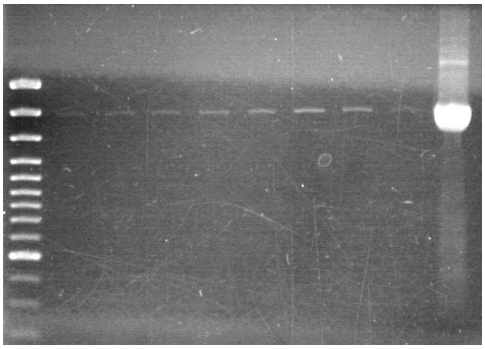

Figure 3.9 PCR screening of yeast bait clones. Order of samples on agarose gel (from left to right): GeneRuler™ 100bp DNA Ladder Plus marker (Fermentas), PCR aliquots of eight individual yeast clones and positive control (pCR3.1-UMOD) PCR aliquot.

In conclusion, we failed to proceed to further steps of two-hybrid screening due to inability to avoid obstacles described above. We also got insecure that YTHS was appropriate tool for studying uromodulin interactions. One of the main drawbacks of classical YTHS is unavailability of proper posttranslational modifications and folding of baits due to the omission of the original signal sequence and due to the fusion to BD directing the resulting fusion protein to the nucleus [236, 237]. In case of uromodulin, which is heavily glycosylated and extensively stabilised by disulfide bridges, this could be critical.

Sequence errors found in constructs prepared by gap repair cloning in yeasts were suggestive of bad tolerance of UMOD cDNA by yeast cells, resulting in higher mutation rate and absence of bait fusion expression. However, correct sequence of the $UMOD^{25-640}$ construct prepared by restriction/ligation spoke against this possibility. In these clones, absence of bait fusion expression could be rather caused by preserving the UMOD C-terminal segment (containing GPI attachment site) in bait constructs that could interfere with proper protein processing. This segment should have been probably omitted in bait design. Finally, PCR amplified bait fragments should had been sequenced in advance of gap repair cloning, which could probably a priori identify potential sequence errors introduced by PCR and suggest the employment of different amplification system.

3.6.2 Concanavalin A (ConA) pull-down assay

3.6.2.1 Introduction

In this assay, we utilised the high oligosaccharide content of uromodulin protein for its immobilisation on sepharose beads with covalently bound lectin (glycan binding protein) ConA [238]. Under certain conditions, lectins are able to bind complex as well as simple saccharides in solution. The majority of known lectins come from plants. In general concept, ConA pull-down assay is similar to immunoprecipitation but instead of capturing antibody immobilised on beads through antibody binding molecule (for example bacterial Protein A or Protein G), protein of which interactors we are intended in (bait) is employed.

3.6.2.2 Specific methods

Buffers and solutions:

Tris-buffered saline (TBS): 0.01 M Tris-Cl, 0.15 M NaCl, pH 7.5 adjusted by 1M NaOH (OP-274 pH/Ion Analyser, Radelkis).

Precondensation of Triton X-114 detergent [239]

As Triton X-114 often contains hydrophilic contaminants, it is reasonable to precondense it by several rounds of phase separation.

1.5 g of detergent was dissolved in 50 mL of TBS in 50 mL tube (TPP) and placed on ice. Solution was then brought to 37°C in a water bath (B.Braun), which made it turbid. Phases were separated by centrifugation at 1000g/10 minutes at RT. Upper phase (detergent-depleted) was removed and discarded. Lower phase (detergent-enriched) was redissolved in an equal

volume of ice-cold TBS and that partitioning was repeated three times. The final detergent-enriched phase contains about 12% of detergent.

Extraction of total proteins from cells by Triton X-114

Buffers and solutions:

Precondensed Triton X-114 (chapter *Precondensation of Triton X-114 detergent*)

2.4-3x10^7 cells of human embryonic kidney cell line 293 (HEK293) (60 mg wet pellet) was resuspended in 5 mL of ice-cold TBS and 1 mL (1/5 volume) of precondensed Triton X-114 (Sigma) and 60 µL (1/100 volume) of PIC (Sigma) were added. Extraction of cells was carried out for 15 minutes on ice with occasional mixing. Lysate was then centrifuged at 10000g/10 minutes at 4°C (centrifuge MR22i, Jouan or 4K15, SIGMA Laborzentrifugen) and supernatant was transferred to a new tube. Pellet was resuspended in 1 mL of ice-cold TBS and homogenised by sonication in cuphorn connected to Ultrasonic Homogenizer 4710 series for 3x15 seconds at 50% output (Cole-Parmer Instrument Co.). Supernatant was warmed to 37°C until it became cloudy. This emulsion was then centrifuged at 1000g/10 minutes and resulting upper and lower phases were collected in separate tubes.

Similarly, 1mL of Tris-Cl homogenate of random kidney tissue (about 75 mg/mL, kindly provided by my colleague Blanka Stibůrková, Ph.D.) was mixed with 4 mL of ice-cold TBS on ice and 1 mL of precondensed Triton X-114 and 60 µL of PIC (Sigma) were added. The mixture was further processed in the same way as described for HEK293 cells. Triton X-114 fractions of the kidney tissue were then tested for uromodulin by SDS-PAGE and WB.

Immobilisation of urinary uromodulin on Concanavalin A-sepharose 4B

Buffers and solutions:

Immobilisation buffer (TBS/Mn/Ca): 0.01 M Tris-Cl, 0.15 M NaCl, 0.001 M $MnCl_2$, 0.001 M $CaCl_2$, pH 7.5 adjusted by 1M NaOH.

For each assay, 50 µL of ConA-sepharose (Sigma #C-9017) suspension was placed to 1.5 mL tube (TPP) and centrifuged at 10000g/1 minute to remove storage buffer (centrifuge MR22i, Jouan or 4K15, SIGMA Laborzentrifugen). Beads were then washed three times with immobilisation buffer and finally resuspended in 50 µL of the same buffer with the addition of 33 µg or 50 µg of uromodulin for HEK293 or kidney tissue assay, respectively. Mixture was incubated at 37°C/1 hour (Biological Thermostat BT 120 M, Ekom) with gentle mixing (Multi RS-60 rotamixer, Biosan), beads were collected by centrifugation and washed three times with

immobilisation buffer and finally resuspended in TBS to the original volume. For blank assay, ConA beads were processed in the same way except that incubation at 37°C was carried out only with immobilisation buffer, without the addition of uromodulin.

ConA pull-down assay

To 50 µL of uromodulin coated beads suspension or blank beads suspension, 100 µL of each HEK293 or kidney tissue fraction were added. The mixture was incubated for 90 minutes on ice with occasional gentle mixing. Beads were then collected in the centrifuge at 10000g/1 minute and washed tree times by ice-cold TBS. After the last wash, supernatant was aspirated and beads were resuspended in 100 µL of 1X SDS-PAGE sample buffer and denatured at 95°C/10 minutes (Dri-Block DB-3, Techne). Beads were then separated in the centrifuge 10000g/5 minutes and 20-µl aliquot of the supernatant was analysed by SDS-PAGE followed by Sypro Ruby (Molecular Probes) staining.

3.6.2.3 Results and discussion

As the bait, we used uromodulin isolated from healthy male urine. Initially, we have determined uromodulin by WB in bead supernatant after immobilisation as well as in subsequent washes to find uromodulin saturation threshold for sepharose beads. Coated beads were incubated with two different cell lysates prepared by means of non-ionic detergent Triton X-114.

Triton X-114 forms two-phase micellar system in aqueous solutions at temperatures above 20°C, while at low temperatures forms a homogenous solution. It is therefore possible to use this detergent for separation of membrane and soluble cell fractions during lysis. Cold lysis buffer first lyses cells and any insoluble material is separated by centrifugation. Resulting pellet contains some of the GPI-anchored species and cellular components insoluble in non-ionic detergents. If the supernatant is warmed, amphiphilic proteins (including GPI-modified) partition to detergent-rich phase while hydrophilic (soluble) proteins partition to detergent-depleted phase. Both phases can be subsequently separated by centrifugation at room temperature with detergent rich phase sedimenting on the bottom of the test tube [239].

Partitioned lysates were prepared from HEK293 cells and from kidney tissue homogenate. HEK293 cell line does not express uromodulin and it was chosen to probe for general interactors. Kidney homogenate, on the other hand was chosen to probe for kidney specific interactors.

WB of the three fractions of kidney homogenate showed uromodulin to be most abundant in the pellet (non-ionic detergent insoluble material) (Figure 3.10). Detergent insolubility of some GPI proteins develops shortly after synthesis [142], and is thought to be due to aggregation of GPI modified proteins with glycosphingolipids during secretion.

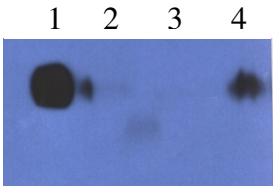

Figure 3.10 Uromodulin WB of Triton X-114 fractions of kidney homogenate. Samples: 1) uromodulin standard (isolated from healthy male urine), 2) detergent depleted (upper) fraction, 3) detergent enriched (lower) fraction, 4) detergent insoluble fraction (pellet).

Uromodulin coated beads were incubated with all three phases (pellet, detergent-rich and detergent depleted phase) recovered by Triton X-114 partitioning of both cell sources. As blanks, we used ConA beads with no uromodulin in ConA binding reaction and otherwise treated in the same way as coated beads. Material bound on beads during incubation with fractions of lysates was released under denaturing condition and analysed by SDS-PAGE (Figure 3.11 and 3.12).

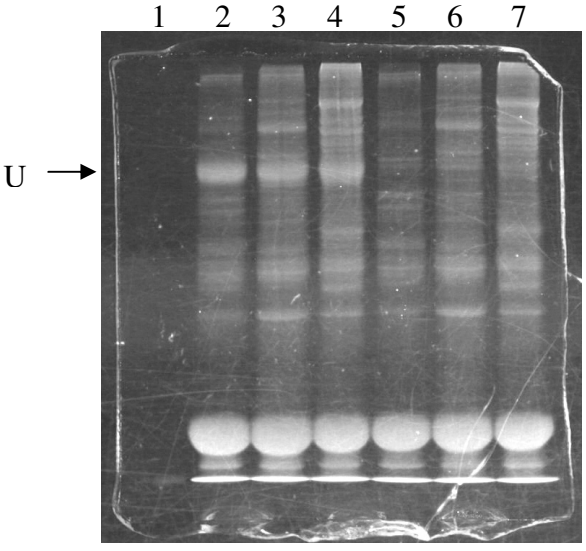

Figure 3.11 ConA pull-down assay of kidney homogenate fractions (SDS-PAGE). Samples: 1) SeeBlue® Pre-Stained Marker (Invitrogen), not stained, 2) detergent insoluble fraction (pellet), 3) detergent depleted (upper) fraction, 4) detergent enriched (lower) fraction, 5) the pellet fraction-blank, 6) upper fraction-blank, 7) lower fraction-blank; U - uromodulin.

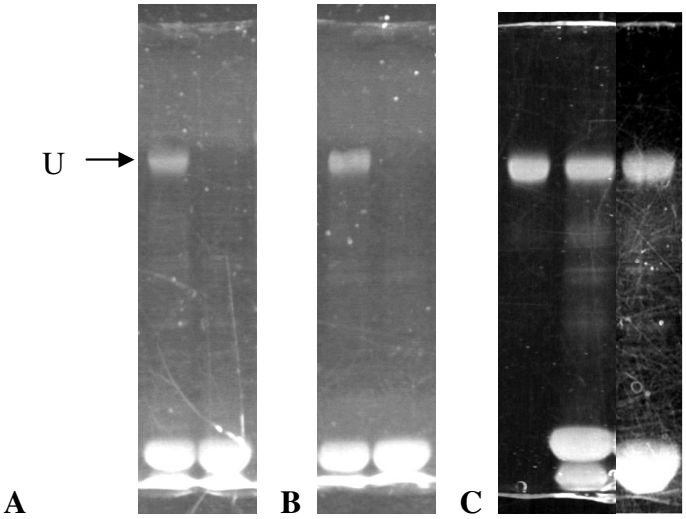

Figure 3.12 ConA pull-down assay of HEK293 fractions (SDS-PAGE). Order of samples (from left to right): A) detergent insoluble fraction (pellet), the pellet fraction-blank B) detergent depleted (upper) fraction, upper fraction-blank, C) uromodulin standard (isolated from healthy male urine), detergent enriched (lower) fraction, lower fraction-blank; U - uromodulin.

By this approach, however, we have never observed a protein(s) specifically present in uromodulin-containing incubations, i.e. not present also in blank reactions. However, uromodulin isolated from urine might not be suitable for this assay. It is known that peptide as well as glycosyl structure of kidney-synthesised uromodulin and its counterpart found in urine differ (chapter 3.1.3). Moreover, binding of uromodulin to solid phase through its glycosyl chains might block its potential binding sites. Low amounts of potential interactors in examined samples or transient character of interaction could also explain our results. Another possibility is that uromodulin has no interacting proteins *in situ*.

In the meantime, there were described interactions between uromodulin and immunoglobulin G (IgG) [240], complement components 1q and 1 [241, 242], recombinant interleukin-1 (rIL-1) [105] and recombinant tumour necrosis factor (rTNF) [243] *in vitro*. Uromodulin was also co-immunoprecipitated with Na^+-K^+-ATPase (NKA) from rat kidney protein extract and cultured TALH cells, which probably reflects their common localization in lipid rafts [244].

4 CONCLUSIONS

1) We were able to gather one of the largest sets of families with UAKD in the world. Through international collaboration and urinary uromodulin screening, we were able to gain biological materials from members of altogether 31 families (including unpublished results).

2) Using genotyping, linkage analysis and *UMOD* sequencing we proved genetic heterogeneity of the disease. We identified *UMOD* mutation in 8 families (including unpublished results) and characterised molecular properties and aberrant cellular trafficking of 6 mutant recombinant UMOD proteins.

3) By genome wide linkage analysis we identified new UAKD locus on chromosome 1q41. In large Belgian family (BE1) with atypical FJHN, we identified single locus and single haplotype segregating with the disease, performed sequence analysis of 9 candidate genes in which we found no classical deleterious mutation. Finally, we found heterozygous deletion mutation in *REN* gene and characterised molecular properties and numerous cellular effects of mutant recombinant renin and suggested probable pathogenetic mechanisms.

4) We provided evidences that alteration of uromodulin biology is common to genetically heterogenous UAKD. We showed decreased UMOD urinary excretion in almost all investigated families. Accordingly, immunohistochemical analyses of kidney sections revealed abnormal uromodulin expression in FJHN/MCKD patients with different genetic backgrounds.

5) We were not able to identify any uromodulin interacting proteins by means of yeast two-hybrid system and concanavalin A pull-down assays.

Practical outputs

1) We introduced numerous molecular genetic, molecular biological and biochemical methods for the analysis of recombinant as well as native UMOD and renin proteins.

2) Western blot of urinary uromodulin is used routinely in our Institute for selective screening of hyperuricaemic conditions. By this approach, we identified 5 Czech UAKD families and subsequently *UMOD* mutation in 3 of them (including unpublished results).

Through international collaboration, we similarly identified 1 Danish family with *UMOD* mutation and 5 families from the United Kingdom, 3 of them with *UMOD* mutation (unpublished results).

3) We provide unique, complex diagnostic service for this group of disorders.

Special notes

1) Oral presentation of our results, subsequently published in our article titled "Alterations of uromodulin biology: a common denominator of the genetically heterogeneous FJHN/MCKD syndrome" (chapter 9.2.2), was awarded the best presentation on the 31st congress of Czech Society for Nephrology held 24. 6. 2006 in Hradec Králové.

2) Figure 5 in our article "Alterations of uromodulin biology: a common denominator of the genetically heterogeneous FJHN/MCKD syndrome" (chapter 9.2.2) titled "Cellular localization of wildtype UMOD and individual UMOD mutants in permeabilised AtT-20 cells studied 18 h after transfection" was selected by the editors of Kidney International journal for cover page of the second September issue (6th issue of 70th volume) in 2006.

5 GENERAL METHODS

Unless otherwise stated, water used in experiments was ultrapure water prepared from common distilled water in Milli-Q® RG Ultrapure Water Purification System (Millipore).

5.1 Isolation of uromodulin from urine

Urinary uromodulin was isolated from one litre of healthy male urine collected between 7 am and 17 pm by the salt out method similar to original procedure reported by Tamm and Horsfall [91]. NaCl was added to urine to 0.58 M and the solution was stirred overnight at 4°C. Precipitate was collected in high-speed benchtop centrifuge (MR22i, Jouan or 4K15, SIGMA Laborzentrifugen) at 5000g/20 minutes into 50 mL tubes (TPP), washed once with 0.58 M NaCl solution and then collected again at 5000g/10 minutes. After aspiration of supernatant, precipitate was dissolved in distilled water, transferred to 1.5 mL test tubes (Deltalab) and centrifuged 5000g/10 minutes to remove insoluble material. Supernatant from all tubes was collected to presoaked 25 mm dialysis tube (Sigma), dialysed against four litres of distilled water at 4°C for 3 days and then lyophilised (Christ Alpha 1-4, B.Braun Biotech International). Lyophilisate was weighted and dissolved in water with 0.02% (w/v) NaN3. The evaluation of purified uromodulin was done by sodium dodecyl sulphate polyacrylamide gel electrophoresis

as well as by Western blot with mouse monoclonal (Cedarlane) or rabbit polyclonal (Biogenesis) anti-THP antibody as described in chapters 5.2 and 5.3.

5.2 Sodium dodecyl sulphate polyacrylamide gel electrophoresis (SDS-PAGE)

Buffers and solutions:

Acrylamide/bisacrylamide stock solution: 29% (w/v) acrylamide (AA), 1% (w/v) methylenebisacrylamide (bisAA).

4X SDS-PAGE separating gel buffer: 1.5 M Tris base, 0.0139 M SDS, pH 8.8 was adjusted by 1 M HCl (OP-274 pH/Ion Analyser, Radelkis).

4X SDS-PAGE stacking gel buffer: 0.5 M Tris base, 0.0139 M SDS, pH 6.8 was adjusted by 1 M HCl.

10X SDS-PAGE running buffer: 1.918 M glycine, 0.248 M Tris base, 0.0347 M SDS, pH 8.3 (not adjusted)

6X SDS-PAGE sample buffer: 0.012% (w/v) bromphenol blue, 30% (v/v) glycerol, 0.347 M SDS, 6% (v/v) β-mercaptoethanol (BME).

10% ammonium persulphate (APS): 1 g of APS was dissolved in 10 mL of water, aliquoted and stored at -20°C.

Coomassie blue staining solution: 0.1% (w/v) coomassie blue R250, 50% methanol (v/v), 10% (v/v) acetic acid. Coomassie blue was dissolved in methanol before addition of other components.

Coomassie blue destain solution: 10% (v/v) methanol, 10% (v/v) acetic acid.

Sypro Ruby fix solution: 50% (v/v) methanol, 7% (v/v) acetic acid, prepared freshly.

Sypro Ruby wash solution: 10% (v/v) methanol, 7% (v/v) acetic acid, prepared freshly.

Separating gels were prepared by mixing AA/bisAA stock solution, 4X SDS-PAGE separating gel buffer and water. Polymerisation was initiated by addition of tetramethyl-ethylenediamine (TEMED) and APS solution to concentration 0.06% (v/v and w/v, respectively). This mixture was poured between assembled glasses and overlaid by water. After minimum 45 minutes, water was poured off and stacking gel prepared by mixing AA/bisAA stock solution, 4X SDS-PAGE stacking gel buffer, water and TEMED and APS solutions to concentrations 0.152% (v/v) and 0.14% (w/v), respectively, was poured. Comb was set immediately and after minimum 15 minutes, assembly was fixed in vertical electrophoresis apparatus (MightySmall II SE250 or SE260, Hoefer). Samples were prepared by mixing with 6X SDS-PAGE sample buffer in 1.5 mL or 0.2 mL (Eppendorf) tubes and denaturation at 100°C for five minutes in dry block thermostat (Dri-Block DB-3, Techne) or PCR thermal cycler

(PTC-225 DNA Engine Tetrad, MJ Research). After pouring 1X SDS-PAGE running buffer, samples were loaded and electrophoresed at 100V in stacking gel and at up to 160V in separating gel.

Gels after electrophoresis were stained in Coomassie blue staining solution for at least 30 minutes and destained by at least two successive washes in Coomassie blue destain solution. Alternatively, gels were stained by SYPRO® Ruby protein gel stain (Molecular Probes) solution according to manufacturer's instructions for Rapid Protocol. Images were acquired by digital camera (Camedia C2000Z, Olympus) on UV transilluminator (Macrovue 2011, LKB).

5.3 Western blotting (WB)

Buffers and solutions:

Blotting buffer: 0.048 M Tris Base, 0.039 M glycine, 0.037% (w/v) SDS, 20% (v/v) methanol, pH 9.2 (not adjusted)

10X Phosphate-buffered saline (10X PBS): 1.37 M NaCl, 0.27 M KCl, 0.78 M Na_2HPO_4, 0.15 M KH_2PO_4, pH 7.3 was adjusted by 1M NaOH (OP-274 pH/Ion Analyser, Radelkis).

1X Phosphate-buffered saline (PBS): prepared by ten-fold dilution of 10X PBS with water.

Blocking buffer (PBS-T/5%BSA): 0.137 M NaCl, 0.027 M KCl, 0.078 M Na_2HPO_4, 0.015 M KH_2PO_4, pH 7.3, 0.05% (v/v) Tween 20, 5% (w/v) bovine serum albumin (BSA).

Washing buffer (PBS-T): 0.137 M NaCl, 0.027 M KCl, 0.078 M Na_2HPO_4, 0.015 M KH_2PO_4, pH 7.3, 0.05% (v/v) Tween 20.

Antibody buffer (PBS-T/0.1%BSA): 0.137 M NaCl, 0.027 M KCl, 0.078 M Na_2HPO_4, 0.015 M KH_2PO_4, pH 7.3, 0.05% (v/v) Tween 20, 0.1% (w/v) BSA.

Proteins separated by SDS-PAGE were transferred onto PVDF membranes (Immobilon-P, Millipore) in semidry blotting apparatus (PHERO-multiblot, Biotec-Ficher). Blotting buffer was prepared and stored without methanol, which was added right before use. Gels were soaked in blotting buffer for at least twenty minutes. In parallel, PVDF membranes were activated in methanol for 20 seconds and then soaked in blotting buffer. Before blotting, six blotting papers were soaked in blotting buffer. Blotting sandwich was assembled onto carbon anode as follows: three blotting papers-PVDF membrane-gel-three blotting papers. Sandwich was then covered by carbon cathode wetted by blotting buffer. Transfer was carried out at 1.6 mA/cm^2 of blotting sandwich for one hour.

Membranes were blocked in blocking buffer for one hour, washed three times for seven minutes in washing buffer and incubated for one hour with primary monoclonal (Cedarlane) or

polyclonal (Biogenesis) anti-THP antibody diluted 1:2000 or 1:10000, respectively, in antibody buffer. Following washing in washing buffer three times for 7 minutes, membranes were incubated for 45 minutes with secondary goat anti-mouse IgG or goat anti-rabbit IgG antibody conjugated to horseradish peroxidase (HRP) (Pierce) diluted 1:5000 or 1:10000, respectively, in antibody buffer. Following washing in washing buffer once for 15 minutes, twice for 7 minutes and finally once for 7 minutes in PBS, membranes were developed by SuperSignal West Pico Chemiluminescent Substrate Kit (Pierce) according to manufacturer's instructions. Chemiluminescent signal was detected manually by exposition to Medical X-ray Blue Films (Agfa). Films were developed for 2 minutes and fixed for 2 minutes in Fomadent set solutions (Foma Bohemia). After extensive washing in tap water, films were let dry.

All antibody incubations and washes were performed during horizontal shaking on KM-2 Miniature Shaker (Edmund-Bühler Gmbh) or Orbital Shaker OS-20 (Biosan) at 60 revolutions per minute (rpm).

5.4 DNA electrophoresis in agarose gel

Buffers and solution:

0.5 M disodium ethylenediamine tetraacetate (EDTA): 18.6 g of $Na_2EDTA.2H_2O$ was mixed with 70 ml of water and 1M NaOH was added during mixing until dissolution of solid, then pH was checked (OP-274 pH/Ion Analyser, Radelkis) and volume was made up to 100 mL.

10X TBE (Tris-Borate-EDTA): 0.89 M Tris Base, 0.89 M Boric acid, 0.02 M EDTA.

50X TAE (Tris-Acetate-EDTA): 2 M Tris Base, 5.7 % (v/v) acetic acid, 0.1 M EDTA.

10X loading buffer: 20% (w/v) Ficoll 400, 0.1 M EDTA, 1% (w/v) SDS, 0.25% (w/v) BPB, 0.25% (w/v) xylene cyanol (optional). 0.5 M EDTA stock solution, pH 8 was used for the preparation of the buffer.

1000X Ethidium bromide solution (EtBr): 0.5 mg/mL EtBr.

Agarose (Serva, #11404) was mixed with 1X TBE buffer to desired concentration and the suspension was boiled in microwave oven (MW 736, Clatronic) until clearing. Hot liquid gel was then cooled to about 40°C, poured to electrophoretic chamber and let solidify. Gel was then covered by 1X TBE buffer, samples were mixed with 10X loading buffer in 1:9 ratio and loaded on the gel together with appropriate DNA molecular weight marker. Electrophoresis was performed at the intensity of 10 V/cm (PS143 electrophoresis power supply, EMBL). For DNA visualisation, the gel was submerged into 1X EtBr solution. Images were acquired by digital camera (Camedia C2000Z, Olympus) on UV transilluminator (Macrovue 2011, LKB). If DNA

fragments were to be isolated from the gel, the same procedure was followed but 1X TAE buffer was used for gel preparation and electrophoresis.

5.5 Isolation of DNA fragments from the agarose gel

After separation of DNA fragments by 1% (w/v) agarose gel electrophoresis (chapter 5.4), gel was briefly submerged to 1X EtBr solution, fragments of interest were excised from the gel by clean scalpel on UV transilluminator (Macrovue 2011, LKB) and slices were placed to 1.5 ml tubes (Deltalab). DNA was then extracted from slices by the Wizard® SV Gel and PCR Clean-Up System (Promega) according to manufacturer's instructions. Briefly, gel slice was differentially weighed and 10 μL of Membrane Binding Solution (kit component) per 10 mg of gel slice was added. Mixture was then vortexed (Vortex-Genie 2, Scientific Industries) and incubated at 65°C (Dri-Block DB-2A thermostat, Techne) with occasional mixing until complete dissolution of the slice. SV Minicolumn and Collection Tube (kit components) were then assembled, gel solution was transferred to the assembly and let stand at RT/1 minute. Assembly was centrifuged at 16000g/1 minute (5415 D centrifuge, Eppendorf), flow-through was discarded and column was washed twice with 700 and 500 μL of Membrane Wash Solution (kit component) with added ethanol at 16000g/1 and 5 minutes, respectively. Empty assembly was then centrifuged at 16000g/1 minute with the centrifuge lid off. Minicolumn was transferred to a clean 1.5 ml tube, 50 μL of Nuclease Free-Water (kit component) was added and after incubation at RT/1 minute, DNA was eluted at 16000g/1 minute.

5.6 Determination of DNA concentration

Concentration and quality of DNA isolated from agarose gels or from bacterial cultures were determined by either BioPhotometer (Eppendorf) or Nanodrop® ND-1000 Spectrophotometer (Nanodrop Technologies). For BioPhotometer (one point measurement at 280 nm), 100 μL of diluted sample (1:99) were used. For Nanodrop ND-1000 (spectral measurement from 220 nm to 350 nm) operated by Nanodrop software v3.1.0, 1.5 μL of neat sample was used. In both cases, appropriate blanking was used.

5.7 DNA sequencing

5.7.1 Cycle sequencing on slab gel platform

Buffers and solutions:

10X TBE for sequencing: 1 M Tris Base, 0.91 M Boric acid, 0.01 M EDTA. The solution components were dissolved in water and solution was filtered through VacuCap® 60 Filter Unit with 0.2 µm membrane (Pall, #4632).

Sequencing polymer: 5.5% Long Ranger Gel Solution (Cambrex), 6 M urea in 1.5X TBE for sequencing. Urea was dissolved in water and then 10X TBE for sequencing stock solution and 50% Long Ranger Gel Solution stock (Cambrex) were added. Solution was then gently stirred at RT/30 minutes (MR 3001K magnetic stirrer, Heidolph) with PlusOne™ Amberlite IRN-150L resin (Amersham Biosciences) added to 10% (w/v) and then filtered through Stericup™ Filter Unit with 0.22 µm Millipore Express PLUS membrane (Millipore, #SCGP U05 RE).

Stop sequencing mix: 0.6% (w/v) dextran blue, 0.02 M EDTA in formamide. Formamide was stirred at RT for 30 minutes (MR 3001K magnetic stirrer, Heidolph) with AG® 501-X8 resin (Bio-Rad, #142-6424) added to 10% (w/v). Mixture was then filtered through Whatmann 1 filter paper and dextran blue and EDTA were added to the filtrate.

Dideoxyadenosine triphosphate (ddATP) termination mix: 1 mM each deoxyadenosine triphosphate (dATP), deoxycytidine triphosphate (dCTP) and deoxythymidine triphosphate (dTTP), 0.67 mM deoxyguanosine triphosphate (dGTP), 0.33 mM 7-deaza-dGTP, 0.00833 mM ddATP.

Dideoxycytidine triphosphate (ddCTP) termination mix: 1 mM each deoxyadenosine triphosphate (dATP), deoxycytidine triphosphate (dCTP) and deoxythymidine triphosphate (dTTP), 0.67 mM deoxyguanosine triphosphate (dGTP), 0.33 mM 7-deaza-dGTP, 0.00833 mM ddCTP.

Dideoxyguanosine triphosphate (ddGTP) termination mix: 1 mM each deoxyadenosine triphosphate (dATP), deoxycytidine triphosphate (dCTP) and deoxythymidine triphosphate (dTTP), 0.67 mM deoxyguanosine triphosphate (dGTP), 0.33 mM 7-deaza-dGTP, 0.00833 mM ddGTP.

Dideoxythymidine triphosphate (ddTTP) termination mix: 1 mM each deoxyadenosine triphosphate (dATP), deoxycytidine triphosphate (dCTP) and deoxythymidine triphosphate (dTTP), 0.67 mM deoxyguanosine triphosphate (dGTP), 0.33 mM 7-deaza-dGTP, 0.00833 mM ddTTP.

10% APS: 1 g of ammonium persulphate was dissolved in 10 mL of water, aliquoted and stored at -20°C.

For cycle sequencing of polymerase chain reaction (PCR) products or plasmids on slab gel platform we used dideoxynucleotide termination approach utilising universal primers

labelled by carbocyanine 5 (Cy5) fluorescent dye on their 5'ends and termostable DNA polymerase (AmpliTaq® FS DNA Polymerase, Applied Biosystems). Accordingly, PCR oligonucleotides were designed to be composed of two distinct parts: target specific part on 3' end and sequence resembling labelled universal primer on 5' end. Target specific parts were designed mainly using Oligo 6.44 software (Molecular Biology Insights). We used following labelled primers for cycle sequencing (Genset Oligos):

T7: 5´ Cy5-AATACGACTCACTATAG 3´
RP: 5´ Cy5-GAAACAGCTATGACCATG 3´

They conform to T7 priming site and M13 Reverse priming site present in the vicinity of multiple cloning site of many cloning vectors. We usually added the T7 sequence to a PCR upper primer and RP sequence to a lower primer.

For single sequence analysis, following reaction mix was set to 1.5 ml tube (Deltalab):

Component	Amount
Template DNA	100-200 fmol*
10X PC2 buffer**	2.8 µL
2 µM Cy-5 labelled sequencing primer	1.5 µL
AmpliTaq® FS DNA Polymerase	0.7 µL
25 mM $MgCl_2$ solution**	3.4 µL
Water	to 21 µL

*Amount of substance of DNA fragments were calculated with the assumption that one base pair corresponds to 660 g/mol.

**Purchased from Ab Peptides, Inc.

5 µL of this mix was dispensed to each of four 0.2 mL tubes (Eppendorf) each containing 2 µL of corresponding dideoxynucleoside triphosphate (ddNTP) termination mix. Tubes were then placed to the thermal cycler (PTC-225 DNA Engine Tetrad, MJ Research) and went through the following thermal program:

Segment	Number of cycles	Temperature (°C)	Time (s)
1	1	95	180
2	35	95	15
		50	25
		68	40
3	1	68	300
4	1	15	for ever

After the program termination, 5 µL of Stop sequencing mix were added to each tube. Reaction tubes were then placed to thermal cycler again, denatured at 95°C/3 minutes and at 85°C/10

minutes and then placed immediately on ice. Usually 9 μL from each tube were loaded on sequencing gel.

The gel was prepared by mixing Sequencing polymer with APS and TEMED to concentrations of 0.054% (w/v and v/v, respectively). As an anodic and cathodic buffer, 0.5X TBE for sequencing was used. Electrophoresis was run in ALFexpress™ or ALFexpress™ II DNA Automated Sequencer under following conditions:

Parameter	Value
Runtime	700 minutes
Voltage	1500 V
Current	60 mA
Power	25 W
Temperature	55°C

ALFexpress™ operation, data collection and their analysis were assisted by Alfwin™ Sequence Analyser 2.0 software (Pharmacia Biotech).

5.7.2 Cycle sequencing on capillary platform

On this platform, we used complete instrumentation and chemistry from Applied Biosystems. BigDye Terminator v3.1 Cycle Sequencing Kit was used for cycle sequencing reactions. This kit contains ddNTPs each labelled by a different fluorescent dye, enabling the use of unlabelled primers for sequencing, including those used for PCR amplification of sequenced DNA fragments. Template DNA was purified by ethanol precipitation according to manufacturer's instructions. Following thermal program was acquired for cycle sequencing:

Segment	Number of cycles	Temperature (°C)	Time (s)
1	1	96	60
2	25	96	10
		50	5
		60	240
3	1	15	for ever

After program termination, Hi-Di™ Formamide was added to each reaction and after denaturation at 95°C/3 minutes and cooling down on ice, samples were run on ABI Prism 3100-Avant™ Genetic Analyzer equipped with 50 cm four-capillary array filled with POP-6™ Polymer for 3100/3100-Avant™ Genetic Analyzers. Electrode buffer was prepared from 10X Running Buffer. Data were collected by 3100-Avant Data Collection Software v2.0 and analysed by Sequencing Analysis Software v5.1.

All the work along the analytical pipeline except for template preparation and the analysis of resulting sequences were performed by my colleague Helena Myšková, B.Sc. at the Institute of Inherited Metabolic Disorders of First Faculty of Medicine of Charles University in Prague.

5.8 Bacteriology

Bacterial media and solutions:

SOC medium: 2% (w/v) Tryptone, 0.5% (w/v) Yeast extract, 10 mM NaCl, 2.5 mM KCl, 10 mM $MgCl_2$, 10 mM $MgSO_4$, 20 mM glucose. Tryptone, Yeast extract and NaCl were completely dissolved in water first followed by KCl. pH was adjusted to 7 - 7.2 by 1 M NaOH (about 1 mL) and the resulting solution was autoclave sterilised. Filter sterilised (0.22 μm filter Milex GP, Millipore) 1 M stock solutions of $MgCl_2$, $MgSO_4$ and D-glucose were added eventually. Medium was aliquoted and stored at -20°C.

LB (Luria-Bertani) medium: 0.5% (w/v) Yeast extract, 1% (w/v) Tryptone, 1% (w/v) NaCl. All components were dissolved in water and pH was adjusted to 7.0 - 7.2 by 1 M NaOH (about 1 mL) and the resulting solution was autoclave sterilised.

Ampicillin stock solution: 50 mg/mL ampicillin. The antibiotic was dissolved in water, aliquoted and stored at -20°C.

LB (Luria-Bertani) ampicillin plates: 0.5% (w/v) Yeast extract, 1% (w/v) Tryptone, 1% (w/v) NaCl. All components were dissolved in water, pH was adjusted to 7.0 - 7.2 by 1 M NaOH (about 1 mL), agar was added to 1.5% (w/v) and the resulting solution was autoclave sterilised. Medium was let cool down to about 50°C, ampicillin was added to 50 μg/mL, plates were poured and after the solidification stored at 4°C.

Glycerol storage solution: 65% (v/v) glycerol, 0.1 M $MgSO_4$, 0.025 M Tris-Cl pH 8. The solution was prepared from 1 M Tris-Cl stock solution, pH 8 (adjusted by 1M NaOH using OP-274 pH/Ion Analyser, Radelkis) and filter sterilised. For long-term storage of *E. coli* clones, overnight cultures were mixed 1:1 with the glycerol storage solution, frozen in mixture of dry ice and denatured ethanol and stored at -70°C.

Bacterial strains:

XL1-Blue strain has genotype *recA1 endA1 gyrA96 thi-1 hsdR17 supE44 relA1 lac* [F´ *proAB lacI*qZΔ*M15* Tn*10* (Tetr)]. Electrocompetent XL1-Blue cells were kindly provided by Martin Pospíšek, Ph.D. from Laboratory of RNA Biochemistry at Department of Genetics and Microbiology, Faculty of Science of Charles University, Czech Republic.

DH5α strain has genotype F^-, φ80d*lacZ*ΔM15, Δ(*lacZYA-argF*)U169, *deoR*, *recA*1, *endA*1, *hsdR*17(rk^-, mk^+), *phoA*, *supE*44, λ^-, *thi*-1, *gyrA*96, *relA*1. Electrocompetent DH5α cells were kindly provided by my former colleague Miroslav Janošík, Ph.D.

OneShot® TOP10 strain (Invitrogen) has genotype F- *mcr*A Δ(*mrr-hsd*RMS-*mcr*BC) φ80*lac*ZΔM15 Δ*lac*X74 *rec*A1 *ara*D139 Δ(*araleu*) 7697 *gal*U *gal*K *rps*L (StrR) *end*A1 *nup*G.

5.8.1 Transformation of E. coli with plasmid DNA

For propagation of pGBD-B bait constructs isolated from yeasts by Lyticase-phenol/chloroform method (previous chapter), electrocompetent *E. coli* strains XL1-Blue or DH5α were transformed by electroporation in E. coli Pulser (Bio-Rad) according to manufacturer's instructions. Transformed cells were then spread over and selected on LB-ampicillin plates.

Briefly, for one transformation, 40 μL of cold competent cells and 1 μL of DNA preparation were mixed and transferred to cold 0.2 cm cuvettes. Cuvettes were then placed to cold cuvette slide and quickly pulsed at 2.5 kV. Immediately after pulse, 1 mL of RT SOC medium was added to the cuvette. Cell suspension was transferred to 15 mL polystyrene tube (Gama Group) and incubated at 37°C/1 hour with shaking (Cellstar incubator, Queue Systems). After the incubation, 200 μL of suspension were spread over LB-ampicillin plates followed by overnight incubation at 37°C (Biological Thermostat BT 120 M, Ekom).

5.8.2 Isolation of plasmid DNA from E. coli

Plasmid DNA was isolated from *E. coli* liquid cultures by QIAprep Spin Miniprep Kit (Qiagen, #27106). Briefly, 5 mL of LB medium supplemented with ampicillin to the concentration of 50 μg/mL were inoculated by bacterial clone transformed with plasmid of interest and incubated at 37°C overnight with shaking (Cellstar incubator, Queue Systems). The following day, cells were harvested from 4 mL of overnight culture by two successive centrifugations in 2 mL tubes (Deltalab) at 4500g/5 minutes (5415 D centrifuge, Eppendorf). Pellets were resuspended in 250 μL of Buffer P1 (kit component) and 250 μL of Buffer P2 (kit component) were added. Tubes were inverted four to six times and 350 μL of Buffer N3 were added. Tubes were inverted four to six times immediately and centrifuged at 16100g/10 minutes. Supernatants were directly applied to the QIAprep spin columns (kit component). Columns were centrifuged at 16100g/30 seconds and the flow-throughs were discarded. Columns were then washed by 0.75 mL of Buffer PE (kit component) at 16100g/30 seconds, flow-throughs were discarded and columns were centrifuged for one additional minute to remove residual wash buffer. Finally, QIAprep columns were placed in a clean 1.5 ml tubes

(Deltalab) and DNA was eluted by 40 μL of water at 16100g/1 minute after one-minute standing at RT.

6 LIST OF SUPPLIERS

6.1 Chemicals

Ab Peptides, Inc.	St. Louis, MO, USA; www.abpeps.com
Amersham Biosciences Corp.	Piscataway, NJ, USA; www.amersham.com or www.gelifesciences.com
Applied Biosystems	Foster City, CA, USA; www.appliedbiosystems.com
BD Biosciences Clontech	Palo Alto, CA; www.bdbiosciences.com
Biogenesis Ltd	Poole, UK; www.biogenesis.co.uk
Bio-Rad, s.r.o.	Prague, Czech Republic; www.bio-rad.com
Cambrex Corporation	East Rutherford, NJ, USA; www.cambrex.com
Cedarlane	Hornby, Ontario, Canada; www.cedarlanelabs.com
CONLAC, s.r.o.	Prague, Czech Republic; www.conlac.cz
Fermentas International, Inc.	Burlington, Ontario, Canada; www.fermentas.com
Foma Bohemia, s.r.o.	Hradec Králové, Czech Republic, www.foma.cz
Generi Biotech, s.r.o.	Hradec Králové, Czech Republic; www.generi-biotech.com
Genset Oligos	La Jolla, CA, USA; www.proligo.com or www.sigmaaldrich.com
Lach-Ner, s.r.o.	Neratovice, Czech Republic; www.lach-ner.com
Molecular Probes	Eugene, OR, USA; http//probes.invitrogen.com
New England Biolabs	Ipswich, MA, USA; www.neb.com
Penta	Prague, Czech Republic; www.penta-chem.cz
Pharmacia Biotech AB	Uppsala, Sweden; www.gelifesciences.com
Pierce	Rockford, IL, USA; www.pircenet.com or www.thermo.com
Promega	Madison, WI, USA; www.promega.com
ProZyme, Inc.	San Leandro, CA, USA; www.prozyme.com
RNDr. Jan Kulich, s.r.o.	Hradec Králové, Czech Republic; www.kulich.cz
Roche, s.r.o.	Prague, Czech Republic; www.roche-applied-science.com
Serva Electrophoresis GmbH	Heidelberg, Germany; www.serva.de

Sigma-Aldrich, s.r.o.	Prague, Czech Republic; www.sigmaaldrich.com
USB Europe GmbH	Staufen, Germany; www.usbweb.com

6.2 Consumables

Agfa-Gevaert N.V.	Mortsel, Belgium; www.agfa.com
Deltalab, S.L.	Rubí (Barcelona), Spain; www.deltalab.es
Eppendorf AG	Hamburg, Germany; www.eppendorf.com
Gama Group, a.s.	Trhové Sviny, Czech Republic; www.gama.cz
Millipore	Billerica, MA, USA; www.millipore.com
Pall Life Sciences	Ann Arbor, MI, USA; www.pall.com
Sigma-Aldrich s.r.o.	Prague, Czech Republic; www.sigma-aldrich.com
TPP	Trasadingen, Switzerland; www.tpp.ch

6.3 Instruments

A&D Engineering, Inc.	San Jose, CA, USA; www.andweighing.com
Amersham Biosciences Corp.	Piscataway, NJ, USA; www.amersham.com or www.gelifesciences.com
Applied Biosystems	Foster City, CA, USA; www.appliedbiosystems.com
B.Braun Biotech International GmbH	Melsungen, Germany; www.sartorius.de
Biosan	Riga, Latvia; www.biosan.lv
Biotec-Fischer GmbH	Reiskirchen, Germany; www.biotec-fischer.de
BioTek Instruments, Inc.	Winooski, VT, USA; www.biotek.com
Clatronic International GmbH	Kempen, Germany; www.clatronic.de
Cole-Parmer Instrument Co.	Chicago, IL, USA; www.coleparmer.com
Consort nv	Turnhout, Belgium; www.consort.be
Edmund Bühler GmbH	Hechingen, Germany; www.edmund-buehler.de
Ekom, s.r.o.	Polná, Czech Republic
EMBL	Heidelberg, Germany
Eppendorf AG	Hamburg, Germany; www.eppendorf.com
Gibco-BRL	Geithersburg, MD, USA; www.gibcobrl.com or www.invitrogen.com
Heidolph Instruments GmbH & Co. KG	Schwabach, Germany; www.heidolph-instruments.de
Hoefer Scientific Instruments	San Francisco, CA, USA; www.hoeferinc.com or

	www.gelifesciences.com
IKA Werke GmbH	Staufen, Germany; www.ika.net
Jouan S.A.	St. Herblain, France; www.thermo.com
LKB-Produkter AB	Bromma, Sweden; www.amersham.com or www.gelifesciences.com
Millipore	Billerica, MA, USA; www.millipore.com
MJ Research, Inc.	Watertown, MA, USA; www.bio-rad.com
NanoDrop Technologies, Inc.	Wilmington, DE, USA; www.nanodrop.com
Ohaus	Pine Brook, NJ, USA; www.ohaus.com
Olympus	Prague, Czech Republic; www.olympus.cz
Pharmacia Biotech AB	Uppsala, Sweden; www.gelifesciences.com
Queue Systems, Inc.	Asheville, NC, USA
Radelkis Kft.	Budapest, Hungary; www.radelkis.hu
SANYO E&E Europe BV	Loughborough, UK; www.sanyo-biomedical.co.uk
Scientific Industries, Inc.	Bohemia, NY, USA; www.scientificindustries.com
SIGMA Laborzentrifugen GmbH	Osterode am Harz, Germany; www.sigma-zentrifugen.de
SLT Laboratory Instruments	Salzburg, Austria; www.tecan.com
Unicam Ltd	Cambridge, UK; www.thermo.com

6.4 Software

Applied Biosystems	Foster City, CA, USA; www.appliedbiosystems.com
Microsoft, s.r.o.	Prague, Czech Republic; www.microsoft.com/cze
Molecular Biology Insights, Inc.	Cascade, CO, USA; www.oligo.net
Pharmacia Biotech AB	Uppsala, Sweden; www.gelifesciences.com
Schoeller Pharma Praha, s.r.o.	Prague, Czech Republic; www.schoeller.cz

7 LIST OF ABBREVIATIONS

AA	acrylamide, amino acid(s)
AD	activation domain, autosomal dominant
AGT	angiotensinogen
APS	ammonium persulphate

BD	binding domain
bisAA	methylenebisacrylamide
BME	β-mercaptoethanol
bp	base pair
BPB	bromphenol blue
BSA	bovine serum albumin
cDNA	complementary or coding DNA
CDS	coding sequence
cM	centimorgan
ConA	Concanavalin A
Cy5	carbocyanine 5
Da	Dalton
DCT	distal convoluted tubule(s)
ddNTP	dideoxynucleoside triphosphate
DNA	deoxyribonucleic acid
dNTP	deoxynucleoside triphosphate
EDTA	ethylenediamine tetraacetate
EGF	epidermal growth factor
ELISA	enzyme-linked immunosorbent assay
EM	electron microscopy
ER	endoplasmic reticulum
ERAD	ER associated protein degradation
ESRD	end-stage renal disease
EtBr	ethidium bromide
FACS	fluorescent automated cell sorting
FE_{ur}	urate fractional excretion
FJHN	familiar juvenile hyperuricaemic nephropathy
GFR	glomerular filtration rate
GPI	glycosyl phosphatidylinositol
HEK	human embryonic kidney
HGPRT	hypoxanthine-guanine phosphoribosyl transferase
HRP	horseradish peroxidase
IVT	*in vitro* translation
JGA	juxtaglomerular apparatus
LiAc	lithium acetate

LOD	logarithm of odds
MCKD	medullary cystic kidney disease
MS	mass spectrometry
MW	molecular weight
NaAc	sodium acetate
NPH, NPHP	nephronophthisis
NTP	nucleoside triphosphate
PAGE	polyacrylamide gel electrophoresis
PIC	protease inhibitor cocktail
PBS	phosphate buffered saline
PCR	polymerase chain reaction
PEG	polyethylene glycol
PRPS	phosphoribosyl pyrophosphate synthetase
PT	proximal tubule(s)
RAS	renin-angiotensin system
RNA	ribonucleic acid
rpm	revolutions per minute
RT	room temperature
SDS	sodium dodecylsulphate
SNP	single nucleotide polymorphism
SRP	signal recognition particle
TALH	thick ascending loop of Henle
TBS	tris-buffered saline
TEMED	tetramethyl ethylenediamine
THP	Tamm-Horsfall protein
UAKD	uromodulin associated kidney disease
UPR	unfolded protein response
UTR	untranslated region
UV	ultraviolet
WB	Western blot(ting)
YTHS	yeast two-hybrid system
ZP	zona pellucida

8 REFERENCES

1. Stiburkova B., Sebesta I. and Kmoch S.: *[Diagnostic aspects of familial juvenile hyperuriceamic nephropathy].* Cas Lek Cesk 144(7): p. 466-471, 2005.
2. Duncan H. and Dixon A.S.: *Gout, familial hypericaemia, and renal disease.* Q J Med 29: p. 127-135, 1960.
3. McBride M.B., Simmonds H.A. and Moro F.: *Familial renal disease or familial juvenile hyperuricaemic nephropathy?* J Inherit Metab Dis 20(3): p. 351-353, 1997.
4. Massari P.U., Hsu C.H., Barnes R.V., Fox I.H., Gikas P.W. and Weller J.M.: *Familial hyperuricemia and renal disease.* Arch Intern Med 140(5): p. 680-684, 1980.
5. Van Goor W., Kooiker C.J. and Mees E.J.: *An unusual form of renal disease associated with gout and hypertension.* J Clin Pathol 24(4): p. 354-359, 1971.
6. Leumann E.P. and Wegmann W.: *Familial nephropathy with hyperuricemia and gout.* Nephron 34(1): p. 51-57, 1983.
7. Puig J.G., Miranda M.E., Mateos F.A., Picazo M.L., Jimenez M.L., Calvin T.S. and Gil A.A.: *Hereditary nephropathy associated with hyperuricemia and gout.* Arch Intern Med 153(3): p. 357-365, 1993.
8. Sebesta I., Krijt J., Pavelka K., Maly J., Simmonds H.A. and McBride M.B.: *Familial juvenile hyperuricaemic nephropathy in adolescents.* Adv Exp Med Biol 370: p. 73-76, 1994.
9. Rosenbloom F.M., Kelley W.N., Carr A.A. and Seegmiller J.E.: *Familial nephropathy and gout in a kindred.* Clin Res 70: p. 270, 1967.
10. Stiburkova B., Majewski J., Sebesta I., Zhang W., Ott J. and Kmoch S.: *Familial juvenile hyperuricemic nephropathy: localization of the gene on chromosome 16p11.2-and evidence for genetic heterogeneity.* Am J Hum Genet 66(6): p. 1989-1994, 2000.
11. Lhotta K., Gruber J., Sgonc R., Fend F. and Konig P.: *Apoptosis of tubular epithelial cells in familial juvenile gouty nephropathy.* Nephron 79(3): p. 340-344, 1998.
12. Dahan K., Fuchshuber A., Adamis S., Smaers M., Kroiss S., Loute G., Cosyns J.P., Hildebrandt F., Verellen-Dumoulin C. and Pirson Y.: *Familial juvenile hyperuricemic nephropathy and autosomal dominant medullary cystic kidney disease type 2: two facets of the same disease?* J Am Soc Nephrol 12(11): p. 2348-2357, 2001.
13. Calado J., Gaspar A., Clemente C. and Rueff J.: *A novel heterozygous missense mutation in the UMOD gene responsible for Familial Juvenile Hyperuricemic Nephropathy.* BMC Med Genet 6: p. 5, 2005.

14. Korom I., Szabo L., Laszlo A., Dallmann L. and Ormos J.: *[Infantile familial hyperuricemia with gouty manifestations].* Orv Hetil 120(10): p. 589-592, 1979.
15. Saeki A., Hosoya T., Okabe H., Saji M., Tabe A., Ichida K., Itoh K., Joh K. and Sakai O.: *Newly discovered familial juvenile gouty nephropathy in a Japanese family.* Nephron 70(3): p. 359-366, 1995.
16. Murakami T., Kawakami H., Nakatsuka K., Jojima K., Nohno H. and Matsuzaki H.: *Underexcretory-type hyperuricemia, disproportionate to the reduced glomerular filtration rate, in two boys with mild proteinuria.* Nephron 56(4): p. 439-442, 1990.
17. Auranen M., Ala-Mello S., Turunen J.A. and Jarvela I.: *Further evidence for linkage of autosomal-dominant medullary cystic kidney disease on chromosome 1q21.* Kidney Int 60(4): p. 1225-1232, 2001.
18. Lam P.W. and Peh W.C.: *Clinics in diagnostic imaging (2). Juvenile gouty arthropathy with associated nephropathy.* Singapore Med J 36(1): p. 85-87, 1995.
19. Reiter L., Brown M.A. and Edmonds J.: *Familial hyperuricemic nephropathy.* Am J Kidney Dis 25(2): p. 235-241, 1995.
20. Badilla A. and Rojas C.: *[Familial gout and nephropathy in a young woman. Report of one case].* Rev Med Chil 129(6): p. 666-670, 2001.
21. Cameron J.S., Moro F. and Simmonds H.A.: *Gout, uric acid and purine metabolism in paediatric nephrology.* Pediatr Nephrol 7(1): p. 105-118, 1993.
22. McBride M.B., Rigden S., Haycock G.B., Dalton N., Van't Hoff W., Rees L., Raman G.V., Moro F., Ogg C.S., Cameron J.S. and Simmonds H.A.: *Presymptomatic detection of familial juvenile hyperuricaemic nephropathy in children.* Pediatr Nephrol 12(5): p. 357-364, 1998.
23. Cameron J.S. and Simmonds H.A.: *Hereditary hyperuricemia and renal disease.* Semin Nephrol 25(1): p. 9-18, 2005.
24. Moro F., Ogg C.S., Simmonds H.A., Cameron J.S., Chantler C., McBride M.B., Duley J.A. and Davies P.M.: *Familial juvenile gouty nephropathy with renal urate hypoexcretion preceding renal disease.* Clin Nephrol 35(6): p. 263-269, 1991.
25. Simmonds H.A., Warren D.J., Cameron J.S., Potter C.F. and Farebrother D.A.: *Familial gout and renal failure in young women.* Clin Nephrol 14(4): p. 176-182, 1980.
26. Farebrother D.A., Pincott J.R., Simmons H.A., Warren D.J., Dillon M.J. and Cameron J.S.: *Uric acid crystal-induced nephropathy: evidence for a specific renal lesion in a gouty family.* J Pathol 135(2): p. 159-168, 1981.
27. Richmond J.M., Kincaid-Smith P., Whitworth J.A. and Becker G.J.: *Familial urate nephropathy.* Clin Nephrol 16(4): p. 163-168, 1981.

28. Yokota N., Yamanaka H., Yamamoto Y., Fujimoto S., Eto T. and Tanaka K.: *Autosomal dominant transmission of gouty arthritis with renal disease in a large Japanese family.* Ann Rheum Dis 50(2): p. 108-111, 1991.
29. Miranda M.E.: *The influence of allopurinol on renal deterioration in familial nepropathy associated with hyperuricemia (FNAH). The Spanish Group for the Study of FNAH.* Adv Exp Med Biol 370: p. 61-64, 1994.
30. Hisatome I., Kosaka H., Ohtahara K., Tsuboi M., Manabe I., Ohtahara A., Sawaguchi M., Igawa O., Tanaka Y., Fujimoto Y., Yoshida A., Takeda A. and Shigemasa C.: *Renal handling of urate in a patient with familial juvenile gouty nephropathy.* Intern Med 35(7): p. 564-568, 1996.
31. Lewis E.J., Hunsicker L.G., Clarke W.R., Berl T., Pohl M.A., Lewis J.B., Ritz E., Atkins R.C., Rohde R. and Raz I.: *Renoprotective effect of the angiotensin-receptor antagonist irbesartan in patients with nephropathy due to type 2 diabetes.* N Engl J Med 345(12): p. 851-860, 2001.
32. Brenner B.M., Cooper M.E., de Zeeuw D., Keane W.F., Mitch W.E., Parving H.H., Remuzzi G., Snapinn S.M., Zhang Z. and Shahinfar S.: *Effects of losartan on renal and cardiovascular outcomes in patients with type 2 diabetes and nephropathy.* N Engl J Med 345(12): p. 861-869, 2001.
33. Lipkowitz M.S., Leal-Pinto E., Rappoport J.Z., Najfeld V. and Abramson R.G.: *Functional reconstitution, membrane targeting, genomic structure, and chromosomal localization of a human urate transporter.* J Clin Invest 107(9): p. 1103-1115, 2001.
34. Roch-Ramel F.: *Renal transport of organic anions.* Curr Opin Nephrol Hypertens 7(5): p. 517-524, 1998.
35. Mazzali M., Hughes J., Kim Y.G., Jefferson J.A., Kang D.H., Gordon K.L., Lan H.Y., Kivlighn S. and Johnson R.J.: *Elevated uric acid increases blood pressure in the rat by a novel crystal-independent mechanism.* Hypertension 38(5): p. 1101-1106, 2001.
36. Messerli F.H., Frohlich E.D., Dreslinski G.R., Suarez D.H. and Aristimuno G.G.: *Serum uric acid in essential hypertension: an indicator of renal vascular involvement.* Ann Intern Med 93(6): p. 817-821, 1980.
37. Mateos F.A. and Puig J.G.: *Renal hemodynamic in familial nephropathy associated with hyperuricemia (FNAH). Spanish Group for the Study of FNAH.* Adv Exp Med Biol 370: p. 31-34, 1994.
38. Prieto C. and Berrocal T.: *Ultrasound imaging and colour Doppler studies in familial nephropathy associated with hyperuricemia (FNAH). The Spanish Group for the Study of FNAH.* Adv Exp Med Biol 370: p. 65-68, 1994.

39. Thorn G.W., Koepf G.F. and Cliniton M.: *Renal failure simulating adrenocortical insufficiency.* New Eng J Med 231: p. 76-85, 1944.
40. Smith C.H. and Graham J.B.: *Congenital medullary cysts of kidney with severe refractory anemia.* Am J Dis Child 69: p. 369-377, 1945.
41. Strauss M.B.: *Clinical and pathological aspects of cystic disease of the renal medulla. An analysis of eighteen cases.* Ann Intern Med 57: p. 373-381, 1962.
42. Wrigley K.A., Sherman R.L., Ennis F.A. and Becker E.L.: *Progressive hereditary nephropathy. A variant of medullary cystic disease?* Arch Intern Med 131(2): p. 240-244, 1973.
43. Giangiacomo J., Monteleone P.L. and Witzleben C.L.: *Medullary cystic disease vs nephronophthisis. A valid distinction?* Jama 232(6): p. 629-631, 1975.
44. Gardner K.D., Jr.: *Evolution of clinical signs in adult-onset cystic disease of the renal medulla.* Ann Intern Med 74(1): p. 47-54, 1971.
45. Whelton A., Ozer F.L., Bias W.B., Williams G.M. and Walker W.G.: *Renal medullary cystic disease: a family study.* Birth Defects Orig Art Ser X(4): p. 154-156, 1974.
46. Goldman S.H., Walker S.R., Merigan T.C., Jr., Gardner K.D., Jr. and Bull J.M.: *Hereditary occurrence of cystic disease of the renal medulla.* N Engl J Med 274(18): p. 984-992, 1966.
47. Scolari F., Viola B.F., Ghiggeri G.M., Caridi G., Amoroso A., Rampoldi L. and Casari G.: *Towards the identification of (a) gene(s) for autosomal dominant medullary cystic kidney disease.* J Nephrol 16(3): p. 321-328, 2003.
48. Fanconi G., Hanhart E., von A.A., Uhlinger E., Dolivo G. and Prader A.: *[Familial, juvenile nephronophthisis (idiopathic parenchymal contracted kidney).].* Helv Paediatr Acta 6(1): p. 1-49, 1951.
49. Strauss M.B. and Sommers S.C.: *Medullary cystic disease and familial juvenile nephronophthisis.* N Engl J Med 277(16): p. 863-864, 1967.
50. Mongeau J.G. and Worthen H.G.: *Nephronophthisis and medullary cystic disease.* Am J Med 43(3): p. 345-355, 1967.
51. Habib R.: *Nephronophthisis and medullary cystic disease.* In: *Pediatric nephrology. Current concepts and management*, Strauss J., Editor. Symposia Specialist, Miami: p. 393-401, 1962.
52. Antignac C., Arduy C.H., Beckmann J.S., Benessy F., Gros F., Medhioub M., Hildebrandt F., Dufier J.L., Kleinknecht C., Broyer M. and et al.: *A gene for familial juvenile nephronophthisis (recessive medullary cystic kidney disease) maps to chromosome 2p.* Nat Genet 3(4): p. 342-345, 1993.

53. Hildebrandt F., Singh-Sawhney I., Schnieders B., Centofante L., Omran H., Pohlmann A., Schmaltz C., Wedekind H., Schubotz C., Antignac C. and et al.: *Mapping of a gene for familial juvenile nephronophthisis: refining the map and defining flanking markers on chromosome 2. APN Study Group.* Am J Hum Genet 53(6): p. 1256-1261, 1993.
54. Haider N.B., Carmi R., Shalev H., Sheffield V.C. and Landau D.: *A Bedouin kindred with infantile nephronophthisis demonstrates linkage to chromosome 9 by homozygosity mapping.* Am J Hum Genet 63(5): p. 1404-1410, 1998.
55. Omran H., Fernandez C., Jung M., Haffner K., Fargier B., Villaquiran A., Waldherr R., Gretz N., Brandis M., Ruschendorf F., Reis A. and Hildebrandt F.: *Identification of a new gene locus for adolescent nephronophthisis, on chromosome 3q22 in a large Venezuelan pedigree.* Am J Hum Genet 66(1): p. 118-127, 2000.
56. Hildebrandt F., Otto E., Rensing C., Nothwang H.G., Vollmer M., Adolphs J., Hanusch H. and Brandis M.: *A novel gene encoding an SH3 domain protein is mutated in nephronophthisis type 1.* Nat Genet 17(2): p. 149-153, 1997.
57. Saunier S., Calado J., Heilig R., Silbermann F., Benessy F., Morin G., Konrad M., Broyer M., Gubler M.C., Weissenbach J. and Antignac C.: *A novel gene that encodes a protein with a putative src homology 3 domain is a candidate gene for familial juvenile nephronophthisis.* Hum Mol Genet 6(13): p. 2317-2323, 1997.
58. Hildebrandt F. and Omram H.: *New insights: nephronophthisis-medullary cystic kidney disease.* Pediatr Nephrol 16(2): p. 168-176, 2001.
59. Scolari F., Ghiggeri G.M., Casari G., Amoroso A., Puzzer D., Caridi G.L., Valzorio B., Tardanico R., Vizzardi V., Savoldi S., Viola B.F., Bossini N., Prati E., Gusmano R. and Maiorca R.: *Autosomal dominant medullary cystic disease: a disorder with variable clinical pictures and exclusion of linkage with the NPH1 locus.* Nephrol Dial Transplant 13(10): p. 2536-2546, 1998.
60. Thompson G.R., Weiss J.J., Goldman R.T. and Rigg G.A.: *Familial occurrence of hyperuricemia, gout, and medullary cystic disease.* Arch Intern Med 138(11): p. 1614-1617, 1978.
61. Burke J.R., Inglis J.A., Craswell P.W., Mitchell K.R. and Emmerson B.T.: *Juvenile nephronophthisis and medullary cystic disease--the same disease (report of a large family with medullary cystic disease associated with gout and epilepsy).* Clin Nephrol 18(1): p. 1-8, 1982.
62. Christodoulou K., Tsingis M., Stavrou C., Eleftheriou A., Papapavlou P., Patsalis P.C., Ioannou P., Pierides A. and Constantinou Deltas C.: *Chromosome 1 localization of a gene*

for autosomal dominant medullary cystic kidney disease. Hum Mol Genet 7(5): p. 905-911, 1998.

63. Scolari F., Puzzer D., Amoroso A., Caridi G., Ghiggeri G.M., Maiorca R., Aridon P., De Fusco M., Ballabio A. and Casari G.: *Identification of a new locus for medullary cystic disease, on chromosome 16p12.* Am J Hum Genet 64(6): p. 1655-1660, 1999.
64. Stavrou C., Koptides M., Tombazos C., Psara E., Patsias C., Zouvani I., Kyriacou K., Hildebrandt F., Christofides T., Pierides A. and Deltas C.C.: *Autosomal-dominant medullary cystic kidney disease type 1: clinical and molecular findings in six large Cypriot families.* Kidney Int 62(4): p. 1385-1394, 2002.
65. Kroiss S., Huck K., Berthold S., Ruschendorf F., Scolari F., Caridi G., Ghiggeri G.M., Hildebrandt F. and Fuchshuber A.: *Evidence of further genetic heterogeneity in autosomal dominant medullary cystic kidney disease.* Nephrol Dial Transplant 15(6): p. 818-821, 2000.
66. Parvari R., Shnaider A., Basok A., Katchko L., Borochovich Z., Kanis A. and Landau D.: *Clinical and genetic characterization of an autosomal dominant nephropathy.* Am J Med Genet 99(3): p. 204-209, 2001.
67. Hateboer N., Gumbs C., Teare M.D., Coles G.A., Griffiths D., Ravine D., Futreal P.A. and Rahman N.: *Confirmation of a gene locus for medullary cystic kidney disease (MCKD2) on chromosome 16p12.* Kidney Int 60(4): p. 1233-1239, 2001.
68. Kamatani N., Moritani M., Yamanaka H., Takeuchi F., Hosoya T. and Itakura M.: *Localization of a gene for familial juvenile hyperuricemic nephropathy causing underexcretion-type gout to 16p12 by genome-wide linkage analysis of a large family.* Arthritis Rheum 43(4): p. 925-929, 2000.
69. Mollet G., Salomon R., Gribouval O., Silbermann F., Bacq D., Landthaler G., Milford D., Nayir A., Rizzoni G., Antignac C. and Saunier S.: *The gene mutated in juvenile nephronophthisis type 4 encodes a novel protein that interacts with nephrocystin.* Nat Genet 32(2): p. 300-305, 2002.
70. Otto E.A., Schermer B., Obara T., O'Toole J.F., Hiller K.S., Mueller A.M., Ruf R.G., Hoefele J., Beekmann F., Landau D., Foreman J.W., Goodship J.A., Strachan T., Kispert A., Wolf M.T., Gagnadoux M.F., Nivet H., Antignac C., Walz G., Drummond I.A., Benzing T. and Hildebrandt F.: *Mutations in INVS encoding inversin cause nephronophthisis type 2, linking renal cystic disease to the function of primary cilia and left-right axis determination.* Nat Genet 34(4): p. 413-420, 2003.
71. Otto E., Hoefele J., Ruf R., Mueller A.M., Hiller K.S., Wolf M.T., Schuermann M.J., Becker A., Birkenhager R., Sudbrak R., Hennies H.C., Nurnberg P. and Hildebrandt F.: *A*

gene mutated in nephronophthisis and retinitis pigmentosa encodes a novel protein, nephroretinin, conserved in evolution. Am J Hum Genet 71(5): p. 1161-1167, 2002.

72. Olbrich H., Fliegauf M., Hoefele J., Kispert A., Otto E., Volz A., Wolf M.T., Sasmaz G., Trauer U., Reinhardt R., Sudbrak R., Antignac C., Gretz N., Walz G., Schermer B., Benzing T., Hildebrandt F. and Omran H.: *Mutations in a novel gene, NPHP3, cause adolescent nephronophthisis, tapeto-retinal degeneration and hepatic fibrosis.* Nat Genet 34(4): p. 455-459, 2003.
73. Otto E.A., Loeys B., Khanna H., Hellemans J., Sudbrak R., Fan S., Muerb U., O'Toole J.F., Helou J., Attanasio M., Utsch B., Sayer J.A., Lillo C., Jimeno D., Coucke P., De Paepe A., Reinhardt R., Klages S., Tsuda M., Kawakami I., Kusakabe T., Omran H., Imm A., Tippens M., Raymond P.A., Hill J., Beales P., He S., Kispert A., Margolis B., Williams D.S., Swaroop A. and Hildebrandt F.: *Nephrocystin-5, a ciliary IQ domain protein, is mutated in Senior-Loken syndrome and interacts with RPGR and calmodulin.* Nat Genet 37(3): p. 282-288, 2005.
74. Sayer J.A., Otto E.A., O'Toole J.F., Nurnberg G., Kennedy M.A., Becker C., Hennies H.C., Helou J., Attanasio M., Fausett B.V., Utsch B., Khanna H., Liu Y., Drummond I., Kawakami I., Kusakabe T., Tsuda M., Ma L., Lee H., Larson R.G., Allen S.J., Wilkinson C.J., Nigg E.A., Shou C., Lillo C., Williams D.S., Hoppe B., Kemper M.J., Neuhaus T., Parisi M.A., Glass I.A., Petry M., Kispert A., Gloy J., Ganner A., Walz G., Zhu X., Goldman D., Nurnberg P., Swaroop A., Leroux M.R. and Hildebrandt F.: *The centrosomal protein nephrocystin-6 is mutated in Joubert syndrome and activates transcription factor ATF4.* Nat Genet 38(6): p. 674-681, 2006.
75. O'Toole J F., Otto E.A., Hoefele J., Helou J. and Hildebrandt F.: *Mutational analysis in 119 families with nephronophthisis.* Pediatr Nephrol 22(3): p. 366-370, 2007.
76. Hildebrandt F. and Otto E.: *Cilia and centrosomes: a unifying pathogenic concept for cystic kidney disease?* Nat Rev Genet 6(12): p. 928-940, 2005.
77. Guay-Woodford L.M.: *Renal cystic diseases: diverse phenotypes converge on the cilium/centrosome complex.* Pediatr Nephrol 21(10): p. 1369-1376, 2006.
78. Stiburkova B., Majewski J., Hodanova K., Ondrova L., Jerabkova M., Zikanova M., Vylet'al P., Sebesta I., Marinaki A., Simmonds A., Matthijs G., Fryns J.P., Torres R., Puig J.G., Ott J. and Kmoch S.: *Familial juvenile hyperuricaemic nephropathy (FJHN): linkage analysis in 15 families, physical and transcriptional characterisation of the FJHN critical region on chromosome 16p11.2 and the analysis of seven candidate genes.* Eur J Hum Genet 11(2): p. 145-154, 2003.

79. Pirulli D., Puzzer D., De Fusco M., Crovella S., Amoroso A., Scolari F., Viola B.F., Maiorca R., Caridi G., Savoldi S., Ghiggeri G. and Casari G.: *Molecular analysis of uromodulin and SAH genes, positional candidates for autosomal dominant medullary cystic kidney disease linked to 16p12.* J Nephrol 14(5): p. 392-396, 2001.
80. Hart T.C., Gorry M.C., Hart P.S., Woodard A.S., Shihabi Z., Sandhu J., Shirts B., Xu L., Zhu H., Barmada M.M. and Bleyer A.J.: *Mutations of the UMOD gene are responsible for medullary cystic kidney disease 2 and familial juvenile hyperuricaemic nephropathy.* J Med Genet 39(12): p. 882-892, 2002.
81. Hodanova K., Majewski J., Kublova M., Vyletal P., Kalbacova M., Stiburkova B., Hulkova H., Chagnon Y.C., Lanouette C.M., Marinaki A., Fryns J.P., Venkat-Raman G. and Kmoch S.: *Mapping of a new candidate locus for uromodulin-associated kidney disease (UAKD) to chromosome 1q41.* Kidney Int 68(4): p. 1472-1482, 2005.
82. Bleyer A.J., Hart T.C., Willingham M.C., Iskandar S.S., Gorry M.C. and Trachtman H.: *Clinico-pathologic findings in medullary cystic kidney disease type 2.* Pediatr Nephrol 20(6): p. 824-827, 2005.
83. Scolari F., Caridi G., Rampoldi L., Tardanico R., Izzi C., Pirulli D., Amoroso A., Casari G. and Ghiggeri G.M.: *Uromodulin storage diseases: clinical aspects and mechanisms.* Am J Kidney Dis 44(6): p. 987-999, 2004.
84. Gersch M., Mutig K., Bachmann S., Kumar S., Ouyang X. and Johnson R.: *Is salt-wasting the long awaited answer to the hyperuricaemia seen in uromodulin storage diseases?* Nephrol Dial Transplant 21(7): p. 2028-2029, 2006.
85. Casari G. and Amoroso A.: *Molecular analysis of uromodulin and SAH genes, positional candidates for autosomal dominant medullary cystic kidney disease linked to 16p12.* J Nephrol 16(3): p. 459, 2003.
86. Calabrese G., Simmonds H.A., Cameron J.S. and Davies P.M.: *Precocious familial gout with reduced fractional urate clearance and normal purine enzymes.* Q J Med 75(277): p. 441-450, 1990.
87. Bingham C., Ellard S., van't Hoff W.G., Simmonds H.A., Marinaki A.M., Badman M.K., Winocour P.H., Stride A., Lockwood C.R., Nicholls A.J., Owen K.R., Spyer G., Pearson E.R. and Hattersley A.T.: *Atypical familial juvenile hyperuricemic nephropathy associated with a hepatocyte nuclear factor-1beta gene mutation.* Kidney Int 63(5): p. 1645-1651, 2003.
88. Edghill E.L., Bingham C., Ellard S. and Hattersley A.T.: *Mutations in hepatocyte nuclear factor-1beta and their related phenotypes.* J Med Genet 43(1): p. 84-90, 2006.

89. Horikawa Y., Iwasaki N., Hara M., Furuta H., Hinokio Y., Cockburn B.N., Lindner T., Yamagata K., Ogata M., Tomonaga O., Kuroki H., Kasahara T., Iwamoto Y. and Bell G.I.: *Mutation in hepatocyte nuclear factor-1 beta gene (TCF2) associated with MODY.* Nat Genet 17(4): p. 384-385, 1997.
90. Tamm I. and Horsfall F.L., Jr.: *Characterization and separation of an inhibitor of viral hemagglutination present in urine.* Proc Soc Exp Biol Med 74(1): p. 106-108, 1950.
91. Tamm I. and Horsfall F.L., Jr.: *A mucoprotein derived from human urine which reacts with influenza, mumps, and Newcastle disease viruses.* J Exp Med 95(1): p. 71-97, 1952.
92. Odin L.: *Carbohydrate residue of a urine mucoprotein inhibiting influenza virus hemagglutination.* Nature 170(4329): p. 663-664, 1952.
93. Gottschalk A.: *Carbohydrate residue of a urine mucoprotein inhibiting influenza virus haemagglutination.* Nature 170(4329): p. 662-663, 1952.
94. Bayer M.E.: *An Electron Microscope Examination of Urinary Mucoprotein and Its Interaction with Influenza Virus.* J Cell Biol 21: p. 265-274, 1964.
95. Wiggins R.C.: *Uromucoid (Tamm-Horsfall glycoprotein) forms different polymeric arrangements on a filter surface under different physicochemical conditions.* Clin Chim Acta 162(3): p. 329-340, 1987.
96. Jovine L., Qi H., Williams Z., Litscher E. and Wassarman P.M.: *The ZP domain is a conserved module for polymerization of extracellular proteins.* Nat Cell Biol 4(6): p. 457-461, 2002.
97. Fletcher A.P., Neuberger A. and Ratcliffe W.A.: *Tamm-Horsfall urinary glycoprotein. The subunit structure.* Biochem J 120(2): p. 425-432, 1970.
98. Fletcher A.P., Neuberger A. and Ratcliffe W.A.: *Tamm-Horsfall urinary glycoprotein. The chemical composition.* Biochem J 120(2): p. 417-424, 1970.
99. Grant A.M. and Neuberger A.: *The development of a radioimmunoassay for the measurement of urinary Tamm-Horsfall glycoprotein in the presence of sodium dodecyl sulphate.* Clin Sci 44(2): p. 163-179, 1973.
100. Dunstan D.R., Grant A.M., Marshall R.D. and Neuberger A.: *A protein, immunologically similar to Tamm-Horsfall glycoprotein, produced by cultured baby hamster kidney cells.* Proc R Soc Lond B Biol Sci 186(1085): p. 297-316, 1974.
101. Wallace A.C. and Nairn R.C.: *Tamm-Horsfall protein in kidneys of human embryos and foreign species.* Pathology 3: p. 303-310, 1971.
102. Muchmore A.V.: *Uromodulin: an immunoregulatory glycoprotein isolated from pregnancy urine that binds to and regulates the activity of interleukin 1.* Am J Reprod Immunol Microbiol 11(3): p. 89-93, 1986.

103. Muchmore A.V. and Decker J.M.: *Uromodulin. An immunosuppressive 85-kilodalton glycoprotein isolated from human pregnancy urine is a high affinity ligand for recombinant interleukin 1 alpha.* J Biol Chem 261(29): p. 13404-13407, 1986.
104. Brown K.M., Muchmore A.V. and Rosenstreich D.L.: *Uromodulin, an immunosuppressive protein derived from pregnancy urine, is an inhibitor of interleukin 1.* Proc Natl Acad Sci U S A 83(23): p. 9119-9123, 1986.
105. Muchmore A.V. and Decker J.M.: *Evidence that recombinant IL 1 alpha exhibits lectin-like specificity and binds to homogeneous uromodulin via N-linked oligosaccharides.* J Immunol 138(8): p. 2541-2546, 1987.
106. Muchmore A.V., Shifrin S. and Decker J.M.: *In vitro evidence that carbohydrate moieties derived from uromodulin, an 85,000 dalton immunosuppressive glycoprotein isolated from human pregnancy urine, are immunosuppressive in the absence of intact protein.* J Immunol 138(8): p. 2547-2553, 1987.
107. Pennica D., Kohr W.J., Kuang W.J., Glaister D., Aggarwal B.B., Chen E.Y. and Goeddel D.V.: *Identification of human uromodulin as the Tamm-Horsfall urinary glycoprotein.* Science 236(4797): p. 83-88, 1987.
108. Orskov I., Ferencz A. and Orskov F.: *Tamm-Horsfall protein or uromucoid is the normal urinary slime that traps type 1 fimbriated Escherichia coli.* Lancet 1(8173): p. 887, 1980.
109. Parkkinen J., Virkola R. and Korhonen T.K.: *Identification of factors in human urine that inhibit the binding of Escherichia coli adhesins.* Infect Immun 56(10): p. 2623-2630, 1988.
110. Pak J., Pu Y., Zhang Z.T., Hasty D.L. and Wu X.R.: *Tamm-Horsfall protein binds to type 1 fimbriated Escherichia coli and prevents E. coli from binding to uroplakin Ia and Ib receptors.* J Biol Chem 276(13): p. 9924-9930, 2001.
111. Sanders P.W. and Booker B.B.: *Pathobiology of cast nephropathy from human Bence Jones proteins.* J Clin Invest 89(2): p. 630-639, 1992.
112. Wenk R.E., Bhagavan B.S. and Rudert J.: *Tamm-Horsfall uromucoprotein and the pathogenesis of casts, reflux nephropathy, and nephritides.* Pathobiol Annu 11: p. 229-257, 1981.
113. McQueen E.G.: *Composition of urinary casts.* Lancet 1(7434): p. 397-398, 1966.
114. Fairley J.K., Owen J.E. and Birch D.F.: *Protein composition of urinary casts from healthy subjects and patients with glomerulonephritis.* Br Med J (Clin Res Ed) 287(6408): p. 1838-1840, 1983.

115. Huang Z.Q. and Sanders P.W.: *Biochemical interaction between Tamm-Horsfall glycoprotein and Ig light chains in the pathogenesis of cast nephropathy.* Lab Invest 73(6): p. 810-817, 1995.
116. Grant A.M., Baker L.R. and Neuberger A.: *Urinary Tamm-Horsfall glycoprotein in certain kidney diseases and its content in renal and bladder calculi.* Clin Sci 44(4): p. 377-384, 1973.
117. Marengo S.R., Chen D.H., Kaung H.L., Resnick M.I. and Yang L.: *Decreased renal expression of the putative calcium oxalate inhibitor Tamm-Horsfall protein in the ethylene glycol rat model of calcium oxalate urolithiasis.* J Urol 167(5): p. 2192-2197, 2002.
118. Hallson P.C., Choong S.K., Kasidas G.P. and Samuell C.T.: *Effects of Tamm-Horsfall protein with normal and reduced sialic acid content upon the crystallization of calcium phosphate and calcium oxalate in human urine.* Br J Urol 80(4): p. 533-538, 1997.
119. Chen W.C., Lin H.S., Chen H.Y., Shih C.H. and Li C.W.: *Effects of Tamm-Horsfall protein and albumin on calcium oxalate crystallization and importance of sialic acids.* Mol Urol 5(1): p. 1-5, 2001.
120. Hess B. and Kok D.J.: *Nucleation, growth and aggregation of stone forming crystals.* In: *Kidney Stones: Medical and Surgical Management*, Coe F.L., Favus M.J., Fak C.Y.C., Parks J.H. and Preminger G.M., Editors. Lippincott-Raven, Philadelphia: p. 3-32, 1996.
121. Seiler M.W. and Hoyer J.R.: *Ultrastructural studies of tubulointerstitial immune complex nephritis in rats immunized with Tamm-Horsfall protein.* Lab Invest 45(4): p. 321-327, 1981.
122. Cohen A.H., Border W.A., Rajfer J., Dumke A. and Glassock R.J.: *Interstitial Tamm-Horsfall protein in rejecting renal allografts. Identification and morphologic pattern of injury.* Lab Invest 50(5): p. 519-525, 1984.
123. Cotran R.S. and Galvanek E.: *Immunopathology of human tubulo-interstitial diseases: localization of immunoglobulins complement and Tamm-Horsfall protein.* Contrib Nephrol 16: p. 126-131, 1979.
124. Resnick J.S., Sisson S. and Vernier R.L.: *Tamm-Horsfall protein. Abnormal localization in renal disease.* Lab Invest 38(5): p. 550-555, 1978.
125. Cavallone D., Malagolini N. and Serafini-Cessi F.: *Binding of human neutrophils to cell-surface anchored Tamm-Horsfall glycoprotein in tubulointerstitial nephritis.* Kidney Int 55(5): p. 1787-1799, 1999.
126. Lynn K.L. and Marshall R.D.: *Excretion of Tamm-Horsfall glycoprotein in renal disease.* Clin Nephrol 22(5): p. 253-257, 1984.

127. Glauser A., Hochreiter W., Jaeger P. and Hess B.: *Determinants of urinary excretion of Tamm-Horsfall protein in non-selected kidney stone formers and healthy subjects.* Nephrol Dial Transplant 15(10): p. 1580-1587, 2000.
128. Thornley C., Dawnay A. and Cattell W.R.: *Human Tamm-Horsfall glycoprotein: urinary and plasma levels in normal subjects and patients with renal disease determined by a fully validated radioimmunoassay.* Clin Sci (Lond) 68(5): p. 529-535, 1985.
129. Tsai C.Y., Wu T.H., Yu C.L., Lu J.Y. and Tsai Y.Y.: *Increased excretions of beta2-microglobulin, IL-6, and IL-8 and decreased excretion of Tamm-Horsfall glycoprotein in urine of patients with active lupus nephritis.* Nephron 85(3): p. 207-214, 2000.
130. Zimmerhackl L.B., Pfleiderer S., Kinne R., Manz F., Schuler G. and Brandis M.: *Tamm-Horsfall-Protein excretion as a marker of ascending limb transport indicates early renal tubular damage in diabetes mellitus type I.* J Diabet Complications 5(2-3): p. 112-114, 1991.
131. Bernard A.M., Ouled A.A., Lauwerys R.R., Lambert A. and Vandeleene B.: *Pronounced decrease of Tamm-Horsfall proteinuria in diabetics.* Clin Chem 33(7): p. 1264, 1987.
132. Hamlin L.M. and Fish W.W.: *Physical properties of Tamm-Horsfall glycoprotein and its glycopolypeptide.* Int J Pept Protein Res 10(4): p. 270-276, 1977.
133. Rampoldi L., Caridi G., Santon D., Boaretto F., Bernascone I., Lamorte G., Tardanico R., Dagnino M., Colussi G., Scolari F., Ghiggeri G.M., Amoroso A. and Casari G.: *Allelism of MCKD, FJHN and GCKD caused by impairment of uromodulin export dynamics.* Hum Mol Genet 12(24): p. 3369-3384, 2003.
134. Tinschert S., Ruf N., Bernascone I., Sacherer K., Lamorte G., Neumayer H.H., Nurnberg P., Luft F.C. and Rampoldi L.: *Functional consequences of a novel uromodulin mutation in a family with familial juvenile hyperuricaemic nephropathy.* Nephrol Dial Transplant 19(12): p. 3150-3154, 2004.
135. Lens X.M., Banet J.F., Outeda P. and Barrio-Lucia V.: *A novel pattern of mutation in uromodulin disorders: autosomal dominant medullary cystic kidney disease type 2, familial juvenile hyperuricemic nephropathy, and autosomal dominant glomerulocystic kidney disease.* Am J Kidney Dis 46(1): p. 52-57, 2005.
136. Yang H., Wu C., Zhao S. and Guo J.: *Identification and characterization of D8C, a novel domain present in liver-specific LZP, uromodulin and glycoprotein 2, mutated in familial juvenile hyperuricaemic nephropathy.* FEBS Lett 578(3): p. 236-238, 2004.
137. Schenk E.A., Schwartz R.H. and Lewis R.A.: *Tamm-Horsfall mucoprotein. I. Localization in the kidney.* Lab Invest 25(1): p. 92-95, 1971.

138. Hoyer J.R., Sisson S.P. and Vernier R.L.: *Tamm-Horsfall glycoprotein: ultrastructural immunoperoxidase localization in rat kidney.* Lab Invest 41(2): p. 168-173, 1979.
139. Sikri K.L., Foster C.L., MacHugh N. and Marshall R.D.: *Localization of Tamm-Horsfall glycoprotein in the human kidney using immuno-fluorescence and immuno-electron microscopical techniques.* J Anat 132(Pt 4): p. 597-605, 1981.
140. Rindler M.J., Naik S.S., Li N., Hoops T.C. and Peraldi M.N.: *Uromodulin (Tamm-Horsfall glycoprotein/uromucoid) is a phosphatidylinositol-linked membrane protein.* J Biol Chem 265(34): p. 20784-20789, 1990.
141. van Rooijen J.J., Voskamp A.F., Kamerling J.P. and Vliegenthart J.F.: *Glycosylation sites and site-specific glycosylation in human Tamm-Horsfall glycoprotein.* Glycobiology 9(1): p. 21-30, 1999.
142. Brown D.A. and Rose J.K.: *Sorting of GPI-anchored proteins to glycolipid-enriched membrane subdomains during transport to the apical cell surface.* Cell 68(3): p. 533-544, 1992.
143. Benting J.H., Rietveld A.G. and Simons K.: *N-Glycans mediate the apical sorting of a GPI-anchored, raft-associated protein in Madin-Darby canine kidney cells.* J Cell Biol 146(2): p. 313-320, 1999.
144. Fukuoka S. and Kobayashi K.: *Analysis of the C-terminal structure of urinary Tamm-Horsfall protein reveals that the release of the glycosyl phosphatidylinositol-anchored counterpart from the kidney occurs by phenylalanine-specific proteolysis.* Biochem Biophys Res Commun 289(5): p. 1044-1048, 2001.
145. Serafini-Cessi F., Malagolini N. and Cavallone D.: *Tamm-Horsfall glycoprotein: biology and clinical relevance.* Am J Kidney Dis 42(4): p. 658-676, 2003.
146. Worcester E.M.: *Urinary calcium oxalate crystal growth inhibitors.* J Am Soc Nephrol 5(5 Suppl 1): p. S46-53, 1994.
147. Hess B., Nakagawa Y. and Coe F.L.: *Inhibition of calcium oxalate monohydrate crystal aggregation by urine proteins.* Am J Physiol 257(1 Pt 2): p. F99-106, 1989.
148. Grover P.K., Moritz R.L., Simpson R.J. and Ryall R.L.: *Inhibition of growth and aggregation of calcium oxalate crystals in vitro--a comparison of four human proteins.* Eur J Biochem 253(3): p. 637-644, 1998.
149. Beshensky A.M., Wesson J.A., Worcester E.M., Sorokina E.J., Snyder C.J. and Kleinman J.G.: *Effects of urinary macromolecules on hydroxyapatite crystal formation.* J Am Soc Nephrol 12(10): p. 2108-2116, 2001.
150. Kobayashi K. and Fukuoka S.: *Conditions for solubilization of Tamm-Horsfall protein/uromodulin in human urine and establishment of a sensitive and accurate enzyme-*

linked immunosorbent assay (ELISA) method. Arch Biochem Biophys 388(1): p. 113-120, 2001.

151. Vylet'al P., Kublova M., Kalbacova M., Hodanova K., Baresova V., Stiburkova B., Sikora J., Hulkova H., Zivny J., Majewski J., Simmonds A., Fryns J.P., Venkat-Raman G., Elleder M. and Kmoch S.: *Alterations of uromodulin biology: a common denominator of the genetically heterogeneous FJHN/MCKD syndrome.* Kidney Int 70(6): p. 1155-1169, 2006.
152. Choi S.W., Ryu O.H., Choi S.J., Song I.S., Bleyer A.J. and Hart T.C.: *Mutant tamm-horsfall glycoprotein accumulation in endoplasmic reticulum induces apoptosis reversed by colchicine and sodium 4-phenylbutyrate.* J Am Soc Nephrol 16(10): p. 3006-3014, 2005.
153. Malagolini N., Cavallone D. and Serafini-Cessi F.: *Intracellular transport, cell-surface exposure and release of recombinant Tamm-Horsfall glycoprotein.* Kidney Int 52(5): p. 1340-1350, 1997.
154. Serafini-Cessi F., Malagolini N., Hoops T.C. and Rindler M.J.: *Biosynthesis and oligosaccharide processing of human Tamm-Horsfall glycoprotein permanently expressed in HeLa cells.* Biochem Biophys Res Commun 194(2): p. 784-790, 1993.
155. Moran P., Raab H., Kohr W.J. and Caras I.W.: *Glycophospholipid membrane anchor attachment. Molecular analysis of the cleavage/attachment site.* J Biol Chem 266(2): p. 1250-1257, 1991.
156. Field M.C., Moran P., Li W., Keller G.A. and Caras I.W.: *Retention and degradation of proteins containing an uncleaved glycosylphosphatidylinositol signal.* J Biol Chem 269(14): p. 10830-10837, 1994.
157. Gusmano R., Caridi G., Marini M., Perfumo F., Ghiggeri G.M., Piaggio G., Ceccherini I. and Seri M.: *Glomerulocystic kidney disease in a family.* Nephrol Dial Transplant 17(5): p. 813-818, 2002.
158. Turner J.J., Stacey J.M., Harding B., Kotanko P., Lhotta K., Puig J.G., Roberts I., Torres R.J. and Thakker R.V.: *UROMODULIN mutations cause familial juvenile hyperuricemic nephropathy.* J Clin Endocrinol Metab 88(3): p. 1398-1401, 2003.
159. Dahan K., Devuyst O., Smaers M., Vertommen D., Loute G., Poux J.M., Viron B., Jacquot C., Gagnadoux M.F., Chauveau D., Buchler M., Cochat P., Cosyns J.P., Mougenot B., Rider M.H., Antignac C., Verellen-Dumoulin C. and Pirson Y.: *A cluster of mutations in the UMOD gene causes familial juvenile hyperuricemic nephropathy with abnormal expression of uromodulin.* J Am Soc Nephrol 14(11): p. 2883-2893, 2003.

160. Wolf M.T., Mucha B.E., Attanasio M., Zalewski I., Karle S.M., Neumann H.P., Rahman N., Bader B., Baldamus C.A., Otto E., Witzgall R., Fuchshuber A. and Hildebrandt F.: *Mutations of the Uromodulin gene in MCKD type 2 patients cluster in exon 4, which encodes three EGF-like domains.* Kidney Int 64(5): p. 1580-1587, 2003.
161. Kudo E., Kamatani N., Tezuka O., Taniguchi A., Yamanaka H., Yabe S., Osabe D., Shinohara S., Nomura K., Segawa M., Miyamoto T., Moritani M., Kunika K. and Itakura M.: *Familial juvenile hyperuricemic nephropathy: detection of mutations in the uromodulin gene in five Japanese families.* Kidney Int 65(5): p. 1589-1597, 2004.
162. Bernascone I., Vavassori S., Di Pentima A., Santambrogio S., Lamorte G., Amoroso A., Scolari F., Ghiggeri G.M., Casari G., Polishchuk R. and Rampoldi L.: *Defective intracellular trafficking of uromodulin mutant isoforms.* Traffic 7(11): p. 1567-1579, 2006.
163. Bleyer A.J., Trachtman H., Sandhu J., Gorry M.C. and Hart T.C.: *Renal manifestations of a mutation in the uromodulin (Tamm Horsfall protein) gene.* Am J Kidney Dis 42(2): p. E20-26, 2003.
164. Wolf M.T., Beck B.B., Zaucke F., Kunze A., Misselwitz J., Ruley J., Ronda T., Fischer A., Eifinger F., Licht C., Otto E., Hoppe B. and Hildebrandt F.: *The Uromodulin C744G mutation causes MCKD2 and FJHN in children and adults and may be due to a possible founder effect.* Kidney Int 71(6): p. 574-581, 2007.
165. Bleyer A.J., Hart T.C., Shihabi Z., Robins V. and Hoyer J.R.: *Mutations in the uromodulin gene decrease urinary excretion of Tamm-Horsfall protein.* Kidney Int 66(3): p. 974-977, 2004.
166. Jennings P., Aydin S., Kotanko P., Lechner J., Lhotta K., Williams S., Thakker R.V. and Pfaller W.: *Membrane targeting and secretion of mutant uromodulin in familial juvenile hyperuricemic nephropathy.* J Am Soc Nephrol 18(1): p. 264-273, 2007.
167. Bates J.M., Raffi H.M., Prasadan K., Mascarenhas R., Laszik Z., Maeda N., Hultgren S.J. and Kumar S.: *Tamm-Horsfall protein knockout mice are more prone to urinary tract infection: rapid communication.* Kidney Int 65(3): p. 791-797, 2004.
168. Mo L., Zhu X.H., Huang H.Y., Shapiro E., Hasty D.L. and Wu X.R.: *Ablation of the Tamm-Horsfall protein gene increases susceptibility of mice to bladder colonization by type 1-fimbriated Escherichia coli.* Am J Physiol Renal Physiol 286(4): p. F795-802, 2004.
169. Raffi H.S., Bates J.M., Jr., Laszik Z. and Kumar S.: *Tamm-Horsfall protein acts as a general host-defense factor against bacterial cystitis.* Am J Nephrol 25(6): p. 570-578, 2005.

170. Mo L., Huang H.Y., Zhu X.H., Shapiro E., Hasty D.L. and Wu X.R.: *Tamm-Horsfall protein is a critical renal defense factor protecting against calcium oxalate crystal formation.* Kidney Int 66(3): p. 1159-1166, 2004.
171. Raffi H., Bates J.M., Laszik Z. and Kumar S.: *Tamm-Horsfall protein knockout mice do not develop medullary cystic kidney disease.* Kidney Int 69(10): p. 1914-1915, 2006.
172. Bachmann S., Mutig K., Bates J., Welker P., Geist B., Gross V., Luft F.C., Alenina N., Bader M., Thiele B.J., Prasadan K., Raffi H.S. and Kumar S.: *Renal effects of Tamm-Horsfall protein (uromodulin) deficiency in mice.* Am J Physiol Renal Physiol 288(3): p. F559-567, 2005.
173. Enomoto A., Kimura H., Chairoungdua A., Shigeta Y., Jutabha P., Cha S.H., Hosoyamada M., Takeda M., Sekine T., Igarashi T., Matsuo H., Kikuchi Y., Oda T., Ichida K., Hosoya T., Shimokata K., Niwa T., Kanai Y. and Endou H.: *Molecular identification of a renal urate anion exchanger that regulates blood urate levels.* Nature 417(6887): p. 447-452, 2002.
174. Fairbanks L.D., Cameron J.S., Venkat-Raman G., Rigden S.P., Rees L., Van T.H.W., Mansell M., Pattison J., Goldsmith D.J. and Simmonds H.A.: *Early treatment with allopurinol in familial juvenile hyerpuricaemic nephropathy (FJHN) ameliorates the long-term progression of renal disease.* Qjm 95(9): p. 597-607, 2002.
175. Puig J.G. and Torres R.J.: *Familial juvenile hyperuricaemic nephropathy.* Qjm 96(2): p. 172-173, 2003.
176. Puig J.G. and Torres R.J.: *Familial juvenile hyperuricaemic nephropathy.* Qjm 97(7): p. 457-458, 2004.
177. Bleyer A.J. and Hart T.C.: *Familial juvenile hyperuricaemic nephropathy.* Qjm 96(11): p. 867-868, 2003.
178. Bleyer A.J., Woodard A.S., Shihabi Z., Sandhu J., Zhu H., Satko S.G., Weller N., Deterding E., McBride D., Gorry M.C., Xu L., Ganier D. and Hart T.C.: *Clinical characterization of a family with a mutation in the uromodulin (Tamm-Horsfall glycoprotein) gene.* Kidney Int 64(1): p. 36-42, 2003.
179. Fairbanks L.D., Marinaki A.M., Simmonds H.A. and Cameron J.S.: *Familial juvenile hyperuricaemic nephropathy.* Qjm 97(2): p. 106-107, 2004.
180. Devonald M.A. and Karet F.E.: *Renal epithelial traffic jams and one-way streets.* J Am Soc Nephrol 15(6): p. 1370-1381, 2004.
181. Rutishauser J. and Spiess M.: *Endoplasmic reticulum storage diseases.* Swiss Med Wkly 132(17-18): p. 211-222, 2002.
182. Yoshida H.: *ER stress and diseases.* Febs J 274(3): p. 630-658, 2007.

183. Schroder M. and Kaufman R.J.: *ER stress and the unfolded protein response.* Mutat Res 569(1-2): p. 29-63, 2005.
184. Chabardes-Garonne D., Mejean A., Aude J.C., Cheval L., Di Stefano A., Gaillard M.C., Imbert-Teboul M., Wittner M., Balian C., Anthouard V., Robert C., Segurens B., Wincker P., Weissenbach J., Doucet A. and Elalouf J.M.: *A panoramic view of gene expression in the human kidney.* Proc Natl Acad Sci U S A 100(23): p. 13710-13715, 2003.
185. Ying W.Z. and Sanders P.W.: *Dietary salt regulates expression of Tamm-Horsfall glycoprotein in rats.* Kidney Int 54(4): p. 1150-1156, 1998.
186. Mattey M. and Naftalin L.: *Mechanoelectrical transduction, ion movement and water stasis in uromodulin.* Experientia 48(10): p. 975-980, 1992.
187. Kahn A.M.: *Effect of diuretics on the renal handling of urate.* Semin Nephrol 8(3): p. 305-314, 1988.
188. Devuyst O., Dahan K. and Pirson Y.: *Tamm-Horsfall protein or uromodulin: new ideas about an old molecule.* Nephrol Dial Transplant 20(7): p. 1290-1294, 2005.
189. Gersch M.S., Sautin Y.Y., Gersch C.M., Henderson G., Bankir L. and Johnson R.J.: *Does Tamm-Horsfall protein-uric acid binding play a significant role in urate homeostasis?* Nephrol Dial Transplant 21(10): p. 2938-2942, 2006.
190. Chambers R., Groufsky A., Hunt J.S., Lynn K.L. and McGiven A.R.: *Relationship of abnormal Tamm-Horsfall glycoprotein localization to renal morphology and function.* Clin Nephrol 26(1): p. 21-26, 1986.
191. Zager R.A., Cotran R.S. and Hoyer J.R.: *Pathologic localization of Tamm-Horsfall protein in interstitial deposits in renal disease.* Lab Invest 38(1): p. 52-57, 1978.
192. Su S.J., Chang K.L., Lin T.M., Huang Y.H. and Yeh T.M.: *Uromodulin and Tamm-Horsfall protein induce human monocytes to secrete TNF and express tissue factor.* J Immunol 158(7): p. 3449-3456, 1997.
193. Thomas D.B., Davies M., Peters J.R. and Williams J.D.: *Tamm Horsfall protein binds to a single class of carbohydrate specific receptors on human neutrophils.* Kidney Int 44(2): p. 423-429, 1993.
194. Kreft B., Jabs W.J., Laskay T., Klinger M., Solbach W., Kumar S. and van Zandbergen G.: *Polarized expression of Tamm-Horsfall protein by renal tubular epithelial cells activates human granulocytes.* Infect Immun 70(5): p. 2650-2656, 2002.
195. Hoyer J.R.: *Tubulointerstitial immune complex nephritis in rats immunized with Tamm-Horsfall protein.* Kidney Int 17(3): p. 284-292, 1980.
196. Mayrer A.R., Kashgarian M., Ruddle N.H., Marier R., Hodson C.J., Richards F.F. and Andriole V.T.: *Tubulointerstitial nephritis and immunologic responses to Tamm-Horsfall*

protein in rabbits challenged with homologous urine or Tamm-Horsfall protein. J Immunol 128(6): p. 2634-2642, 1982.

197. Pahl H.L. and Baeuerle P.A.: *A novel signal transduction pathway from the endoplasmic reticulum to the nucleus is mediated by transcription factor NF-kappa B.* Embo J 14(11): p. 2580-2588, 1995.
198. Kaneko M., Niinuma Y. and Nomura Y.: *Activation signal of nuclear factor-kappa B in response to endoplasmic reticulum stress is transduced via IRE1 and tumor necrosis factor receptor-associated factor 2.* Biol Pharm Bull 26(7): p. 931-935, 2003.
199. Hu P., Han Z., Couvillon A.D., Kaufman R.J. and Exton J.H.: *Autocrine tumor necrosis factor alpha links endoplasmic reticulum stress to the membrane death receptor pathway through IRE1alpha-mediated NF-kappaB activation and down-regulation of TRAF2 expression.* Mol Cell Biol 26(8): p. 3071-3084, 2006.
200. Paul M., Poyan Mehr A. and Kreutz R.: *Physiology of local renin-angiotensin systems.* Physiol Rev 86(3): p. 747-803, 2006.
201. Campbell D.J.: *Critical review of prorenin and (pro)renin receptor research.* Hypertension 51(5): p. 1259-1264, 2008.
202. Walter P., Ibrahimi I. and Blobel G.: *Translocation of proteins across the endoplasmic reticulum. I. Signal recognition protein (SRP) binds to in-vitro-assembled polysomes synthesizing secretory protein.* J Cell Biol 91(2 Pt 1): p. 545-550, 1981.
203. Morris B.J.: *Molecular biology of renin. I: Gene and protein structure, synthesis and processing.* J Hypertens 10(3): p. 209-214, 1992.
204. Yoshida H., Matsui T., Yamamoto A., Okada T. and Mori K.: *XBP1 mRNA is induced by ATF6 and spliced by IRE1 in response to ER stress to produce a highly active transcription factor.* Cell 107(7): p. 881-891, 2001.
205. Wilson F.H., Disse-Nicodeme S., Choate K.A., Ishikawa K., Nelson-Williams C., Desitter I., Gunel M., Milford D.V., Lipkin G.W., Achard J.M., Feely M.P., Dussol B., Berland Y., Unwin R.J., Mayan H., Simon D.B., Farfel Z., Jeunemaitre X. and Lifton R.P.: *Human hypertension caused by mutations in WNK kinases.* Science 293(5532): p. 1107-1112, 2001.
206. Gribouval O., Gonzales M., Neuhaus T., Aziza J., Bieth E., Laurent N., Bouton J.M., Feuillet F., Makni S., Ben Amar H., Laube G., Delezoide A.L., Bouvier R., Dijoud F., Ollagnon-Roman E., Roume J., Joubert M., Antignac C. and Gubler M.C.: *Mutations in genes in the renin-angiotensin system are associated with autosomal recessive renal tubular dysgenesis.* Nat Genet 37(9): p. 964-968, 2005.

207. Lacoste M., Cai Y., Guicharnaud L., Mounier F., Dumez Y., Bouvier R., Dijoud F., Gonzales M., Chatten J., Delezoide A.L., Daniel L., Joubert M., Laurent N., Aziza J., Sellami T., Amar H.B., Jarnet C., Frances A.M., Daikha-Dahmane F., Coulomb A., Neuhaus T.J., Foliguet B., Chenal P., Marcorelles P., Gasc J.M., Corvol P. and Gubler M.C.: *Renal tubular dysgenesis, a not uncommon autosomal recessive disorder leading to oligohydramnios: Role of the Renin-Angiotensin system.* J Am Soc Nephrol 17(8): p. 2253-2263, 2006.
208. Zingg-Schenk A., Bacchetta J., Corvol P., Michaud A., Stallmach T., Cochat P., Gribouval O., Gubler M.C. and Neuhaus T.J.: *Inherited renal tubular dysgenesis: the first patients surviving the neonatal period.* Eur J Pediatr 167(3): p. 311-316, 2008.
209. Burckle C. and Bader M.: *Prorenin and its ancient receptor.* Hypertension 48(4): p. 549-551, 2006.
210. Kaneshiro Y., Ichihara A., Sakoda M., Takemitsu T., Nabi A.H., Uddin M.N., Nakagawa T., Nishiyama A., Suzuki F., Inagami T. and Itoh H.: *Slowly progressive, angiotensin II-independent glomerulosclerosis in human (pro)renin receptor-transgenic rats.* J Am Soc Nephrol 18(6): p. 1789-1795, 2007.
211. Pentz E.S., Moyano M.A., Thornhill B.A., Sequeira Lopez M.L. and Gomez R.A.: *Ablation of renin-expressing juxtaglomerular cells results in a distinct kidney phenotype.* Am J Physiol Regul Integr Comp Physiol 286(3): p. R474-483, 2004.
212. Cioffi J.A., Allen K.L., Lively M.O. and Kemper B.: *Parallel effects of signal peptide hydrophobic core modifications on co-translational translocation and post-translational cleavage by purified signal peptidase.* J Biol Chem 264(25): p. 15052-15058, 1989.
213. Arnold A., Horst S.A., Gardella T.J., Baba H., Levine M.A. and Kronenberg H.M.: *Mutation of the signal peptide-encoding region of the preproparathyroid hormone gene in familial isolated hypoparathyroidism.* J Clin Invest 86(4): p. 1084-1087, 1990.
214. Fitches A.C., Appleby R., Lane D.A., De Stefano V., Leone G. and Olds R.J.: *Impaired cotranslational processing as a mechanism for type I antithrombin deficiency.* Blood 92(12): p. 4671-4676, 1998.
215. Siggaard C., Rittig S., Corydon T.J., Andreasen P.H., Jensen T.G., Andresen B.S., Robertson G.L., Gregersen N., Bolund L. and Pedersen E.B.: *Clinical and molecular evidence of abnormal processing and trafficking of the vasopressin preprohormone in a large kindred with familial neurohypophyseal diabetes insipidus due to a signal peptide mutation.* J Clin Endocrinol Metab 84(8): p. 2933-2941, 1999.

216. Hon L.S., Zhang Y., Kaminker J.S. and Zhang Z.: *Computational prediction of the functional effects of amino acid substitutions in signal peptides using a model-based approach.* Hum Mutat 2008.
217. Jarjanazi H., Savas S., Pabalan N., Dennis J.W. and Ozcelik H.: *Biological implications of SNPs in signal peptide domains of human proteins.* Proteins 70(2): p. 394-403, 2008.
218. Datta R., Waheed A., Shah G.N. and Sly W.S.: *Signal sequence mutation in autosomal dominant form of hypoparathyroidism induces apoptosis that is corrected by a chemical chaperone.* Proc Natl Acad Sci U S A 104(50): p. 19989-19994, 2007.
219. Kutz W.E., Wang L.W., Dagoneau N., Odrcic K.J., Cormier-Daire V., Traboulsi E.I. and Apte S.S.: *Functional analysis of an ADAMTS10 signal peptide mutation in Weill-Marchesani syndrome demonstrates a long-range effect on secretion of the full-length enzyme.* Hum Mutat 2008.
220. Marciniak S.J. and Ron D.: *Endoplasmic reticulum stress signaling in disease.* Physiol Rev 86(4): p. 1133-1149, 2006.
221. Schroder M.: *Endoplasmic reticulum stress responses.* Cell Mol Life Sci 65(6): p. 862-894, 2008.
222. Kaufman R.J.: *Orchestrating the unfolded protein response in health and disease.* J Clin Invest 110(10): p. 1389-1398, 2002.
223. Ito M., Jameson J.L. and Ito M.: *Molecular basis of autosomal dominant neurohypophyseal diabetes insipidus. Cellular toxicity caused by the accumulation of mutant vasopressin precursors within the endoplasmic reticulum.* J Clin Invest 99(8): p. 1897-1905, 1997.
224. Bonapace G., Waheed A., Shah G.N. and Sly W.S.: *Chemical chaperones protect from effects of apoptosis-inducing mutation in carbonic anhydrase IV identified in retinitis pigmentosa 17.* Proc Natl Acad Sci U S A 101(33): p. 12300-12305, 2004.
225. Rebello G., Ramesar R., Vorster A., Roberts L., Ehrenreich L., Oppon E., Gama D., Bardien S., Greenberg J., Bonapace G., Waheed A., Shah G.N. and Sly W.S.: *Apoptosis-inducing signal sequence mutation in carbonic anhydrase IV identified in patients with the RP17 form of retinitis pigmentosa.* Proc Natl Acad Sci U S A 101(17): p. 6617-6622, 2004.
226. Persson P.B.: *Renin: origin, secretion and synthesis.* J Physiol 552(Pt 3): p. 667-671, 2003.
227. Nangaku M. and Fujita T.: *Activation of the renin-angiotensin system and chronic hypoxia of the kidney.* Hypertens Res 31(2): p. 175-184, 2008.

228. Cruzado J.M., Rico J. and Grinyo J.M.: *The renin angiotensin system blockade in kidney transplantation: pros and cons.* Transpl Int 21(4): p. 304-313, 2008.
229. Safirstein R., Megyesi J., Saggi S.J., Price P.M., Poon M., Rollins B.J. and Taubman M.B.: *Expression of cytokine-like genes JE and KC is increased during renal ischemia.* Am J Physiol 261(6 Pt 2): p. F1095-1101, 1991.
230. James P., Halladay J. and Craig E.A.: *Genomic libraries and a host strain designed for highly efficient two-hybrid selection in yeast.* Genetics 144(4): p. 1425-1436, 1996.
231. Fields S. and Song O.: *A novel genetic system to detect protein-protein interactions.* Nature 340(6230): p. 245-246, 1989.
232. Ma H., Kunes S., Schatz P.J. and Botstein D.: *Plasmid construction by homologous recombination in yeast.* Gene 58(2-3): p. 201-216, 1987.
233. Petermann R., Mossier B.M., Aryee D.N. and Kovar H.: *A recombination based method to rapidly assess specificity of two-hybrid clones in yeast.* Nucleic Acids Res 26(9): p. 2252-2253, 1998.
234. Bendixen C., Gangloff S. and Rothstein R.: *A yeast mating-selection scheme for detection of protein-protein interactions.* Nucleic Acids Res 22(9): p. 1778-1779, 1994.
235. Fromont-Racine M., Rain J.C. and Legrain P.: *Toward a functional analysis of the yeast genome through exhaustive two-hybrid screens.* Nat Genet 16(3): p. 277-282, 1997.
236. Van Criekinge W. and Beyaert R.: *Yeast Two-Hybrid: State of the Art.* Biol Proced Online 2: p. 1-38, 1999.
237. Serebriiskii I.G., Toby G.G., Finley R.L., Jr. and Golemis E.A.: *Genomic analysis utilizing the yeast two-hybrid system.* Methods Mol Biol 175: p. 415-454, 2001.
238. Sumner J.B. and Howell S.F.: *Identification of Hemagglutinin of Jack Bean with Concanavalin A.* J Bacteriol 32(2): p. 227-237, 1936.
239. Doering T.L. and Englund P.T.: *Detection of Glycophospholipid Anchors on Proteins.* In: *Current Protocols in Molecular Biology*, Ausubel F.M., Brent R., Kingston R.E., Moore D.D., Seidman J.G., Smith J.A. and Struhl K., Editors. John Wiley & Sons, Inc., New York: p. 17.18.11-17.18.13, 2000.
240. Rhodes D.C., Hinsman E.J. and Rhodes J.A.: *Tamm-Horsfall glycoprotein binds IgG with high affinity.* Kidney Int 44(5): p. 1014-1021, 1993.
241. Rhodes D.C.: *Binding of Tamm-Horsfall protein to complement 1q measured by ELISA and resonant mirror biosensor techniques under various ionic-strength conditions.* Immunol Cell Biol 78(5): p. 474-482, 2000.

242. Rhodes D.C.: *Binding of Tamm-Horsfall protein to complement 1q and complement 1, including influence of hydrogen-ion concentration.* Immunol Cell Biol 80(6): p. 558-566, 2002.
243. Sherblom A.P., Decker J.M. and Muchmore A.V.: *The lectin-like interaction between recombinant tumor necrosis factor and uromodulin.* J Biol Chem 263(11): p. 5418-5424, 1988.
244. Welker P., Geist B., Fruhauf J.H., Salanova M., Groneberg D.A., Krause E. and Bachmann S.: *Role of lipid rafts in membrane delivery of renal epithelial Na+-K+-ATPase, thick ascending limb.* Am J Physiol Regul Integr Comp Physiol 292(3): p. R1328-1337, 2007.

9 SUPPLEMENT

9.1 List of author's publications and presentations

9.1.1 Presentations

Kublová M., **Vyleťal P.**, Hodaňová K., Kalbáčová M., Blažková H., Majewski J., Simmonds A., Matthijs G. and Kmoch S.: Uromodulin urinary excretion in patients with familial juvenile hyperuricaemic nephropathy (FJHN). Poster presentation. 19th workshop Inherited Metabolic Disorders, Podbanské, Slovakia, 26. - 28. 5. 2004.

Kublová M., **Vyleťal P.**, Hodaňová K., Kalbáčová M., Hůlková H., Majewski J., Simmonds A., Matthijs G. and Kmoch S.: Uromodulin urinary excretion in patients with familial juvenile hyperuricaemic nephropathy (FJHN). Poster presentation. 45th Annual Short Course in Medical and Experimental Mammalian Genetics, The Jackson Laboratory, Bar Harbor, Maine, USA, 18. - 30. 7. 2004.

Kublová M., **Vyleťal P.,** Hodaňová K., Barešová V., Kalbáčová M., Sikora J., Živný J., Sovová J., Majewski J., Marinaki A., Simmonds A., Fryns J.-P., Venkat-Raman G. and Kmoch S.: Familial Juvenile Hyperuricaemic Nephropathy (FJHN), molecular analysis of 23 families, identification and functional consequences of 6 uromodulin mutations. Poster presentation. 37th European Human Genetics Conference, Prague, Czech Republic, 7. - 10. 5. 2005.

Kublová M., **Vyleťal P.,** Hodaňová K., Barešová V., Kalbáčová M., Sikora J., Živný J., Sovová J., Majewski J., Marinaki A., Simmonds A., Fryns J.-P., Venkat-Raman G. and Kmoch S.: Familial Juvenile Hyperuricaemic nephropathy (FJHN), molecular analysis of 23 families, identification and functional consequences of 6 uromodulin mutations. Poster presentation. 20th workshop Inherited Metabolic Disorders, Lednice, Czech Republic, 18. - 20. 5. 2005.

Kublová M., Hodaňová K., Majewski J., **Vyleťal P.**, Kalbáčová M., Stibůrková B., Hůlková H., Chagnon Y. C., Lanouette Ch. M., Marinaki A., Fryns J.-P., Venkat-Raman G. and Kmoch S.: Mapping of a new candidate locus for uromodulin-associated kidney disease (UAKD) to chromosome 1q41. Poster presentation. Functional Genomics and Disease, 2nd ESF Functional Genomics Conference, Oslo, Norway, 6. - 10. 9. 2005.

Kmoch S., **Vyleťal P.**, Kublová M., Kalbáčová M., Hodaňová K., Stibůrková B., Hůlková H., Majewski J., Simmonds A., Fryns J.-P., Venkat-Raman G. and Elleder M.: Alterations of uromodulin biology: a common denominator of the genetically heterogeneous FJHN/MCKD syndrome. Oral presentation. 31st congress of the Czech Society for Nephrology, Hradec Králové, Czech Republic, 24. 6. 2006.

Kublová M., **Vyleťal P.**, Kalbáčová M., Hodaňová K., Barešová V., Stibůrková B., Sikora J., Hůlková H., Živný J., Majewski J., Simmonds A., Fryns J.-P., Venkat-Raman G., Elleder M. and Kmoch S.: Alterations of Uromodulin Biology - a Common Denominator of the Genetically Heterogeneous FJHN/MCKD Syndrome. Poster presentation. The American Society for Cell Biology - 46th Annual Meeting, San Diego, USA, 9. - 13. 12. 2006.

Vyleťal P., Hůlková H., Živná M., Berná L., Novák P., Elleder M. and Kmoch S.: Abnormal processing of uromodulin (UMOD) in Fabry disease patients reflects kidney tubular cell storage alteration and is reversible by enzyme replacement therapy. Poster presentation. The American Society for Cell Biology - 47th Annual Meeting, Washington, DC, USA, 1. - 5. 12. 2007.

Thesis unrelated presentations

Vyleťal P., Sokolová J., Cooper D. N., Krawczak M., Kraus J. P., Pepe G., Rickards O., Koch H. G., Linnebank M., Kluijtmans L. A., Blom H. J., Boers G. H., Gaustadnes M., Skovby F., Wilcken B., Wilcken D. E., Andria G., Sebastio G., Naughten E. R., Yap S., Ohura T., Pronicka E., Laszlo A., and Kožich V.: Evolutionary relatedness of cystathionine β-synthase (CBS)

alleles bearing the common homocystinuria mutation c.833T>C (I278T). Poster presentation. 17th workshop Inherited Metabolic Disorders, Piešťany, Slovakia, 15. - 17. 5. 2002.

9.1.2 Publications

Stibůrkova B., Majewski J., Hodaňonová K., Ondrová L., Jeřábková M., Zikánová M., **Vyleťal P.**, Šebesta I., Marinaki A., Simmonds A., Matthijs G., Fryns J. P., Torres R., Puig J. G., Ott J. and Kmoch S.: Familial juvenile hyperuricaemic nephropathy (FJHN): linkage analysis in 15 families, physical and transcriptional characterisation of the FJHN critical region on chromosome 16p11.2 and the analysis of seven candidate genes. Eur J Hum Genet. 2003 Feb;11(2):145-154. **IF 3.669** (2003)

Hodaňová K., Majewski J., Kublová M., **Vyleťal P.**, Kalbáčová M., Stibůrková B., Hůlková H., Chagnon Y. C., Lanouette Ch. M., Marinaki A., Fryns J.-P., Venkat-Raman G. and Kmoch S.: Mapping of a new candidate locus for uromodulin-associated kidney disease (UAKD) to chromosome 1q41. Kidney Int. 2005 Oct;68(4):1472-1482. **IF 4.927** (2005)

Vyleťal P., Kublová M., Kalbáčová M., Hodaňová K., Barešová V., Stibůrková B., Sikora J., Hůlková H., Živný J., Majewski J., Simmonds A., Fryns J.-P., Venkat-Raman G., Elleder M. and Kmoch S.: Alterations of uromodulin biology: a common denominator of the genetically heterogeneous FJHN/MCKD syndrome. Kidney Int. 2006 Sep;70(6):1155-1169. **IF 4.773** (2006)

Vyleťal P., Hůlková H., Živná M., Berná L., Novák P., Elleder M. and Kmoch S.: Abnormal expression and processing of uromodulin in Fabry disease reflects tubular cell storage alteration and is reversible by enzyme replacement therapy. J Inherit Metab Dis. 2008 Aug;31(4): p. 508-517. **IF 1.668** (2007)

Živná M., Hůlková H., Hodaňová K., **Vyleťal P.**, Kalbáčová M., Barešová V., Sikora J., Blažková H., Živný J., Iványek R., Sovová J., Claes K., Matthijs G., Elleder M., Kapp K. and Kmoch S.: Preprorenin signal sequence mutation affecting renin biosynthesis and intra-renal RAS expression in a family with uromodulin associated kidney disease. Manuscript in preparation, 2008.

Thesis unrelated publications

Vyleťal P., Sokolová J., Cooper D. N., Kraus J. P., Krawczak M., Pepe G., Rickards O., Koch H. G., Linnebank M., Kluijtmans L. A., Blom H. J., Boers G. H., Gaustadnes M., Skovby F., Wilcken B., Wilcken D. E., Andria G., Sebastio G., Naughten E. R., Yap S., Ohura T., Pronicka E., Laszlo A., and Kožich V.: Diversity of cystathionine beta-synthase haplotypes bearing the most common homocystinuria mutation c.833T>C: a possible role for gene conversion. Hum Mutat. 2007 Mar;28(3):255-64. **IF 6.473** (2006)

9.2 Manuscript in preparation - Preprorenin signal sequence mutation affecting renin biosynthesis and intra-renal RAS expression in a family with uromodulin associated kidney disease

Preprorenin signal sequence mutation affecting renin biosynthesis and intra-renal RAS expression in a family with uromodulin associated kidney disease

Martina Živná[1,2], Helena Hůlková[2], Kateřina Hodaňová[1,2], Petr Vyleťal[1,2] , Marie Kalbáčová[1,2], Veronika Barešová[1,2], Jakub Sikora[2], Hana Blažková[2], Jan Živný[3], Robert Ivánek[1,2], Jana Sovová[2], Kathleen Claes[4], Gert Matthijs[5], Milan Elleder[1,2], Katja Kapp[6] and Stanislav Kmoch[1,2*]

[1]Center for Applied Genomics, [2]Institute for Inherited Metabolic Disorders and [3]Institute of Pathophysiology, Charles University, 1st Faculty of Medicine, Prague; [4]Department of Nephrology, University Hospital Gasthuisberg, Leuven; [5]Center for Human Genetics, University of Leuven; [6]ZMBH (Center for Molecular Biology Heidelberg), University of Heidelberg

*Corresponding author and reprint address:

Stan Kmoch

Center for Applied Genomics, Institute for Inherited Metabolic Disorders,

Ke Karlovu 2, 128 00 Prague 2, Czech Republic

Phone: 420-2-24967691, FAX: 420-2-24919392, Email: SKMOCH@LF1.CUNI.CZ

Running title: Renin signal sequence mutation in UAKD family

Abstract

We analysed family with autosomal-dominant tubulointerstitial nephropathy characterized by combination of hyperuricemia, decreased urinary uromodulin (UMOD) excretion and abnormal UMOD expression in the kidney. Using positional cloning we identified in affected individuals deletion of one of the leucine residues forming hydrophobic pentaleucine motif of the preprorenin signal sequence. We found that the mutation decreases signal peptide hydrophobicity required for efficient ER translocation, changes property of the out cleaved signal peptide and limits biosynthesis of secretory competent and catalytically active prorenin and renin proteins. Cells stably expressing mutant protein retained prorenin and renin intracellularly and showed reduced growth rate and signs of activated ER stress, unfolded protein response and pronounced autophagy. The immunohistochemical analysis of kidney tissues showed in patients reduced expression of prorenin and renin in site of juxtaglomerular apparatus, absence of renin expressing cells along the tubules and enhanced ectopic expression of prorenin and renin in arterioles and arteries. Our results indicates that the identified mutation leads to aberrant prorenin and renin biosynthesis, ER-stress mediated cytotoxicity and slowly progressing damage of renin expressing cells which probably affects structure and function of juxtaglomerular apparatus, changes sensitivity of the tubuloglomerular feedback mechanism and alters renal blood flow autoregulation, which lead to ischemia, loss of glomeruli, tubulointerstitial injury and end-stage renal disease. We believe that the presented genetic defect and phenotype define and document the range and functional importance of juxtaglomerular cells and the intra-renal RAS system, which is still not well understood in humans.

Introduction

The term of the uromodulin-associated kidney diseases (UAKD) emerged recently for a group of autosomal-dominant tubulointerstitial nephropathies characterized by combination of hyperuricemia, gouty arthritis, decreased urinary uromodulin (UMOD) excretion and abnormal UMOD expression in the kidney [1]. UAKD comprises phenotypes known as a familial juvenile hyperuricemic nephropathy (FJHN) (OMIM 162000) [2, 3], medullary cystic kidney diseases type 1 (MCKD1) (OMIM 174000) [4], and type 2 (MCKD2) (OMIM 603860) [5]. The association of these phenotypes with disturbances of the UMOD biology was established following the identification of *UMOD* mutations in some of the families [6]. Although present in majority of the cases [7-12], UMOD mutations are clearly not the only cause of the UAKD phenotype [1, 13-18]. The other disease causing gene(s) still remain(s) to be identified.

In this work we advanced our analysis in a single UAKD family showing linkage to chromosome 1q41 [19], and identified in affected individuals a deletion of one of the leucine residues forming hydrophobic pentaleucine motif of the preprorenin signal sequence. Preprorenin is expressed by juxtaglomerular (JG) cells in the kidney. It is a biosynthetic precursor of prorenin and renin which are produced by glycosylation and proteolytic processing of the nascent preproprotein [20]. Both, prorenin and renin are secretory proteins active in the renin-angiotensin system (RAS) [21], and the (pro)renin receptor signal transduction pathway which is distinct from RAS receptor signalling [22]. Both pathways play an important role in kidney physiology and pathology. Mutations in the RAS system components cause autosomal recessive renal tubular dysgenesis [23-25]. The (pro)renin receptor knockout in mouse was lethal [26], and human (pro)renin receptor transgenic rats developed gradual proteinuria and glomerulosclerosis [27]. Moreover renin-1 in mice is essential for normal JG cell granulation, macula densa morphology and tubuloglomerular feedback signalling [28] and selective ablation of JG cells resulted into renin insufficiency and led to alteration of renal functions and morphology [29].

Signal peptides are typically N-terminus located 15-25 amino acid residues creating characteristic hydrophilic-hydrophobic structures fundamental for proper ER co-translational translocation and modulation of secretory proteins biogenesis [30]. In addition to that some of the signal peptides removed from the nascent preproprotein by signal peptidase (SPase), and their fragments produced by signal peptide peptidase (SPPase) have other post-targeting function [31-34]. Considering their biological importance, it is therefore not surprising, that about 30 human genetic disorders, both dominant and recessive, have been described as to be associated with mutations in signal sequences [35-38].

Inspired by these facts, we therefore further studied biosynthesis, catalytic properties and cellular localization of the prorenin and renin expressed from the wild-type and mutant preprorenin cDNA constructs, assessed effect of the expressed proteins on cell viability and correlated the results with expression of prorenin, renin, other phenotype related proteins and selected tubular markers in available kidney biopsies. Our results provided several lines of evidence indicating that the identified mutation leads to aberrant prorenin and renin biosynthesis, cytotoxic stress and slowly progressing damage of renin expressing cells which affects local intra-renal RAS system, alters structure and function of JG apparatus, and similarly to renal tubular dysgenesis [23] and animal model with ablated JG cells [29], end up in deterioration of kidney functions and observed clinical abnormalities.

Results

Genotyping and linkage analysis identified single genomic region on chromosome 1.

To corroborate the results of the medium-dense scan [19], we performed genome-wide linkage analysis and identified single genomic region with statistically significant LOD score of 3.24 on chromosome 1 (Fig. 1*A*). Using haplotype analysis we delimited the candidate region between the SNP_A_1517951 and SNP_A_1509750 markers (Fig. 1*B*). The identified 24.7 Mb region, (position chr1:186,798,293-211,538,405) have contained 242 genes (NCBI Build 36.2). It has overlapped partially with recently defined candidate region for the Gordon syndrome (OMIM 145260), which is characterized by hyperkalemia, mild hyperchloremia, suppressed plasma renin activity and hypertension [39].

Sequencing of candidate genes revealed mutation in the signal sequence of renin.

Sequencing candidate genes we revealed in the proband heterozygous deletion c.[44_46delTGC] in exon 1 of the renin gene (*REN*) (Fig. 2*A*). The mutation causes a deletion of one of the leucine residues forming hydrophobic pentaleucine motif of the preprorenin signal sequence ($\Delta L16^{REN}$). Subsequent genotyping showed that the identified deletion is present in all affected individuals, while healthy individuals from the family as well as 200 unrelated Caucasian controls have normal genotype (Fig. 2*B*).

$\Delta L16^{REN}$ mutation may affect various steps of prorenin and renin biosynthesis.

Human prorenin and renin are synthesized in JG cells from 406 amino acid preproprotein composed of a 23 amino acid N-terminal signal sequence, 43 amino acid “pro“ domain, and 340 amino acid mature renin [20]. Deleted leucine residue is located in the conserved hydrophobic core of the preprorenin signal sequence (Fig.3 *A* and *B*), which ensures insertion of the signal sequence into translation-translocation channel in the endoplasmic reticulum (ER) membrane [40]. Following proteosynthesis, glycosylation and signal sequence removal, both the prorenin

and renin are sorted to secretory granules from where they are released in highly regulated manner into the circulation [41]. Based on its position, the pathogenic effect(s) of the $\Delta L16^{REN}$ mutation may be associated either with aberrant prorenin and renin biosynthesis, intracellular trafficking and secretion or with the loss or gain of function effect of the mutated signal peptide.

***In silico* analysis suggests decreased hydrophobicity of the $\Delta L16^{REN}$ signal sequence.**

The hydrophobic region of the human preprorenin signal sequence is not perfectly conserved among the mammals (Fig. 3*B*). Using SignalP 3.0 server [42], we noticed that $\Delta L16^{REN}$ mutation decreases the signal sequence prediction probability, (*D* score value) [35] by 4%, and has no effect on predicted signal peptide cleavage site (data not shown). Other calculation [43] showed decrease in the hydrophobicity of the $\Delta L16^{REN}$ signal sequence compare to that of the WT^{REN} (1,689 vs. 2,156, respectively) (Fig. 3*C*).

$\Delta L16^{REN}$ mutation reduces the translocation efficiency and mutant signal peptide behaves differently under *in vitro* conditions.

To study the effect of the identified mutation on biosynthesis of prorenin and renin *in vitro*, we cloned the WT^{REN}, $\Delta L16^{REN}$ and an artificial, effect enhancing mutant $\Delta L14\text{-}16^{REN}$ cDNAs into pCR3.1 expression vector and transcribed and translated encoding transcripts in rabbit reticulocyte lysate in the absence/presence of rough microsomes (RMs) and tripeptide glycosylation acceptor (AP) (Fig. 4*A*). *In vitro* translation performed in the absence of RMs produced from all three transcripts a single protein of 42 kDa that correlates with the theoretical molecular weight of preprorenin precursor (Fig. 4*A*; lanes 1, 6, 11). In the presence of RMs, the *in vitro* translation reactions were separated into membranes and cytosol fractions. $\underline{WT^{REN}}$ transcript produced an additional protein of 47 kDa, which appeared predominately in the membrane fraction, while the 42 kDa protein was mainly detected in the supernatant (Fig. 4*A*; lanes 2 and 3). In the presence of AP, the 42 kDa protein was found again in the supernatant (Fig. 4*A*; lane 4), while the 47 kDa protein amount was reduced and a 41 kDa protein appeared in the pellet fraction (Fig. 4*A*; lane 5). Considering the signal sequence cleavage and two N-glycosylation sites in preprorenin sequence (N71 and N141), which alter the molecular weight by 2-3 kDa each, the 47 kDa represents probably the signal sequence cleaved, ER-translocated and fully glycosylated prorenin, while the 41 kDa protein represent the signal sequence cleaved, unglycosylated prorenin. The other minor protein bands represent probably bi- and mono-glycosylated forms which were produced due to incomplete inhibitory effect of AP. Mutant $\underline{\Delta L16^{REN}}$ transcript produced protein that was also translocated (Fig. 4*A*; lanes 7-10) but less efficiently than WT^{REN} (compare Fig. 4*A*; lanes 3 and 8). Furthermore, a higher amount of precursor molecules was detected in the pellet fraction (Fig. 4*A*; lane 8), which suggests that

these molecules are attached but not inserted into RMs. The artificial mutant *ΔL14-16*^{REN} transcript was also translated, but not translocated (Fig. 4*A*; lanes 12-15).

To further investigate the WT^{REN} and ΔL16^{REN} signal sequence properties, the *in vitro* translation/translocation assay was performed in the presence/absence of signal peptide peptidase inhibitor $(ZZ\text{-}L)_2$ – ketone and the resulting products were analysed using high resolution SDS-PAGE for small peptides (Fig. 4*B*). The analysis revealed in case of WT^{REN} presence of a 3 kDa peptide in the pellet fraction (Fig. 4*B*; lane 4). In the absence of RMs, this peptide was not identified (data not shown), which suggests that this molecule is the renin precursor-derived signal peptide, SP$^{WT\text{-}REN}$. When SPPase inhibitor was added to the *in vitro* translation/translocation reaction, the amount of SP$^{WT\text{-}REN}$ increased accordingly (Fig. 4*B*; lane 6). In case of ΔL16^{REN}, only small amounts of a 3 kDa SP$^{\Delta L16\text{-}REN}$ peptide was observed and the addition of the SPPase inhibitor had no effect on its presence (Fig. 4*B*; lanes 8 and 9). The translation and translocation of mature WT^{REN} or ΔL16^{REN} proteins was not affected by the SPPase inhibitor or its organic solvent (data not shown).

Normal renin activity but decreased prorenin and renin secretion in AtT-20 cells transiently expressing ΔL16^{REN}.

To investigate co-translational translocation efficiency, post-translational processing and secretion rate of prorenin and renin and renin activity *in vivo*, we used *WT*^{REN}, *ΔL16*^{REN} and Δ*L14-16*^{REN} cDNA expression vectors and transiently expressed corresponding recombinant proteins in AtT-20 cells. We measured and found numerical, but not significant decrease in renin enzymatic activity between WT^{REN} and ΔL16^{REN} proteins in cell lysates and medium (Fig. 5*A*). Measuring active renin amount, we found significant decrease in total prorenin and renin amount in cell lysates as well as significant decrease of prorenin and renin secreted into medium from *ΔL16*^{REN} cDNA construct. Prorenin and renin synthesis from Δ*L14-16*^{REN} cDNA construct and the renin activity were negligible (Fig. 5*B*). Reduced rate and time delay in ΔL16^{REN} protein synthesis compared to WT^{REN} were apparent also from Western blot analysis, which further showed no differences in post-translational processing between WT^{REN} and ΔL16^{REN} protein products (Fig. 5*C-F*). We obtained similar results from transiently transfected HEK 293 cells (data not shown).

Prorenin and renin secretion is impaired in ΔL16^{REN} stable cell lines.

To overcome limitations of transient expression for quantitative renin analysis and intracellular localization studies, we transfected HEK 293 cell lines with *WT*^{REN} and *ΔL16*^{REN} cDNA constructs and selected stable prorenin and renin producing clones. Using IRMA assay detecting selectively active renin we found significant decrease in prorenin and renin amounts in lysates and medium of ΔL16^{REN} cells (Fig. 6*A*). Contrary to this result, Western blot analysis, detecting

whole protein mass, showed significant intracellular accumulation of prorenin and renin in $\Delta L16^{REN}$ cells (Fig. 6*B*). Prorenin and renin amounts in medium of $\Delta L16^{REN}$ cells were reduced on Western blot in accordance with IRMA assay (Fig. 6*C*). As in transient expression experiments, we found no differences in post-translational processing of prorenin and renin between WT^{REN} and $\Delta L16^{REN}$ stable cell lines (Fig. 6 *B* and *C*).

To investigate differences in a mode (semi-quantum vs. continuous) and dynamics of the renin secretion between WT^{REN} and $\Delta L16^{REN}$ stable cell lines, we modified commercially available fluorescence resonance energy transfer (FRET) method based on renin mediated cleavage of 5-FAM and QXL520 containing renin substrate. We continuously monitored the activity of the renin secreted by live cells by means of 5-FAM fluorescent signal release from the cleaved substrate. We found no difference in the mode of renin secretion, however the rate of renin synthesis was considerably decreased in $\Delta L16^{REN}$ cell lines (Fig. 6*D*).

$\Delta L16^{REN}$ stable cells show reduced growth rate and a signs of unfolded protein response.

To asses the effect of the signal sequence mutation on cell viability, we determined and compared cell growth characteristics of HEK 293 and MDCK cell lines stably expressing WT^{REN} and $\Delta L16^{REN}$. As a control we also determined growth rate curves in antibiotics selected cell lines, which showed no renin expression by, RT-PCR and Western blot analysis (0^{REN} cell lines). The WT^{REN} and 0^{REN} cells showed very similar exponential growth rates with population-doubling times of 46 hours during seven days of the cultivation. Compared to the WT^{REN} and 0^{REN}, the $\Delta L16^{REN}$ cells showed significant lag phase delay with population-doubling time of 78 hours during first three days of the cultivation. Following this period the cell growth curve and population-doubling time of $\Delta L16^{REN}$ cells became similar to that of the WT^{REN} and 0^{REN} cells (Fig. 7*A* and *B*). RT-PCR analysis further showed in $\Delta L16^{REN}$ cells presence of the spliced *XBP1(S)* mRNA variant, which is a key effector of the mammalian unfolded protein response (UPR) [44] (Fig. 7*C)*.

$\Delta L16^{REN}$ mutation has no effect on prorenin and renin localization in stable cell lines.

To see whether signal sequence mutation affects cellular distribution of prorenin and renin, we studied their localization in WT^{REN} and $\Delta L16^{REN}$ stable cell lines by immunofluorescence and confocal microscopy. The analysis showed expected localization of prorenin and renin containing granules in cytosol of the investigated cells. We did not find any visible differences in granule size, shape and localization and found no signs of prorenin and renin retention in ER, Golgi apparatus, cytoskeleton or plasma membrane neither in WT^{REN} nor $\Delta L16^{REN}$ expressing cell lines (Fig. 8).

Macroautophagy and distension of rough endoplasmic reticulum cisternae seems to be more pronounced in $\Delta L16^{REN}$ cells.

To reveal eventual impacts of reduced translocation efficiency of $\Delta L16^{REN}$ on cellular ultrastructure we analysed WT^{REN} and $\Delta L16^{REN}$ stable cell lines and non-transfected HEK 293 cells (NT) by electron microscopy (EM). The images (Fig. 9) showed in the cytosol of both WT^{REN} and $\Delta L16^{REN}$ cells numerous, variously sized, round, electron dense and membrane delimited granules, which characteristic is compatible with those of secretory renin granules (Fig. 9*A*-*C*) and [45]. These structures were not present in NT cells (data not shown). Despite extensive evaluation, no direct sites of active exocytosis were observed; nevertheless, a number of granules were localized in close vicinity to plasma membrane. In addition to renin granules, cells of both lines contained numerous, often double membrane bound bodies with pleomorphic content which was suggestive of degraded cytoplasmic contents including remnants of organelles (Fig. 9*D* and *E*). These ultrastructural features are characteristic [46] and therefore highly suggestive of autophagic origin of this compartment. Furthermore we observed considerably distended rough endoplasmic reticulum cisternae (compare Fig. 9*F* to Fig. 9*A*). Even though focused quantification of these changes (macroautophagy and ER distension) was not performed, both changes seemed to be more frequent and pronounced in $\Delta L16^{REN}$ cells.

Plasma renin activity is normal in affected individuals.

To correlate the results from *in vitro* and *in vivo* studies with the situation in the patients, we measured plasma renin activity (PRA) and aldosterone (Ald) concentration in patients DIII.6 (PRA 0,7 and 1,00 µg/L/h; Ald 158 and 390 ng/L, respectively), DIV4 (PRA 3,10 µg/L/h; Ald 134 ng/L) and DIV.7 (PRA 0,50 µg/L/h, Ald 255 ng/L). Measured values were within control ranges (PRA 0,40-2,78 µg/L/h; Ald 20-330 ng/L). This may be well explained by activated extra renal prorenin and renin production - see bellow and [47], and correspond with normal blood pressure of the investigated individuals.

Reduced expression and abnormal localization of prorenin and renin and altered expression of RAS components in patients´ kidney.

To asses prorenin and renin expression in patients´ kidney samples, we performed in three patients immunohistochemical staining with antibody specifically detecting prorenin, prorenin + renin, and active renin. In addition to that and to previous immunohistochemical study of UMOD and MUC1 [1], we further investigated expression of other RAS components (renin receptor, angiotensinogen, angiotensin II), KNK2 (TREK-1) as another candidate gene located within the identified genomic region and WNK4 kinase as a marker of proximal tubule brush border and protein involved in the pathogenesis of Gordon syndrome [48].

Compared to control tissues (Fig.10A-C), we found in patients considerably reduced expression of both, renin and prorenin. In early disease stage, the signal was strongly decreased in JG granular cells and undetectable in tubular cells (Fig.10D-F). In advanced destructive stage of the

disease, the signal was absent in both JGA and tubular epithelium (Fig.10G-I). However, we observed abnormal localization/induction of both, renin and prorenin inside the vessel wall of several arterioles and small arteries in all three patients (Fig.10J-L). Staining intensities of other analyzed renal RAS components, angiotensinogen, angiotensin II and pro/renin receptor, were decreased compared to controls. The decrease was proportional to the stage of the disease (Figure 11). TREK-1 (apical pole of PT) and WNK4 (apical pole of TALH and CD) showed tendency to weakened immunostaining similarly to UMOD and MUC-1 [1] (not shown).
From a morphological point of view, patients´ kidney showed progressive destruction of both glomeruli and renal tubules with some differences in severity between individual nephrons (details are given in legend to Figure 10).

Discussion

We identified $\Delta L16^{REN}$ mutation in the signal sequence of preprorenin segregating with a phenotype of autosomal dominant tubulointerstitial nephropathy fulfilling the clinical and biochemical criteria of UAKD [1]. We found, that the mutation decreases sequence hydrophobicity required for efficient ER translocation, changes property of the out cleaved signal sequence and limits biosynthesis of secretory competent and catalytically active prorenin and renin proteins. The mutation further causes intracellular retention of prorenin and renin, and cells expressing mutant protein have shown reduced growth rate, signs of activated ER stress, unfolded protein response (UPR) and pronounced autophagy, a features having potentially serious consequences especially for tissues dedicated to extracellular protein synthesis [49]. Constant ER stress and activated UPR signalling have generally serious impact on ER function and structure, trigger apoptosis, inflammation and eventually lead to reduced viability or even cell death [50] and disease development [51]. This pathogenetic mechanism is well plausible for the $\Delta L16^{REN}$ mutation as is in ER-stress and apoptosis inducing signal sequence mutations found in autosomal dominant neurohypophyseal diabetes insipidus [52], carbonic anhydrase IV causing retinitis pigmentosa [53, 54] or parathyroid hormone in autosomal dominant form of hypoparathyroidism [37].
The major site of prorenin and renin synthesis are JG cells [55]. JG cells execute tight control on renin synthetic capacity and secretion rate in order to regulate precisely blood pressure, renal hemodynamics and electrolyte balance [56]. The patients with $\Delta L16^{REN}$ mutation presented with small kidney, progressive hyalinosis of glomeruli, tubular atrophy or cystic dilatation, interstitial renal fibrosis, reduced glomerular filtration rate (GFR), urinary concentration defect with mild hyperkalemia and hyperchloremia [19], which phenotype is remarkably similar to mice with ablated JG cells [29]. The immunohistochemical analysis of kidney tissue showed reduced

expression of prorenin and renin in site of JG apparatus and absence of renin expressing cells along the tubules with enhanced ectopic expression or uptake of prorenin and renin in arterioles and arteries. These observations provide evidence for malfunction of the autocrine and paracrine effects of renin in the intra-renal RAS [57], and explains (enhanced ectopic expression) normotension, near normal plasma renin activity as well as normal endocrine function of RAS system in affected individuals.

Based on our experiments and observations, it is conceivable to predict, that the $\Delta L16^{REN}$ mutation reduces ability of regulated renin secretion *in vivo*. This probably affects renal development [23], sensitivity of the tubuloglomerular feedback mechanism and autoregulation of renal blood flow [56], which through altered renal hemodynamics and resulting hypoxia may lead to loss of glomeruli, tubulointerstitial injury and end-stage renal disease [58]. Mechanism of RAS blockage corresponds to anemia, hyperkalemia and reduced GFR presented in the patients [59] and renal ischemia well explains reduced expression of UMOD [60] and other tubular proteins.

We believe that the genetic defect and phenotype presented by affected individuals directly defines and documents functional importance of JG cells and the local intra-renal RAS system which is not well understood in humans. Detailed clinical, biochemical and molecular investigations of the patients together with further characterization of the wild-type and mutant preprorenin expressing cell lines are therefore of great interest.

Methods

Patients

The investigated family was described in detail in our previous studies [1, 19].

Genotyping and linkage analysis

Genomic DNA was isolated by standard methods. Samples were genotyped using Affymetrix GeneChip Mapping 10K 2.0 Xba Arrays according to the manufacturer's protocol. Raw feature intensities were extracted from the Affymetrix GeneChip Scanner 3000 7G images using the GeneChip Operating Software. Individual SNP calls were generated using GeneChip Genotyping Analysis Software (GTYPE) 4.0. Resulting genotypes were exported and analysed in the Merlin software v1.1.2 [61] . Multipoint parametric linkage analysis along with determination of the most likely haplotypes were carried out under the assumption of a dominant mode of inheritance with a 0.99 constant, age independent penetrance, 0.01 phenocopy rate and 0.001 frequency of disease allele. The results were visualized in the HaploPainter software v29.5 [62] and in the R-project v2.1.

REN gene analysis

Genomic fragments covering promoter region and all of the exons with their corresponding exon-intron boundaries of the *REN* were PCR amplified from genomic DNA and sequenced as previously described [63]. Segregation of the c.[88_90delTGC] mutation in the family was assessed by PCR-RFLP analysis of the mutation that created *MwoI* restriction site. Presence of the mutation in a control population was assessed by sizing and determination of the trinucleotide repeat number on Li-CoR IR^2 system [19].

***REN* cDNA expression constructs**

WT^{REN} cDNA was reverse transcribed and PCR amplified from the human total kidney RNA and cloned into pCR4- TOPO vector (Invitrogen, Paisley, UK). $\Delta L16^{REN}$ cDNA was prepared by subcloning of the corresponding DNA fragment obtained by PCR amplification of the patient DNA. Both constructs were introduced into the *Escherichia coli* TOP 10´F strain (Invitrogen, Paisley, UK) and individual clones were sequence verified. $\Delta L14\text{-}16^{REN}$ cDNA was identified among the clones during the sequencing process. Mammalian expression constructs WT^{REN}/pCR3.1, $\Delta L16^{REN}$/pCR3.1 and $\Delta L14\text{-}16^{REN}$/pCR3.1 were prepared by subcloning of corresponding inserts into pCR3.1 vector (Invitrogen, Paisley, UK) using *PmeI* and *NotI* restriction sites.

***In silico* analysis**

Signal peptide sequences were obtained from the UniProtKB/Swiss-Prot database. Multiple alignment and evaluation of the amino acids conservation were performed by ClustalW2 software (EMBL-EBI database).

***In vitro* translation and translocation**

WT^{REN}, $\Delta L16^{REN}$ and $\Delta L14\text{-}16^{REN}$ encoding plasmid DNA were linearised, purified and used for *in vitro* transcription with T7 polymerase as described previously [64]. Transcripts were treated with RQ1 DNase (Promega, Mannheim, Germany) and purified with G-25 columns (GE Healthcare, Freiburg, Germany). *In vitro* translation was performed in 10 µl reactions with 70% rabbit reticulocyte lysate (Promega, Mannheim, Germany) and 150 ng of each transcript in the presence of 35S EasyTag EXPRESS35S Protein Labeling Mix (Perkin Elmer, Rodgau Jügesheim, Germany). Reactions were incubated at 30°C for 30 min in the absence or presence of 1 eq of *Micrococcus* nuclease-treated rough microsomes (RMs) produced according to the protocol of Walter and Blobel [65]. Acceptor tripeptide (AP, N-benzoyl-Asn-Gly-Thr-methylamide, Bachem, Weil am Rhein, Germany) was dissolved in MetOH. 7.5 µl of 0.5 M solution were lyophilised in an Eppendorf tube prior to the addition of the *in vitro* translation reaction components to a final concentration of 375 µM. The signal peptide peptidase inhibitor (Z-LL)2-ketone (Calbiochem, Darmstadt, Germany) was dissolved in DMSO and added to a final concentration of 10 µM. *In vitro* reactions were either directly precipitated or membranes

were separated by centrifugation through a sucrose cushion as described elsewhere [34], except that the sucrose cushion contained 250 mM KAc. The pellet was resuspended either in SDS sample buffer or Wiltfang gel sample buffer, and the supernatant was precipitated as described above.

For a time course experiment, *in vitro* translation was stopped after 30 min by the addition of 1.25 mM cycloheximide (Sigma, Taufkirchen, Germany), and the reaction was incubated at 30°C for different periods of time prior to the separation of membranes.

Translation products were separated in 10% SDS gels (T: 10%, C: 0.8% according to Lämmli) or in Wiltfang gels [66] with the following modifications: gels were sized up to 200 x 200 mm, the AA-bisAA concentration of the separating gel was 15% and the gels were run at constant voltage of 180V with cooling.

Transient expression of REN

AtT-20, HEK 293, and MDCK cells were maintained in DMEM High Glucose medium supplemented with 10% (v/v) fetal calf serum (PAA), 100 U/ml penicillin G (Sigma, Prague, Czech Republic) and 100 µg/ml streptomycin sulphate (PAA Laboratories GmbH, Pashing, Austria). Transfections were carried out using Lipofectamine 2000^{TM} (Invitrogen, Paisley, UK) and either 1,5 µg or 4µg of DNA for 1,5x10^5 or 8x10^5 cells, respectively.

REN expressing stable cell lines

HEK 293 and MDCK cells were maintained as described above and transfected at 85% confluence using cell specific kits and Amaxa Nucleofector System (Amaxa, Koln, Germany). Three days post nucleofection, cells were trypsinised and diluted in selective medium containing 0,8 mg/ml G418 (Invitrogen-Gibco, Paisley, UK). 1, 10 or 100 cells per well were seeded into 96-well plates. Selected cells were transferred into 12-well plates and later into 25 cm^2 flasks. Integration of *REN* construct and REN expression were confirmed using PCR, sequencing and Western blot analyses. All the selected, sequence verified and REN positive clones were maintained for further analyses in the selective medium supplemented with 0,5 mg/ml of G418 or cryopreserved with 10% DMSO in FCS.

REN analysis

Western blot analysis and deglycosylation studies

Cells were seeded into 6-well plate (8x10^5 cells/well) and grown in standard, serum-supplemented medium. 24 hours before the analyses the supplemented medium was replaced by serum free medium. For secreted renin analysis, the medium was collected and centrifuged at 800g/5 min and then at 15000g/5 min for residual cells and cellular debris removal, respectively. Resulting supernatant was mixed with Protease inhibitor cocktail (Sigma, Prague, Czech Republic) in 100:1 (v/v) ratio. 500µl of this medium was then concentrated on Microcon YM-10

filters (Millipore, Billerica, MA) and total protein was recovered and mixed with SDS sample buffer.

Harvested cells were resuspended in PBS containing Protease inhibitor cocktail, sonicated twice for 30 sec on ice and centrifuged at 15000 g/5 min. Supernatant was mixed with SDS sample buffer.

Denatured protein samples were separated on 13% SDS-PAGE, blotted onto PVDF membrane, probed either with Rabbit Anti-Preprorenin (288-317) (detection of renin and prorenin) or Rabbit Anti-Preprorenin 21-64 (detection of prorenin) antibody (Yanaihara, Shizuoka, Japan) and detected with Anti-Rabbit IgG antibody conjugated to horseradish peroxidase (Pierce, Rockford, IL).

Deglycosylation experiments were performed on medium extracts or cell lysates using the GlycoPro™ enzymatic deglycosylation kit (ProZyme Inc., San Leandro, CA). Deglycosylated products were analysed by SDS-PAGE and Western blot as described above.

Renin activity measurement

Renin activity was measured using Angiotensin I RIA kit (Immunotech, Prague, Czech Republic) following manufacturer's instructions. Briefly, cells were seeded into 6-well plates and transfected. 24 hours after the transfection, the medium was collected and the cell lysate was prepared as described above. For renin activity, 50 µl of medium and 5 µl of lysate were diluted to final volume of 200 µl with PBS. For trypsine activated renin activity 5 µl of medium and 2,5 µl of lysate were incubated at 37°C for 30 minutes in 50 µl PBS reactions containing 20 µg and 5 µg of trypsine, respectively. The reaction was stopped by 1 µl of 10mg/mL trypsine inhibitor (PMSF, Roche, Prague, Czech Republic) and diluted to a final volume of 200 µl with PBS. 20 µl of the trypsinised mixtures were mixed with 80 µl of a solution containing 25 µl PBS, 5 µl of 0,5 µg/µl human angiotensinogen (Sigma, Prague, Czech Republic) and 50 µl of the ACE inhibitor (part of the RIA kit). This mixture was incubated at 37°C for 1 hour.

Active renin IRMA measurement

Renin amount was measured by Active Renin IRMA kit (DSL, Webster, TX) following manufacturer's instructions. Cell culturing, media collection, lysate preparation and sample trypsinisation was essentially the same as described above. 10 µl of the trypsinised mixtures were mixed with 190 µl of PBS and 100 µl of the anti-hRenin (I-125) reagent (kit component).

Renin secretion, FRET measurement

Stably transfected HEK 293 cells were seeded at 1,5 x 10^5 cells per well and cultured in 96-well plate in standard, serum-supplemented medium without phenol red. After 20 hours, the medium was replaced with medium containing renin substrate conjugated with 5-FAM and QXL520 (component of SensoLyte 520 Renin Assay Kit, AnaSpec, San Jose, CA). Fluorescent signal

was monitored at 520 nm every 5 minute for 8 hours at 37°C or 42°C on Synergy 2 Microplate Reader (BioTek, Winooski, VT).

Immunofluorescence analysis

Stably transfected HEK 293 cells were grown on glass chamber slides (BD Falcon - 4Chamber Polystyrene Vessel Tissue Culture Treated Glass Slide). After 48 hours the cells were washed with PBS, fixed with 100% ice-cold methanol, blocked with 5% FCS and incubated with rabbit Anti-Preprorenin (288-317) and rabbit Anti-Preprorenin (21-64) polyclonal antibodies for renin detection. Organelle specific primary antibodies and fluorescent-labelled secondary antibodies were described previously [1]. Nucleus was stained by 4´, 6-diamidino-2-phenylindole (DAPI). Slides were mounted in fluorescence mounting medium Immu-Mount (Shandon Lipshaw, Pittsburgh, PA) and analysed by confocal microscopy [1].

Growth rate analysis

Stably transfected HEK 293 cells were seeded in a 6-well plate at $4x10^5$ cells per well and cultured in the selective, G418 containing medium. Cells were counted every 24 hours for 7 days using standard Bürger's cell. The medium was changed at 3rd, 5th and 6th day.

***XBP1* analysis**

Total RNA was isolated from cells using TRIZOL (Invitrogen, Carlsbad, Ca) and reverse-transcribed with oligo-dT primer and SuperScript II (Invitrogen, Carlsbad, Ca). *XBP1* was PCR amplified from the corresponding cDNA with gene specific primers.

Electron microscopy

Pellets of stably transfected HEK 293 cells were fixed with 3% glutaraldehyde (GA) in 0.1 M phosphate buffer for 30 min and by buffered 1% OsO_4 for 2 h, then dehydrated and embedded into Epon. Thin sections were double-contrasted with uranylacetate and lead nitrate. Grids were observed and photographs were obtained on JEOL 1200 electron microscope.

Plasma renin activity measurement

Plasma renin activity was measured by Angiotensin I RIA kit (Immunotech, Prague, Czech Republic) according to manufacturer's instructions.

Immunohistochemistry studies

Formaldehyde or ethanol-fixed kidney samples from 5 controls and patients DII.1, DIV.3 and DIV.7 were analysed essentially as previously described [1]. Selected antigens were investigated using the following primary antibodies: prorenin - Rabbit Anti-Preprorenin (21-64); prorenin + renin - Rabbit Anti-Preprorenin (288-317); active renin - Mouse Anti-Renin R3-36-16 (a gift from Novartis AG, Basel Switzerland); Pro/renin receptor - Rabbit Anti-P/RR, (a gift from Genevieve Nguyen, Paris); angiotensinogen - Mouse Anti-Angiotensinogen (US Biological, Swampscott, MA); angiotensin II - Mouse Anti-Angiotensin II (Acris, Herford, Germany);

TREK-1 - Rabbit Anti- TREK-1 (H-75); WNK4 – Goat Anti-WNK4 (N-12), both from Santa Cruz Biotechnology, Heidelberg, Germany.

Acknowledgements

We thank Elly Pijkels and Evelyne Lerut for their efforts in collection of biological materials and patient's data, Maria Leidenberger for technical support with in vitro translation experiments, Novartis Pharma AG for R3-36-16 renin antibody, Genevieve Nguyen for pro/renin antibody and Genomics and Bioinformatics Facility of the Institute of Molecular Genetics AS CR for genotyping. This work was supported by the Grant Agency of Charles University of Prague (257672 to M.Ž., and 257750 to P.V.). Institutional support was provided by the Ministry of Education of the Czech Republic (projects MSM0021620806, and 1M6837805002).

Disclosure

None

References

1. Vylet'al, P., et al., *Alterations of uromodulin biology: a common denominator of the genetically heterogeneous FJHN/MCKD syndrome.* Kidney Int, 2006. **70**(6): p. 1155-69.
2. Duncan, H. and A.S. Dixon, *Gout, familial hypericaemia, and renal disease.* Q J Med, 1960. **29**: p. 127-35.
3. Cameron, J.S., F. Moro, and H.A. Simmonds, *Gout, uric acid and purine metabolism in paediatric nephrology.* Pediatr Nephrol, 1993. **7**(1): p. 105-18.
4. Goldman, S.H., et al., *Hereditary occurrence of cystic disease of the renal medulla.* N Engl J Med, 1966. **274**(18): p. 984-92.
5. Scolari, F., et al., *Identification of a new locus for medullary cystic disease, on chromosome 16p12.* Am J Hum Genet, 1999. **64**(6): p. 1655-60.
6. Hart, T.C., et al., *Mutations of the UMOD gene are responsible for medullary cystic kidney disease 2 and familial juvenile hyperuricaemic nephropathy.* J Med Genet, 2002. **39**(12): p. 882-92.
7. Kudo, E., et al., *Familial juvenile hyperuricemic nephropathy: detection of mutations in the uromodulin gene in five Japanese families.* Kidney Int, 2004. **65**(5): p. 1589-97.
8. Rampoldi, L., et al., *Allelism of MCKD, FJHN and GCKD caused by impairment of uromodulin export dynamics.* Hum Mol Genet, 2003. **12**(24): p. 3369-84.

9. Rezende-Lima, W., et al., *Homozygosity for uromodulin disorders: FJHN and MCKD-type 2.* Kidney Int, 2004. **66**(2): p. 558-63.
10. Turner, J.J., et al., *UROMODULIN mutations cause familial juvenile hyperuricemic nephropathy.* J Clin Endocrinol Metab, 2003. **88**(3): p. 1398-401.
11. Calado, J., et al., *A novel heterozygous missense mutation in the UMOD gene responsible for Familial Juvenile Hyperuricemic Nephropathy.* BMC Med Genet, 2005. **6**: p. 5.
12. Lens, X.M., et al., *A novel pattern of mutation in uromodulin disorders: autosomal dominant medullary cystic kidney disease type 2, familial juvenile hyperuricemic nephropathy, and autosomal dominant glomerulocystic kidney disease.* Am J Kidney Dis, 2005. **46**(1): p. 52-7.
13. Wolf, M.T., et al., *Mutations of the Uromodulin gene in MCKD type 2 patients cluster in exon 4, which encodes three EGF-like domains.* Kidney Int, 2003. **64**(5): p. 1580-7.
14. Dahan, K., et al., *A cluster of mutations in the UMOD gene causes familial juvenile hyperuricemic nephropathy with abnormal expression of uromodulin.* J Am Soc Nephrol, 2003. **14**(11): p. 2883-93.
15. Stacey, J.M., et al., *Genetic mapping studies of familial juvenile hyperuricemic nephropathy on chromosome 16p11-p13.* J Clin Endocrinol Metab, 2003. **88**(1): p. 464-70.
16. Ohno, I., et al., *Familial juvenile gouty nephropathy: exclusion of 16p12 from the candidate locus.* Nephron, 2002. **92**(3): p. 573-5.
17. Kroiss, S., et al., *Evidence of further genetic heterogeneity in autosomal dominant medullary cystic kidney disease.* Nephrol Dial Transplant, 2000. **15**(6): p. 818-21.
18. Auranen, M., et al., *Further evidence for linkage of autosomal-dominant medullary cystic kidney disease on chromosome 1q21.* Kidney Int, 2001. **60**(4): p. 1225-32.
19. Hodanova, K., et al., *Mapping of a new candidate locus for uromodulin-associated kidney disease (UAKD) to chromosome 1q41.* Kidney Int, 2005. **68**(4): p. 1472-82.
20. Imai, T., et al., *Cloning and sequence analysis of cDNA for human renin precursor.* Proc Natl Acad Sci U S A, 1983. **80**(24): p. 7405-9.
21. Paul, M., A. Poyan Mehr, and R. Kreutz, *Physiology of local renin-angiotensin systems.* Physiol Rev, 2006. **86**(3): p. 747-803.
22. Campbell, D.J., *Critical review of prorenin and (pro)renin receptor research.* Hypertension, 2008. **51**(5): p. 1259-64.
23. Gribouval, O., et al., *Mutations in genes in the renin-angiotensin system are associated with autosomal recessive renal tubular dysgenesis.* Nat Genet, 2005. **37**(9): p. 964-8.

24. Lacoste, M., et al., *Renal tubular dysgenesis, a not uncommon autosomal recessive disorder leading to oligohydramnios: Role of the Renin-Angiotensin system.* J Am Soc Nephrol, 2006. **17**(8): p. 2253-63.
25. Zingg-Schenk, A., et al., *Inherited renal tubular dysgenesis: the first patients surviving the neonatal period.* Eur J Pediatr, 2008. **167**(3): p. 311-6.
26. Burckle, C. and M. Bader, *Prorenin and its ancient receptor.* Hypertension, 2006. **48**(4): p. 549-51.
27. Kaneshiro, Y., et al., *Slowly progressive, angiotensin II-independent glomerulosclerosis in human (pro)renin receptor-transgenic rats.* J Am Soc Nephrol, 2007. **18**(6): p. 1789-95.
28. Clark, A.F., et al., *Renin-1 is essential for normal renal juxtaglomerular cell granulation and macula densa morphology.* J Biol Chem, 1997. **272**(29): p. 18185-90.
29. Pentz, E.S., et al., *Ablation of renin-expressing juxtaglomerular cells results in a distinct kidney phenotype.* Am J Physiol Regul Integr Comp Physiol, 2004. **286**(3): p. R474-83.
30. Hegde, R.S. and H.D. Bernstein, *The surprising complexity of signal sequences.* Trends Biochem Sci, 2006. **31**(10): p. 563-71.
31. Martoglio, B., *Intramembrane proteolysis and post-targeting functions of signal peptides.* Biochem Soc Trans, 2003. **31**(Pt 6): p. 1243-7.
32. Henderson, R.A., et al., *HLA-A2.1-associated peptides from a mutant cell line: a second pathway of antigen presentation.* Science, 1992. **255**(5049): p. 1264-6.
33. Martoglio, B., R. Graf, and B. Dobberstein, *Signal peptide fragments of preprolactin and HIV-1 p-gp160 interact with calmodulin.* Embo J, 1997. **16**(22): p. 6636-45.
34. Dultz, E., et al., *The signal peptide of the mouse mammary tumor virus Rem protein is released from the endoplasmic reticulum membrane and accumulates in nucleoli.* J Biol Chem, 2008. **283**(15): p. 9966-76.
35. Jarjanazi, H., et al., *Biological implications of SNPs in signal peptide domains of human proteins.* Proteins, 2008. **70**(2): p. 394-403.
36. Hon, L.S., et al., *Computational prediction of the functional effects of amino acid substitutions in signal peptides using a model-based approach.* Hum Mutat, 2008.
37. Datta, R., et al., *Signal sequence mutation in autosomal dominant form of hypoparathyroidism induces apoptosis that is corrected by a chemical chaperone.* Proc Natl Acad Sci U S A, 2007. **104**(50): p. 19989-94.
38. Kutz, W.E., et al., *Functional analysis of an ADAMTS10 signal peptide mutation in Weill-Marchesani syndrome demonstrates a long-range effect on secretion of the full-length enzyme.* Hum Mutat, 2008.

39. Mansfield, T.A., et al., *Multilocus linkage of familial hyperkalaemia and hypertension, pseudohypoaldosteronism type II, to chromosomes 1q31-42 and 17p11-q21.* Nat Genet, 1997. **16**(2): p. 202-5.
40. Walter, P., I. Ibrahimi, and G. Blobel, *Translocation of proteins across the endoplasmic reticulum. I. Signal recognition protein (SRP) binds to in-vitro-assembled polysomes synthesizing secretory protein.* J Cell Biol, 1981. **91**(2 Pt 1): p. 545-50.
41. Morris, B.J., *Molecular biology of renin. I: Gene and protein structure, synthesis and processing.* J Hypertens, 1992. **10**(3): p. 209-14.
42. Bendtsen, J.D., et al., *Improved prediction of signal peptides: SignalP 3.0.* J Mol Biol, 2004. **340**(4): p. 783-95.
43. Kyte, J. and R.F. Doolittle, *A simple method for displaying the hydropathic character of a protein.* J Mol Biol, 1982. **157**(1): p. 105-32.
44. Yoshida, H., et al., *XBP1 mRNA is induced by ATF6 and spliced by IRE1 in response to ER stress to produce a highly active transcription factor.* Cell, 2001. **107**(7): p. 881-91.
45. Sagnella, G.A. and W.S. Peart, *Studies on the isolation and properties of renin granules from the rat kidney cortex.* Biochem J, 1979. **182**(2): p. 301-9.
46. Eskelinen, E.L., *To be or not to be? Examples of incorrect identification of autophagic compartments in conventional transmission electron microscopy of mammalian cells.* Autophagy, 2008. **4**(2): p. 257-60.
47. Krop, M., et al., *Renin and prorenin disappearance in humans post-nephrectomy: evidence for binding?* Front Biosci, 2008. **13**: p. 3931-9.
48. Wilson, F.H., et al., *Human hypertension caused by mutations in WNK kinases.* Science, 2001. **293**(5532): p. 1107-12.
49. Marciniak, S.J. and D. Ron, *Endoplasmic reticulum stress signaling in disease.* Physiol Rev, 2006. **86**(4): p. 1133-49.
50. Schroder, M., *Endoplasmic reticulum stress responses.* Cell Mol Life Sci, 2008. **65**(6): p. 862-94.
51. Kaufman, R.J., *Orchestrating the unfolded protein response in health and disease.* J Clin Invest, 2002. **110**(10): p. 1389-98.
52. Ito, M., J.L. Jameson, and M. Ito, *Molecular basis of autosomal dominant neurohypophyseal diabetes insipidus. Cellular toxicity caused by the accumulation of mutant vasopressin precursors within the endoplasmic reticulum.* J Clin Invest, 1997. **99**(8): p. 1897-905.

53. Bonapace, G., et al., *Chemical chaperones protect from effects of apoptosis-inducing mutation in carbonic anhydrase IV identified in retinitis pigmentosa 17.* Proc Natl Acad Sci U S A, 2004. **101**(33): p. 12300-5.
54. Rebello, G., et al., *Apoptosis-inducing signal sequence mutation in carbonic anhydrase IV identified in patients with the RP17 form of retinitis pigmentosa.* Proc Natl Acad Sci U S A, 2004. **101**(17): p. 6617-22.
55. Sequeira Lopez, M.L., et al., *Embryonic origin and lineage of juxtaglomerular cells.* Am J Physiol Renal Physiol, 2001. **281**(2): p. F345-56.
56. Persson, P.B., *Renin: origin, secretion and synthesis.* J Physiol, 2003. **552**(Pt 3): p. 667-71.
57. Kobori, H., et al., *The intrarenal renin-angiotensin system: from physiology to the pathobiology of hypertension and kidney disease.* Pharmacol Rev, 2007. **59**(3): p. 251-87.
58. Nangaku, M. and T. Fujita, *Activation of the renin-angiotensin system and chronic hypoxia of the kidney.* Hypertens Res, 2008. **31**(2): p. 175-84.
59. Cruzado, J.M., J. Rico, and J.M. Grinyo, *The renin angiotensin system blockade in kidney transplantation: pros and cons.* Transpl Int, 2008. **21**(4): p. 304-13.
60. Safirstein, R., et al., *Expression of cytokine-like genes JE and KC is increased during renal ischemia.* Am J Physiol, 1991. **261**(6 Pt 2): p. F1095-101.
61. Abecasis, G.R., et al., *Merlin--rapid analysis of dense genetic maps using sparse gene flow trees.* Nat Genet, 2002. **30**(1): p. 97-101.
62. Thiele, H. and P. Nurnberg, *HaploPainter: a tool for drawing pedigrees with complex haplotypes.* Bioinformatics, 2005. **21**(8): p. 1730-2.
63. Kmoch, S., et al., *Human adenylosuccinate lyase (ADSL), cloning and characterization of full-length cDNA and its isoform, gene structure and molecular basis for ADSL deficiency in six patients.* Hum Mol Genet, 2000. **9**(10): p. 1501-13.
64. Lyko, F., et al., *Signal sequence processing in rough microsomes.* J Biol Chem, 1995. **270**(34): p. 19873-8.
65. Walter, P. and G. Blobel, *Preparation of microsomal membranes for cotranslational protein translocation.* Methods Enzymol, 1983. **96**: p. 84-93.
66. Wiltfang, J., N. Arold, and V. Neuhoff, *A new multiphasic buffer system for sodium dodecyl sulfate-polyacrylamide gel electrophoresis of proteins and peptides with molecular masses 100,000-1000, and their detection with picomolar sensitivity.* Electrophoresis, 1991. **12**(5): p. 352-66.

Figure legends

Figure 1 Linkage analysis in the UAKD family. (A) A whole genome parametric linkage analysis showing single statistically significant region on chromosome 1q41. (B) Haplotype analysis delimiting the candidate region between the markers SNP_A_1517951 and SNP_A_1509750. Black symbols denote affected individuals, open symbols denote unaffected individuals.

Figure 2 Mutation $\Delta L16^{REN}$ in the preprorenin gene. (A) Chromatogram of preprorenin genomic DNA sequence showing deletion of a trinucleotide repeat in the proband. (B) PCR RFLP analysis showing segregation of the mutation in affected individuals.

Figure 3 Bioinformatic analysis of the preprorenin. (A) Diagram of the preprorenin sequence showing the locations of the identified $\Delta L16^{REN}$ mutation and epitopes recognized by prorenin (21-64) and preprorenin (288-317) specific antibodies. (B) Homology of the mutant and wild-type human preprorenin signal peptide sequences with those of higher mammals. (C) Hydrophobicity plot of the WT^{REN}, $\Delta L16^{REN}$, $\Delta L14\text{-}16^{REN}$ signal sequences calculated using the Kyte and Doolittle method and scale.

Figure 4 *In vitro* transcription, translation and translocation. (A) Corresponding transcripts transcribed and translated in nuclease-treated rabbit reticulocyte lysate in the absence (-), or presence (+), of rough microsomes (RM) and tripeptide glycosylation acceptor (AP). (B) Translation/translocation assay performed in the presence (+), and absence (-) of signal peptide peptidase inhibitor $(ZZ\text{-}L)_2$. The s and p denote supernatant and pellet fractions.

Figure 5 Transient expression of preprorenin in AtT-20 cells. (A) Renin (REN) and trypsine activated total renin + prorenin (ProREN+REN) activities, and (B) active renin (REN) and trypsine activated total renin + prorenin (ProREN+REN) amounts measured in cell lysates and medium 24 hours after the transfection with WTREN, ΔL16REN, ΔL14-16REN constructs and an empty Vector. The values represent means ± s.d. from three transfection experiments carried out in triplicates. The statistical significance of the differences between WT^{REN} and $\Delta L16^{REN}$ protein activities and amounts was tested by t-test (Microsoft Office Excel 2003). *P<0,05; ** P<0,01; NS - not significant. (C-D) Western blot analysis of prorenin and renin in cell lysates collected at indicated time point after the transfection. (C) (21-64) antibody detection of prorenin in untreated lysates; (D) (21-64) antibody detection of prorenin in N-deglycosylated lysates; (E) (288-311) antibody detection of prorenin and renin in untreated lysates; (F) (288-317) antibody detection of prorenin and renin in N-deglycosylated lysates; - denotes WT^{REN} protein product before deglycosylation.

Figure 6 Stable expression of prorenin and renin in HEK 293 cell lines. (A) Active renin (REN) and trypsine activated total renin + prorenin (ProREN+REN) amounts measured in cell lysates

and medium. The values represent means ± s.d. of the measurements performed in two independent clones for each of the constructs. The individual measurements were carried out in triplicates. The statistical significance of the differences between WT^{REN} and $\Delta L16^{REN}$ protein amounts was tested by t-test. *P<0,05; ** P<0,01; *** P<0,001. 0^{REN} is antibiotics selected cell line, which showed no renin expression by RT-PCR and Western blot analysis. (B) Western blot analysis of prorenin and renin in cell lysates before (-) and after (+) N-deglycosylation. (C) Western blot analysis of prorenin and renin in medium before (-) and after (+) N-deglycosylation. (D) Renin secretion from living HEK 293 cell lines. The fluorescent signal is released from 5-FAM and QXL520 conjugated renin substrate and corresponds to the activity of the renin secreted in medium.

Figure 7 Growth curves and *XBP1* expression in stably transfected WT^{REN} and $\Delta L16^{REN}$ cell lines. (A) HEK 293 cells. (B) MDCK cells. (C) RT-PCR detection of *XBP1* splicing variants in WT^{REN}, $\Delta L16^{REN}$ and 0^{REN} cells. *XBP1(U)* is constitutively expressed form. XBP1(S) is formed by alternative splicing upon ER stress and encoded protein is a key effector of the mammalian unfolded protein response (UPR).

Figure 8 Cellular localisation of the prorenin and renin in stably transfected WT^{REN} and $\Delta L16^{REN}$ HEK 293 cells. (A, B) Prorenin and renin detected using renin 288-317 antibodies (green signal) and its colocalisation with (C, D) endoplasmic reticulum detected using PDI antibody; (E, F) Golgi apparatus detected using GS28 antibody; (G, H) cytoskeleton detected using Acetylated alpha-Tubulin antibody and (I, J) plasma membrane detected using Pan-Cadherin antibody (red signals).

Figure 9 Electron microscopy of stably transfected WT^{REN} and $\Delta L16^{REN}$ HEK 293 cells. (A) Overview of the WT^{REN} cell with numerous electron dense granules marked by the arrows. (B) Detail of the electron dense granules in WT^{REN} cell. (C) Granules in $\Delta L16^{REN}$ cell. Compare the morphology of these granules to additional numerous membrane bound bodies containing pleomorphic and partly degraded cytosolic components (compatible with autophagic compartment) both in (D) WT^{REN} and (E) $\Delta L16^{REN}$ cells. (F) Considerable distension of ER cisternae (asterisk) observed more frequently in $\Delta L16^{REN}$ cells. Actual magnification in thousands is provided for each of the images.

Figure 10 Immunohistochemistry and nephropathology. (A, B, C) Renin expression in control kidney. (A) Renin expression in JG cells and individual cells of collecting ducts; a 7 years aged control. (B, C) Renin staining in an adult control (B) in JG apparatus and (C) in renal cortical tubules where the signal is restricted to individual cells of the collecting ducts.
(D, E, F) Kidney biopsies in an early disease stage. The common denominator is a strong reduction of renin signal in the JG apparatus and its absence in the surrounding tubules. (D)

Structural abnormalities in patient DIV.3 at 8 years of age are minimal with enlarged glomeruli and borderline tubulointerstitial changes. In patient DIV.7 at 4 years of age, there were (E) some glomeruli in various stages of hyalinization and (F) occasionally foci of tubular atrophy with mild interstitial fibrosis.

(G, H, I) Patient DII.1 at 60 years of age in advanced stage of kidney disease. (G, H) Pronounced tubular atrophy and loss of tubules is accompanied with prominent interstitial fibrosis. Some of the atrophic tubules are surrounded by thickened basement membranes. Many of the remaining tubules reveal cystic dilatation (see G). Glomeruli exhibit various degrees of sclerosis. Some glomeruli are collapsed in the enlarged Bowman spaces suggesting block in tubular fluid passage (see H). Periglomerular fibrosis is frequently present, (see H). Note regional heterogeneity in the severity of structural alteration. H&E staining. (I) Renin staining is absent in both JG apparatus and tubular epithelium even in relatively well preserved regions.

(J, K, L) Renin expression inside the wall of small size vessels, probably in a sub/endothelial localization, more prominent in patient DII.1 (the main pictures) than in patients in early stage of the disease (inserts). (J) Prorenin and renin detected by preprorenin antibody, (K) mouse monoclonal antibody, and (L) prorenin antibody. Insert (J) demonstrates situation in patient 1, inserts (K) and (L) in patient 2.

Figure 11 Detection of renal RAS components. (A-E) Immunodetection of pro/renin receptor. (A,B) Strong signal at the basolateral pole of distal convoluted tubules and thick ascending loop of Henle in (A) 7 years aged control, and (B) adult control. Expression pro/renin receptor is in patients reduced proportionally to the disease stage (C) patient DIV.7, (D) patient DIV.3, (E) patient DII1.

(F-J) Immunodetection of angiotensinogen (AGT). (F) Mild and heterogenous intracellular granular positivity in proximal tubules in 7 years aged control and (H, I) comparable or slightly weakened signal in patients in early stage of the disease (H) patient DIV.7, (I) patient DIV.3. (G) Pronounced AGT expression in proximal tubules in adult control and (J) significantly decreased intensity in the kidney of patient DII1.

(K-O) Immunodetection of angiotensin II. (K) Presence of angiotensin II at the apical pole of proximal tubules, in the tubular fluid and in distal nephron epithelium in 7 years aged control and reduced signal in both (M) patient DIV.7, and (N) patient DIV.3. (L) Positivity in adult control kidney is seen in the same locations as in the infantile control but with an increased intensity. This contrasts with (O) markedly decreased signal in adult patient DII.1. In the advanced stage of the disease (patient DII.1) immunostaining signals of all the followed RAS components were always restricted to the foci of relatively preserved renal parenchyma.

Figure 1

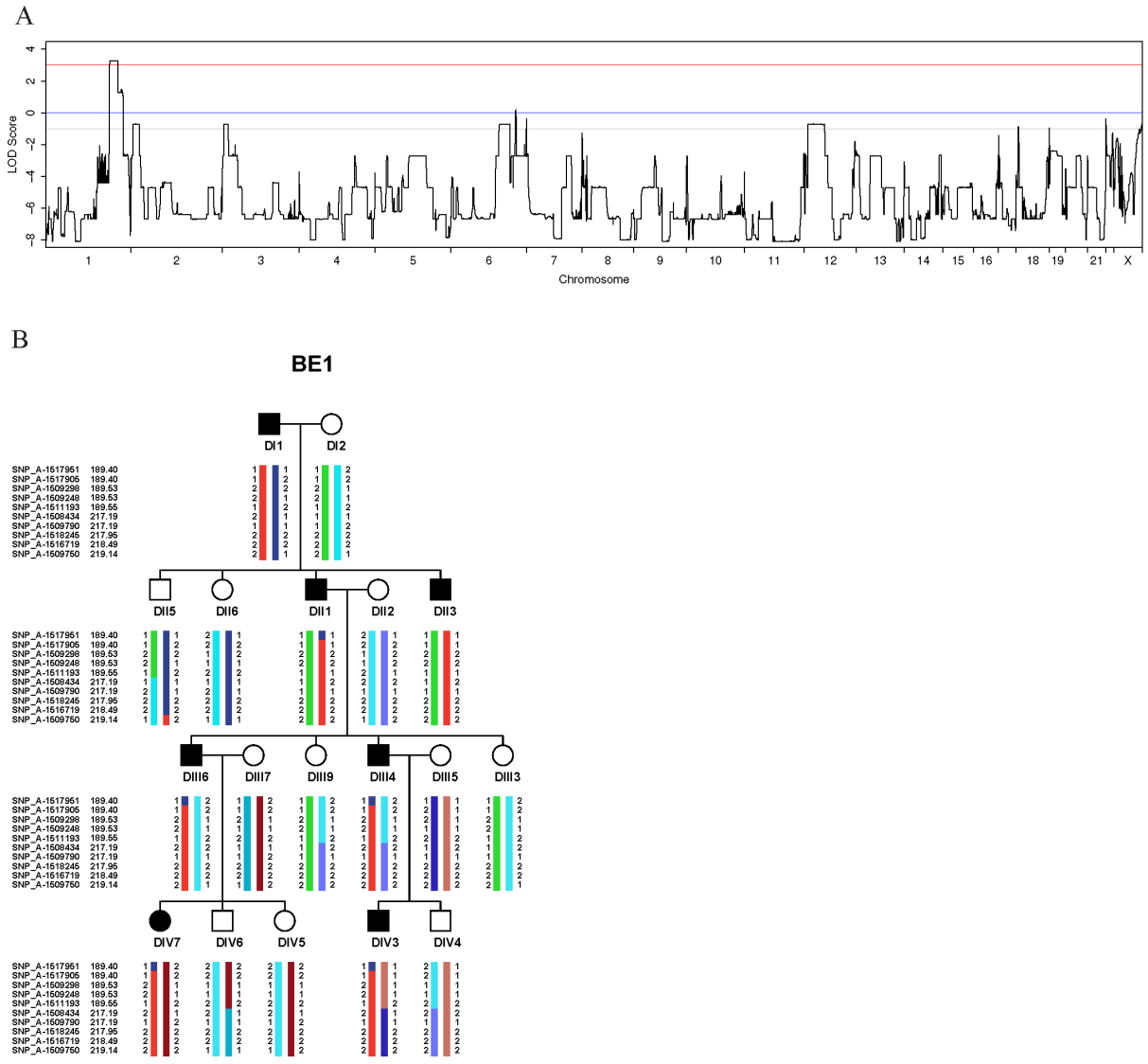

Figure 2

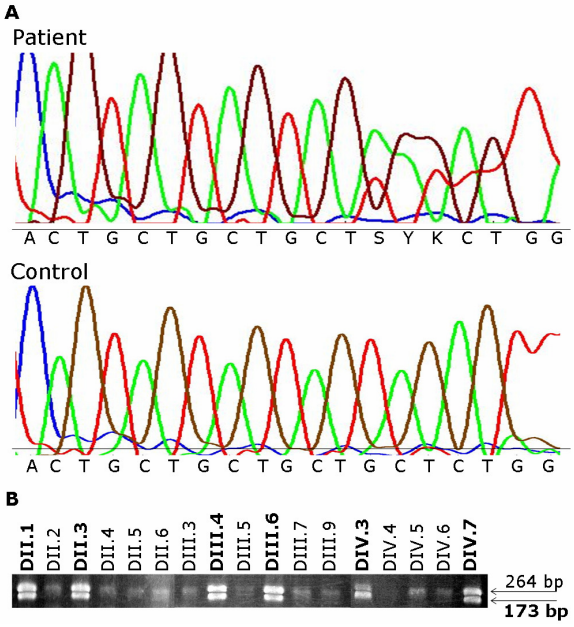

Figure 3

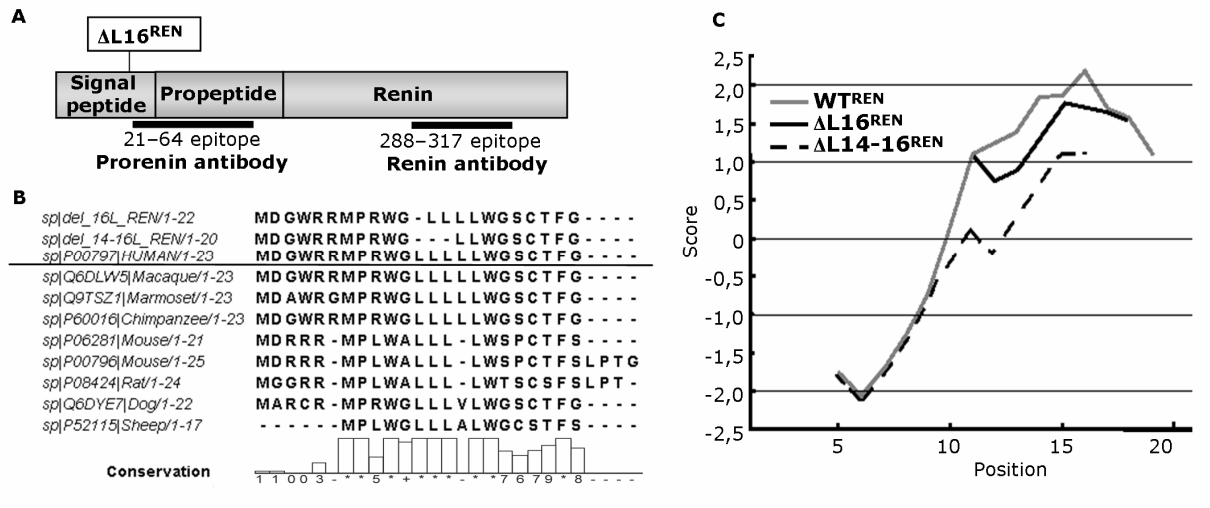

Figure 4

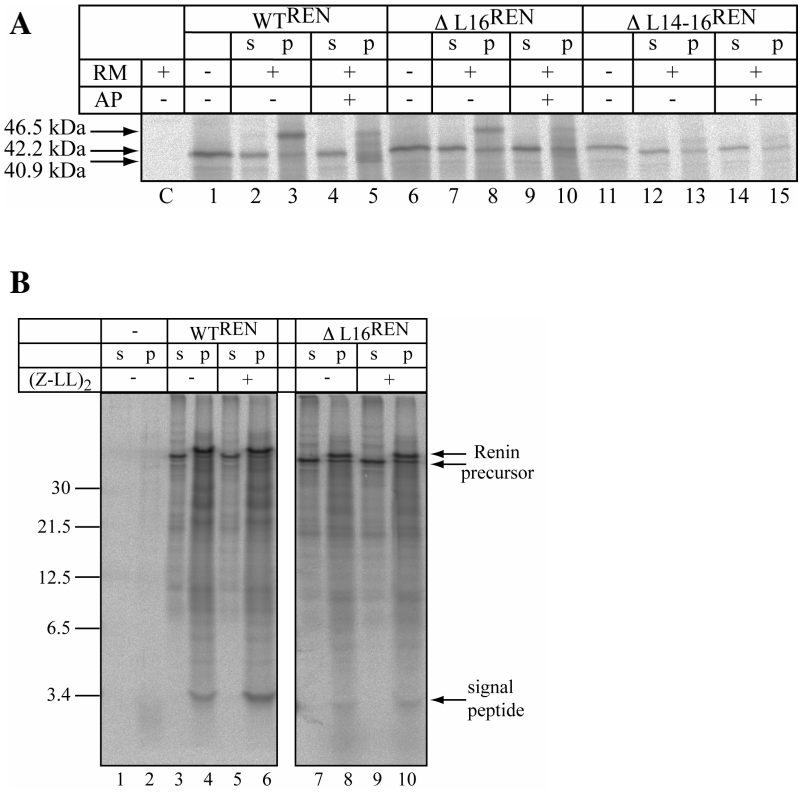

Figure 5

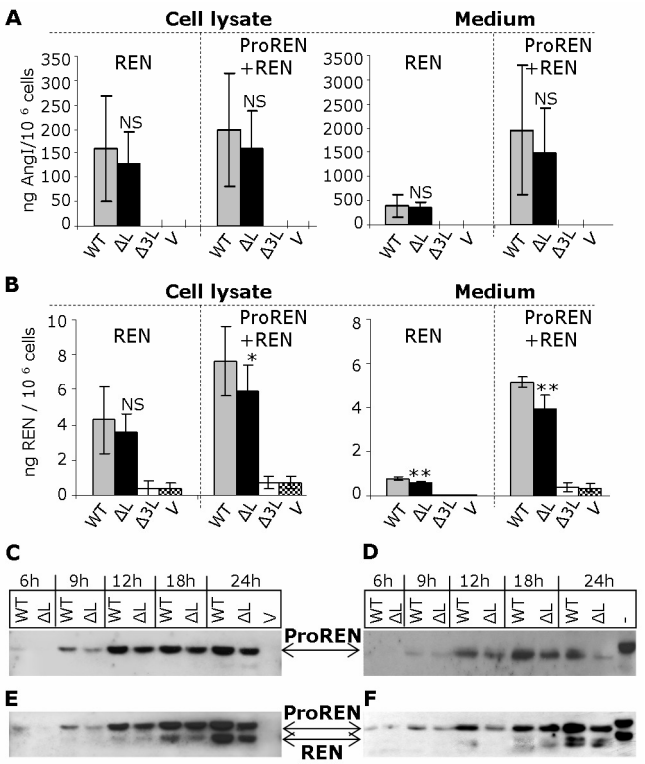

Figure 6

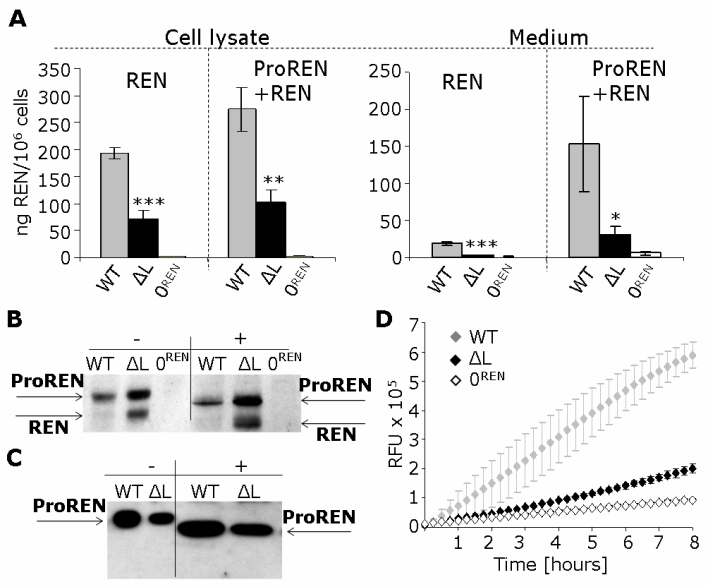

Figure 7

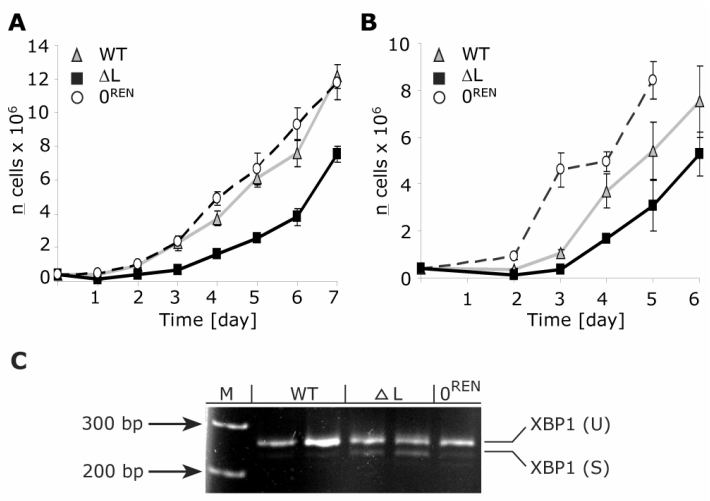

Figure 8

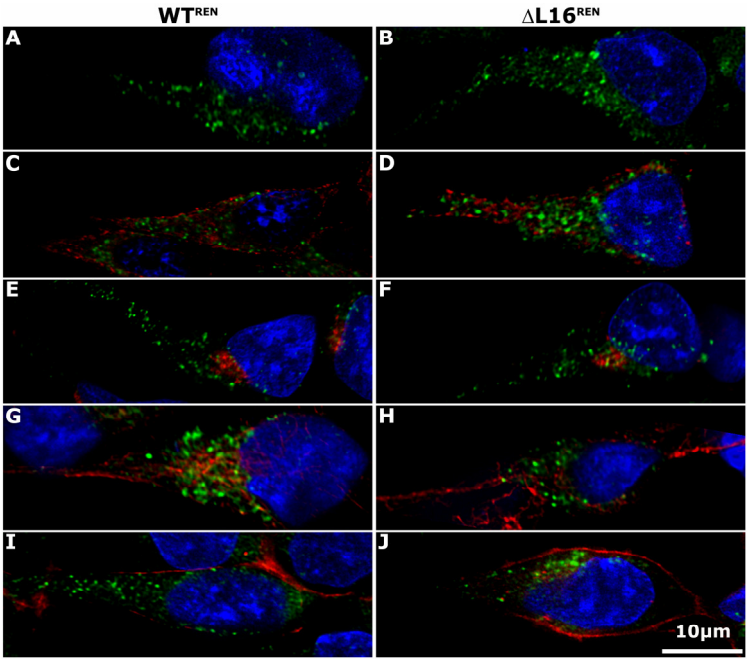

Figure 9

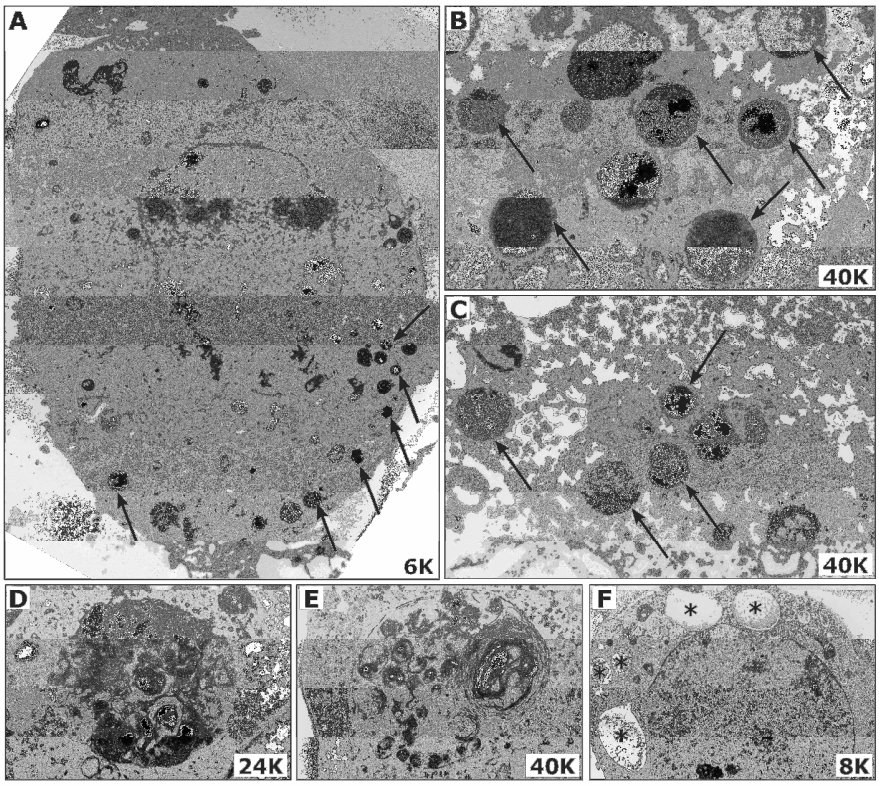

Figure 10

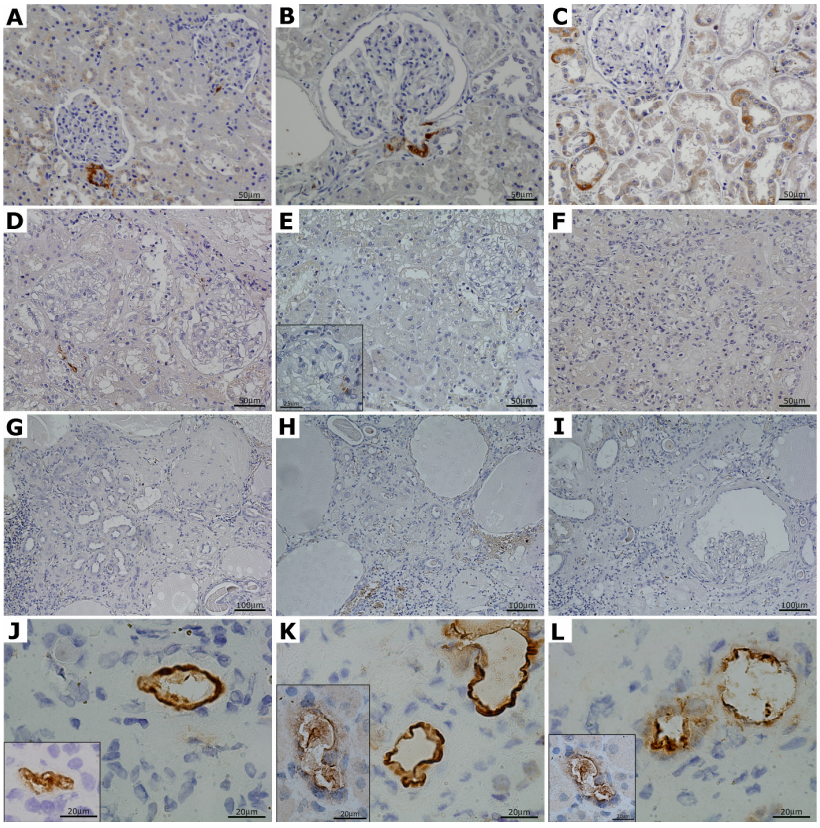

Figure 11